CANADIAN THESES

THÈSES CANADIENNES

NOTICE

The quality of this microfiche is heavily dependent upon the quality of the original thesis submitted for microfilming. Every effort has been made to ensure the highest quality of reproduction possible.

If pages are missing, contact the university which granted the degree.

Some pages may have indistinct print especially if the original pages were typed with a poor typewriter ribbon or if the university sent us an inferior photocopy.

Previously copyrighted materials (journal articles, published tests, etc.) are not filmed.

Reproduction in full or in part of this film is governed by the Canadian Copyright Act, R.S.C. 1970, c. C-30. Please read the authorization forms which accompany this thesis.

AVIS

La qualité de cette microfiche dépend grandement de la qualité de la thèse soumise au microfilmage. Nous avons tout fait pour assurer une qualité supérieure de reproduction.

S'il manque des pages, veuillez communiquer avec l'université qui a conféré le grade.

La qualité d'impression de certaines pages peut laisser à désirer, surtout si les pages originales ont été dactylographiées à l'aide d'un ruban usé ou si l'université nous a fait parvenir une photocopie de qualité inférieure.

Les documents qui font déjà l'objet d'un droit d'auteur (articles de revue, examens publiés, etc.) ne sont pas microfilmés.

La reproduction, même partielle, de ce microfilm est soumise à la Loi canadienne sur le droit d'auteur, SRC 1970, c. C-30. Veuillez prendre connaissance des formules d'autorisation qui accompagnent cette thèse.

THIS DISSERTATION
HAS BEEN MICROFILMED
EXACTLY AS RECEIVED

LA THÈSE A ÉTÉ
MICROFILMÉE TELLE QUE
NOUS L'AVONS REÇUE

Canada

Transition Boiling Under Slightly Pressurized Conditions and Measurements of Rewetting Temperature

by

Kwan Tong Poon

A thesis
presented to the School of Graduate Studies and Research
at the University of Ottawa
in partial fulfillment of the
requirements for the degree of
Master of Applied Science
in
Department of Mechanical Engineering

ACKNOWLEDGEMENT

The author wishes to express his appreciation to Dr. S.C. Cheng who initiated this project for his support, guidance and encouragement.

The author wishes to thank Dr. Groeneveld and Mr. W.W.L. Ng for their valuable advice during the course of this experiment. He also wishes to express his appreciation to Miss T. Chung for her efforts in typing this manuscript, and to the technical staff of the Mechanical Engineering Workshop for their technical assistance.

This work was supported financially by Argonne National Laboratory, Illinois, U.S.A. An expression of thanks is extended to Atomic Energy of Canada Limited for providing technical information and testing material.

ABSTRACT

Transition boiling heat flux at pressures from 101 to 686 kPa and the rewetting temperature at atmospheric pressure have been obtained for distilled water.

For transition boiling, water flowed in a composite test section with 1.19 cm ID tube heated by cartridge heaters. The thermocouples were placed at the outer wall of the tube. From the temperature history of the data thermocouple during a quenching process, the boiling curve could be constructed. The transition heat flux results seemed to be mainly affected by pressure and mass flux, but no significant influence by inlet subcooling was observed.

The rewetting temperature of a single rod and a three-rod bundle was investigated by an electric resistance probe. The thermocouple inside the rod could also provide the temperature history for constructing the boiling curve in which the rewetting temperature was compared with the signal from the probe. The experimental results indicated that the rewetting temperature for single rod from both probe signal and boiling curve were close, but not so successful for the three rod test section.

CONTENTS

LIST OF FIGURES

NOMENCLATURE

A	Area
C	Specific Heat
CHF	Critical Heat Flux
D	Diameter
G	Mass Flux
g	Gravitational Constant
h	Heat Transfer Coefficient
HP	Horsepower
ID	Inside Diameter
k	Thermal Conductivity
L	Length
OD	Outside Diameter
p	Pressure
Q	Heat
q	Heat Transfer Rate
r	Radius
T	Temperature
t	Time
T.C.	Thermocouple
T.B.	Transition Boiling
x	quality

Greek Symbols

	Thermal Diffisivity, Void Fraction
	Thickness
	Height of Surface Roughness
	Dynamic Viscosity
	Density
	Surface Tension of Liquid-Vapour
	Heat Flux

Subscripts

a	Atmospheric
amb	ambient
c	Copper
CHF	Critical Heat Flux
DNP	Departure from Nucleate Boiling
e	Equivalent
f	Film Temperature
i	ith Nodal Point
in	inside
g	Saturated Vapour
l	Liquid
n	nth Nodal Point
min	Minimum
out	Outside
sat	Saturated
sub	Subcooling
t	tube
TB	Transition Boiling
v	Vapour

Chapter I

INTRODUCTION

Heat transfer in boiling has been investigated intensively for the last thirty years. Scientists in this field have succeeded in explaining many individual phenomena and in gathering extensive information. However, the knowledge in transition boiling, including the minimum film boiling point, is limited. The study of transition boiling under moderate pressure is important to the safety evaluation of water-cooled nuclear reactors analysis.

All types of power producing water reactors have coolant circuits which operate at high pressure, ranging from about 70 bar (6.86 MPa or 1000 psia) in the Boiling Water Reactor (BWR) and Steam-Generating Heavy Water Reactor (SGHWR), to 150 bar (15.4 MPa or 2250 psia) in the Pressurized-Water Reactor(PWR). The accidental loss of coolant through small breaches will lead to depressurization in the system. Many different types of Emergency Core-Cooling Systems are used for different reactors. One of them is the low pressure Emergency Core-Cooling System (ECCS), which is designed to operate when the circuit is largely depressurized to reflood the core region. The knowledge of transition boiling and

rewetting phenomena is needed in order to design a safe and efficient emergency core cooling system.

For this reason, a research program was carried out to obtain the post CHF heat transfer data under different system pressure, mass flux and subcooling, and to detect the CHF and rewetting points via an electric resistance probe at atmospheric pressure.

1.1 POOL BOILING CURVE

Figure 1 illustrates the typical dependence between the heat flux, q/A, and the temperature difference, $\Delta T_w = T_w - T_{sat}$ on a heating surface. There are four distinct regions and two important points:

1. The natural convection region AB, where no boiling is observed. The liquid is found to be slightly superheated on the heating surface. Energy is transported from the heating surface to the liquid-vapour interface by free convection.
2. The nucleate boiling region, BC where vapour nucleation occurs at the heating surface, grows in size, and eventually breaks off. In this regime the fluid around the heating element becomes highly agitated -- much more so than in the case of the free convection regime. This increased fluid motion tends,

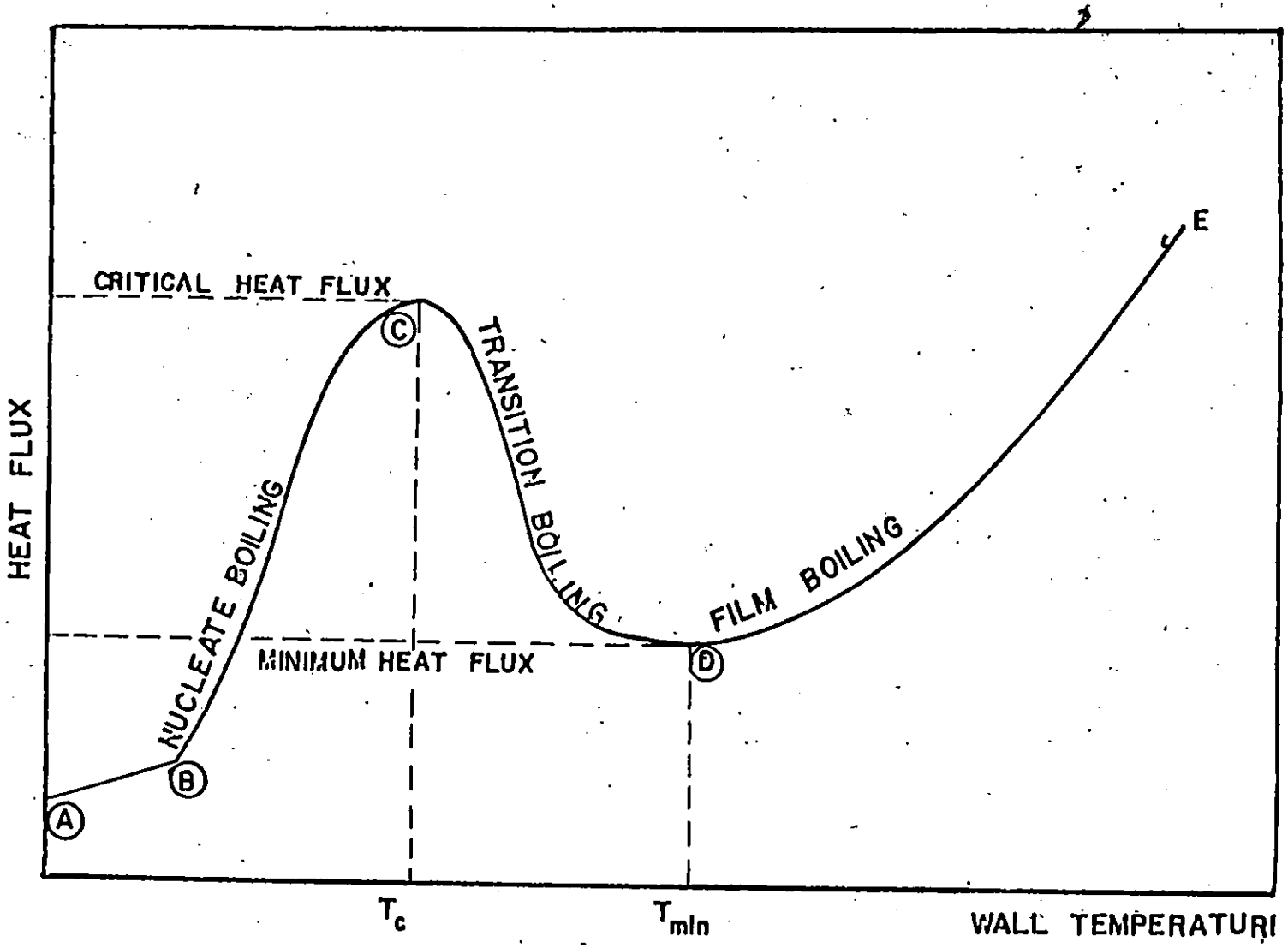

FIG. 1 POOL BOILING CURVE

naturally, to intensify the heat transfer process, causing an upturn in the boiling curve.

3. The transition boiling region CD(the descending branch of surface heat flux), with an increase of surface temperature, characterizing the region between nucleate and film boiling. Berenson [1] has provided a concise description of the transition boiling mechanism: "Transition boiling is a combination of unstable film boiling and unstable nucleate boiling alternately existing at any given location on a heating surface. The variation in heat transfer rate with temperature is primarily a result of a change in the fraction of time each boiling regime exists at a given location." As illustrated in Figure 1, the transition boiling region starts at critical heat flux point (point C) and ends at Leidenfrost point (point D); or vice versa, depending on whether it is heating from nucleate to film boiling or a quenching process, from film boiling to nucleate boiling.

4. The film boiling region DE is where a stable vapour film covers the entire heating surface and vapour is released from the film periodically in the form of regularly spaced bubbles. Heat transfer is accomplished principally by conduction and convection

through the vapour film, with radiation becoming significant as the surface temperature is increased.

5. Maximum heat flux (point C) is where the maximum limit of nucleate boiling is reached. The heat flux at this point is called critical heat flux. There exists a great number of empirical correlations of critical heat flux. Their application, however, is very limited, because many important parameters governing the heat flux are unknown. As a result, most correlations are applicable to a specific geometry, physical and thermal properties of heated surface material, and a certain range of flow parameters.

6. Minimum heat flux (point D) is the lower limit of film boiling, which is determined by analogous physical phenomena, namely the establishment and collapse of a stable vapour film. Liquid-solid contacts, under stable film boiling condition were observed by Bradfield [2], and it was found that the liquid subcooling and surface roughness played important roles in the occurance of contacts. Recently, Fung [3] and Stewart [4] measured the quench temperature (rewetting temperature) under forced convection with different qualities of water and under different pressures, and concluded that

only subcooling and pressure affected the minimum film boiling temperature.

1.2 EVAPORATION IN A VERTICAL TUBE

The study of the evaporation in a vertical tube has attracted most researchers in the boiling heat transfer field. Because of its simple geometry, it is easier to perform experiments and to determine the effect of parameters. The vertical tube has also been widely used in industrial applications. Figure 2 shows schematially the various stages of two-phase flow and boiling during the evaporation of a liquid in a vertical tube as the heat flux is increased. In tube A the heat flux is just sufficient to bring the fluid up to saturation at the outlet. Tube B has twice amount of this heat input, tube C three times and so on. The main features shown on Figure 2 are as follows:

1. Lines of constant quality (x) are shown, and the range of quality covered as the flow passes through the tube is increased as the heat input is increased.
2. The line xx denotes the onset of nucleate boiling. At low heat inputs (tube B), nucleation does not start until the bulk fluid has become superheated. At high heat flux, nucleation occurs near the wall even when $x<0$, corresponding to the onset of subcooled boiling.

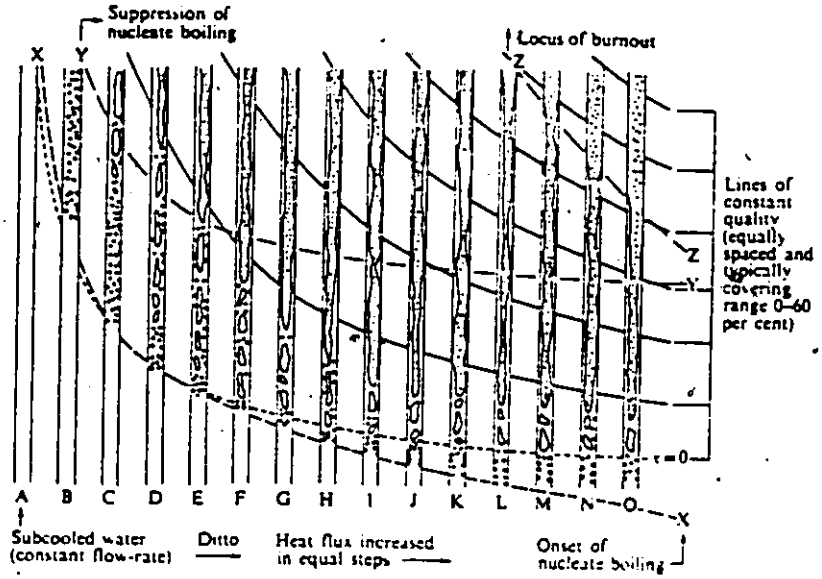

FIG.2 REGIMES OF FLOW AND HEAT TRANSFER

IN A HEATED TUBE

3. It will be seen that the flow patterns develop progressively as the heat input increases. Initially, the bubble flow occurs at the end of a tube, and as the vapour content increases, this changes to slug flow, churn flow, and finally annular flow.

4. As the two phase quality increases, the wall temperature decreases because of improved heat transfer. Ultimately, the wall temperature is insufficient to sustain nucleate boiling and this is suppressed along the line YY. Downstream of this line, the evaporation is filmwise.

5. The liquid film thins along the channel by means of evaporation and entrainment of droplets from it, then the film dries up, giving rise to a region of poor heat transfer. This region is propagated upstream as the heat flux is increased and ultimately penetrates the region of subcooled boiling, where the transition is of a somewhat different nature. This transition, known as 'burnout' is shown as line ZZ on Figure 2.

6. In the region beyond burnout the wall temperature can be very high, and locus VV might be representative of the melting of the tube.

Figures 3, 4, and 5 (Collier [5]) illustrate various aspects of behavior within the regions as shown in Figure 2. Figure 3 shows the various regions of flow and heat transfer as the fluid is evaporated. It also illustrates how the wall and fluid temperature might vary along the channel. Figure 4 shows schematically the various regions of heat transfer as they occur in terms of heat flux and quality. Each horizontal line on Figure 4 represents a given level of heat flux. The variation of heat transfer coefficient with quality at each heat flux level is illustrated in Figure 5. Consider for instance, the variation corresponding to lever (ii). Initially, the heat transfer coefficient is approxmately constant, corresponding to single-phase forced convection heat transfer to the liquid. When the subcooled boiling region is reached, the heat transfer coefficient increases.

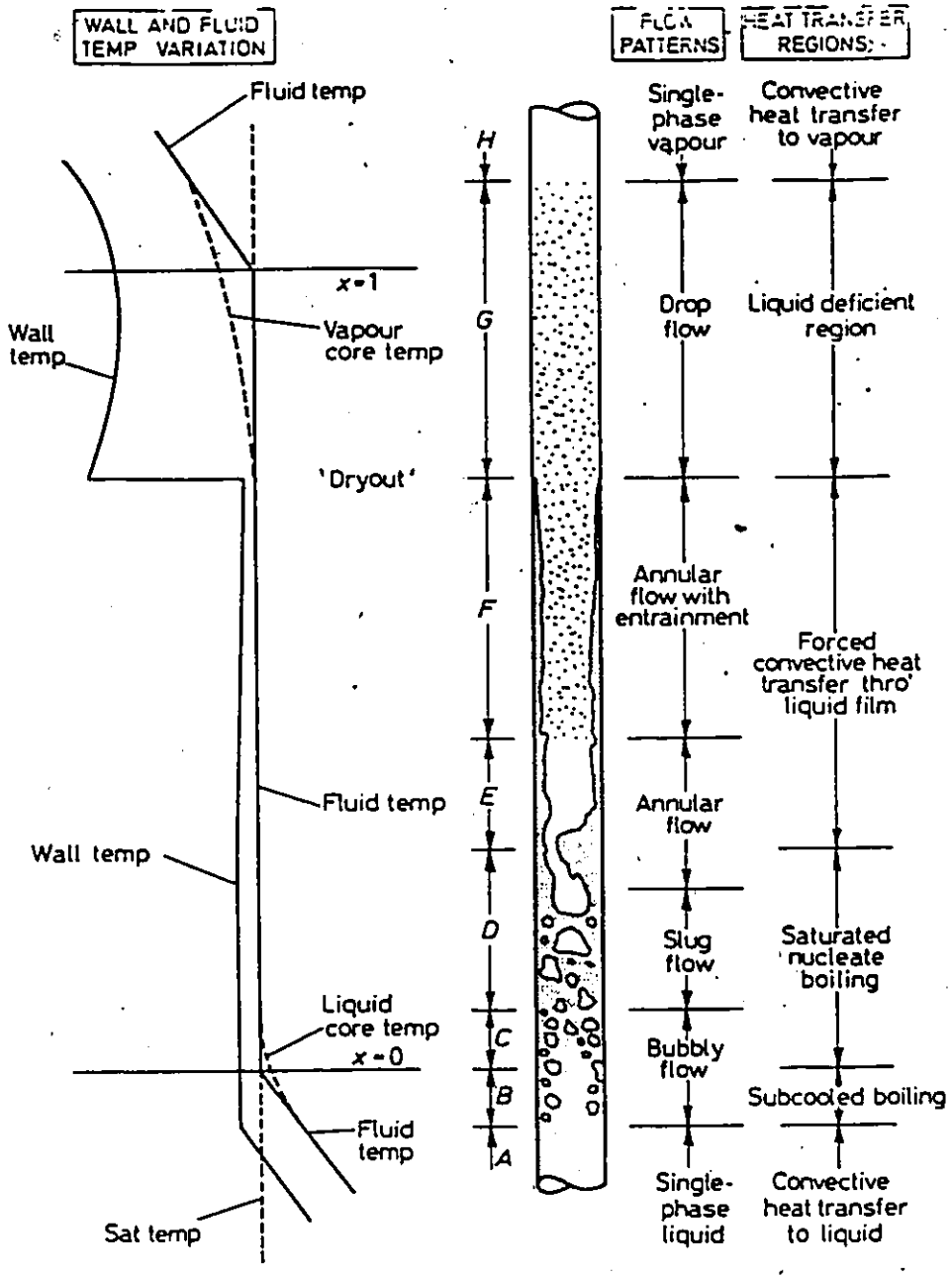

FIG. 3 REGIONS OF HEAT TRANSFER IN CONVECTIVE BOILING

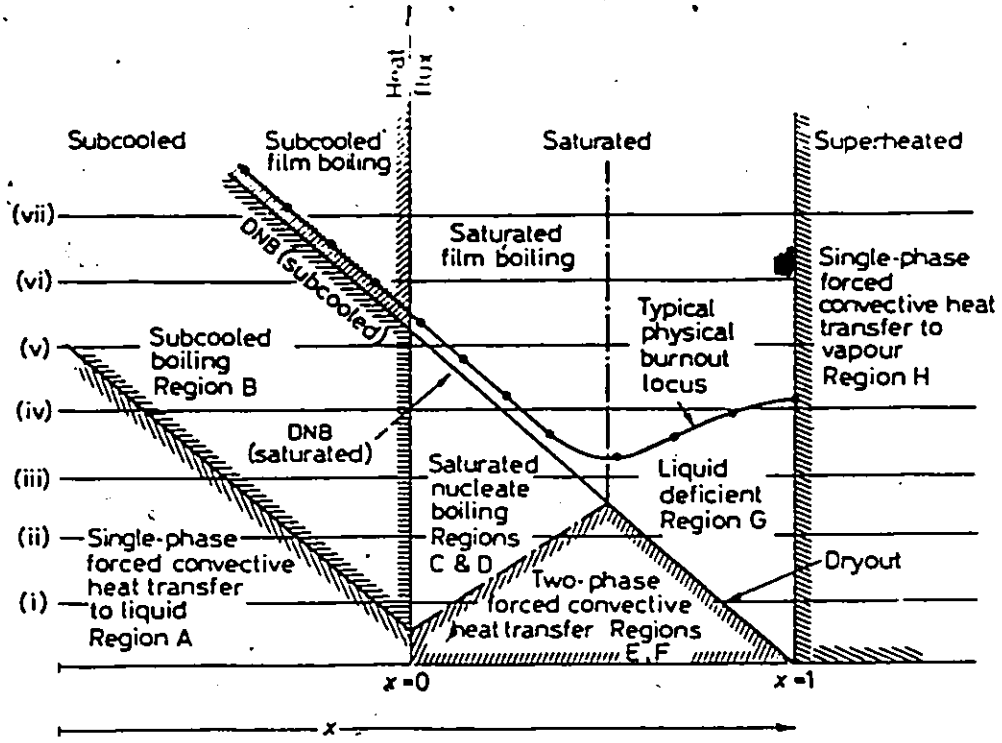

FIG.4 REGION OF TWO-PHASE FORCED CONVECTIVE FLOW

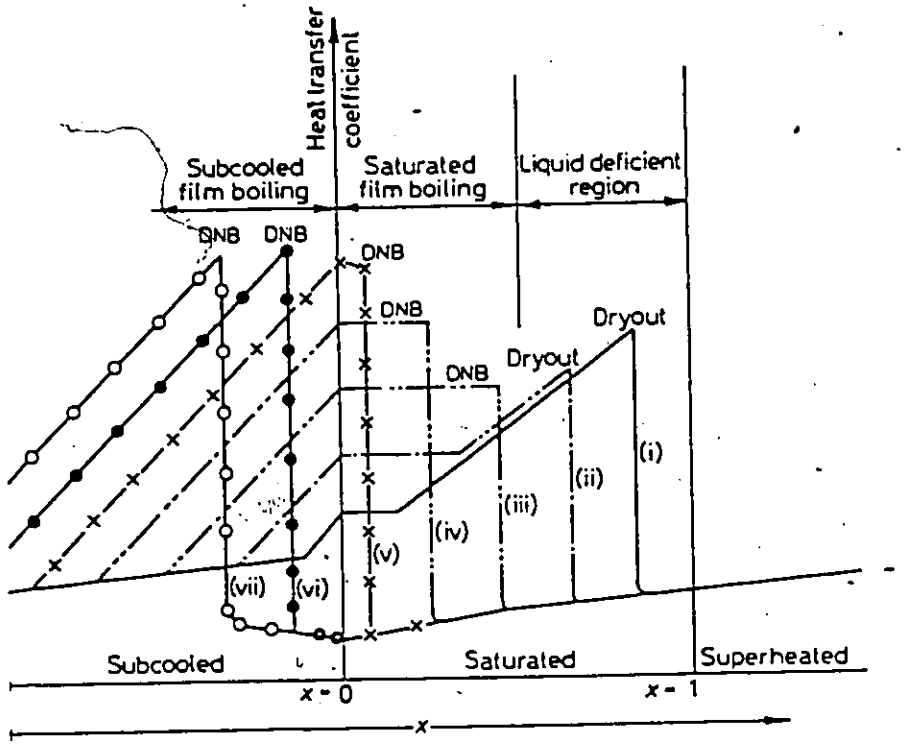

FIG.5 VARIATION OF HEAT TRANSFER COEFFICIENT

Chapter II

LITERATURE SURVEY

2.1 REVIEW OF EXPERIMENTAL STUDIES

2.1.1 Transition Boiling Studies

The most widely used system in forced convective boiling studies is a heat flux controlled system where the heat output of an electrically heated element is increased gradually. Such a system, however, does not permit the measurement of transition boiling data. A variety of temperature controlled systems have been used in transition boiling studies. Some of them are discussed in the following paragraphs.

McDonough et al [6] used NaK liquid (an alloy of sodium and potassium) as heating fluid in a two-fluid system. The liquid flowed along the shell side of test section while the water passed through the Inconel tube with 0.25" OD and 0.049" wall thickness. The test was conducted at pressures of 5.5, 8.0, and 13.7 MPa. From their experiment, the proposed correlation for water in a round tube is

$$\frac{\phi_{BO} - \phi_z}{T_w - T_{DNB}} = 730\, e^{\frac{576}{P}}$$

where ϕ_{BO} is the local burnout flux, ϕ_z is local transition boiling heat flux, P is absolute system pressure in kPa, T_w is local tube wall temperature (°F), and T_{DNB} is the wall temperature predicted by the Jens and Lottes [7] correlation.

Their experiment results indicate that the transition boiling heat flux is dependent upon pressure, burnout heat flux, wall temperature and temperature of departure from nucleate boiling. Once these values are available, the transition heat flux can be calculated. This equation can only apply to the pressure range of 5.5 to 13.7 MPa (800 to 2000 psia). Since the burnout heat flux and T_{DNB} depend on mass flux and pressure, the transition heat flux is affected by pressure as well as by mass flux. Their major aim was to study the prediction of transition heat flux at the pressure range mentioned above. They concluded that the observed data were within 35% of prediction, but the pressure effect was not mentioned.

Weisman et al [8] used the same method as McDonough's, but the heating fluid was mercury instead of NaK. Pressurized water passed through a 1.02 cm ID tube with 50 cm heated length. The experiment was conducted at pressure of 1.72 to 5.17 bars and mass flux from 19 to 190 kg/m^2 sec. The transition heat flux data, which agreed reasonably with

their previously proposed correlation [9], indicated that the transition heat flux increased with mass flux and pressure within their experimental range.

By using a stabilizing secondary coolant inside of an electrically heated tube, Ellion [10] was able to obtain transition data with water as a test fluid at pressures between 115 and 400 kPa and liquid velocities from 0.34 to 1.52 m/sec. High pressure water, as stabilizing fluid flowing inside of 2.25" ID tube with 3" heated length, was used to avoid a dryout temperature excursion. Once the water temperature, power supply, stabilizing fluid temperature and heat transfer coefficient were known, the transition heat flux of test fluid could be calculated. One criterion must be met for this experiment: The gradient $(\frac{d\phi}{dT})$ of stabilizing coolant should be greater than the absolute slope of actual boiling curve at transition regime. The choice of stabilizing fluids which have sufficiently high transport properties is very limited. Hence, the flow parameters of transition boiling are restricted by using Ellion's method.

More recently, Cheng et al [11] obtained the transition boiling data by a transient method. The test section basically consisted of a high thermal inertia cylindrical block (copper or brass), with or without a flow tube

(Inconel, stainless steel, or zircaloy) located along the centre bore. The block was heated by cartridge heaters inserted in copper block at some distance from the centre of the flow channel. By quenching the heated block with water at atmospheric pressure, the transition boiling data were obtained for mass flux from 68 to 203 kg/m^2sec and subcooling from 0 to 27.8°C. Their experimental results concluded that the transition heat flux increases with mass flux and inlet subcooling, but decreases with $k\rho C_p$ of wall material.

2.1.2 Minimum Film Temperature Measurement Studies

A number of experiments for the rewetting temperature and minimum film boiling temperature have been conducted.

Bradfield [2] observed liquid-solid contacts under stable film boiling conditions in his experiment. It was found that the liquid subcooling and surface roughness played important roles in the occurence of contacts. The liquid-solid contact behavior of water and ethanol on flat horizontal copper and stainless steel surfaces at elevated pressure was also investigated by Yao et al [12]. In their experiment, the minimum film boiling point was determined by an increase in the rate of cooling as the wall temperature decreased and by visual observations as well. Figures 6 and

7 show their results comparing with others. There was no conclusive relationship between the minimum film boiling temperature and the system pressure.

Dua [13] studied the rewetting of a copper tube by a falling film of liquid nitrogen. The measured rewetting temperature was found to be very close to the Leidenfrost temperature of liquid nitrogen on a copper surface. His experimental results indicated that the rewetting temperature was not dependent upon the mass flow rate. Lee et al [14] studied the propagation of rewetting by flooding the heated channels. They concluded that the measured quenching temperature was affected by propagation of rewetting front, and therefore was not the true rewetting temperature.

Recently Stewart [3] and Fung [4] developed a steady state film boiling method, with which axial conduction could be eliminated. They both concluded that the minimum film boiling temperature decreased as the quality in the subcooled region increased. At high quality, the minimum temperature remained relatively constant. Stewart claimed that it could also measure the true quench temperature. He also found that there was no effect due to mass flux, and the minimum film boiling temperature superheat decreased slightly as pressure increased for pressure less than 4 MPa and quality larger than -0.04.

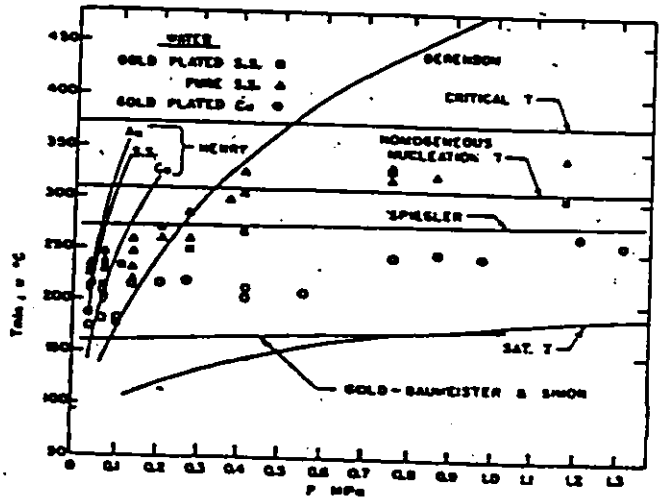

Fig-6 Measured film boiling wall temperatures for water on various surfaces

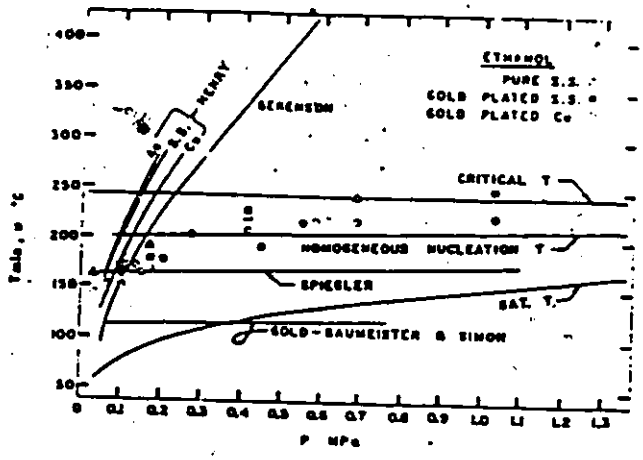

Fig. 7 Measured minimum film boiling wall temperatures for ethanol and various surfaces

2.2 USE OF ELECTRIC PROBES IN TWO PHASE FLOW EXPERIMENT.

There are basically two types of electrical probes to measure the conductance and the capacitance. The probes can be used as measuring techniques in studies of two-phase flow behavior.

2.2.1 Conductance Probe.

The most common and convenient electrical probes are those of the conductance type. The conductance to be measured can be either between a single electrode in the flow and another electrode on the wall, or between two electrodes both located in the stream.

2.2.1.1 Two Electrode Method

The two-electrode conductance probe is used to detect the bridging of two electrodes by a drop. Thus, the chief application is for droplet flow. By varying the distance between the two electrodes, it is possible to determine the drop sizes which are larger than the span between the probes.

Hewitt [15] used an electric probe (conductance type) to determine the average value of the film thickness in upwards annual flow of air-water mixture. The conductance increased

with increasing film thickness. Figure 8 shows this arrangement along with a calibration cell.

2.2.1.2 Probe-to-Wall

Through the use of an electric conductance probe, Griffith [16] investigated the location of transition between slug flow and annular flow. His probe as shown in Figure 9 was used to determine the electrical resistance between the centre of the pipe and the wall. The probe was used to determine whether or not there were bridges of liquid across the channel.

With an arrangment similar to that of Griffith, Ragheb [17] used the zirconium-platinum probe (as shown in Figure 10) to detect the flow pattern on the vertical heated wall. Tests were conducted for water at atmospheric pressure under flow boiling conditions with G, mass flux, varying from 34 to 102 kg/m^2 sec. and ΔT_{sub}, inlet subcooling, varying from 0 to 28°C.

Yao and Henry [12] examined the area and duration of liquid-solid contacts in the film boiling of saturated ethanol and water on a horizontal, flat, stainless steel and copper surface with electrical conductance probes. It was observed that, at the atmospheric pressure, contacts occurred over a wide temperature range, and at the elevated

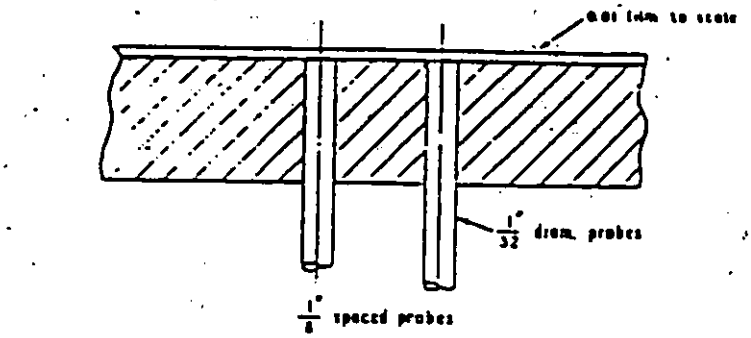

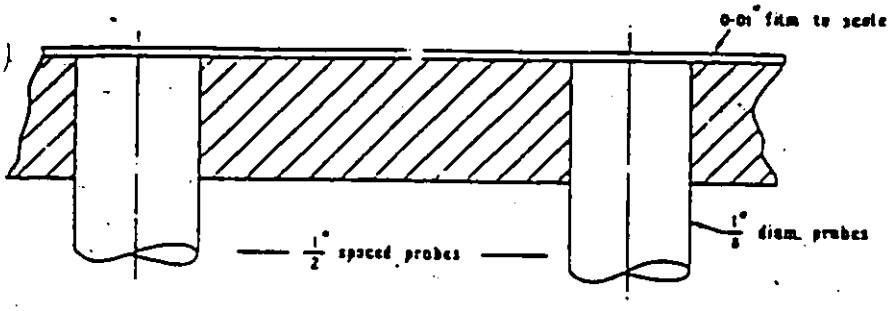

SCALE DRAWING OF $\frac{1}{8}$" AND $\frac{1}{2}$" SPACED PROBES COVERED BY 0·01" FILM.

A.E.R.E.-R.3921

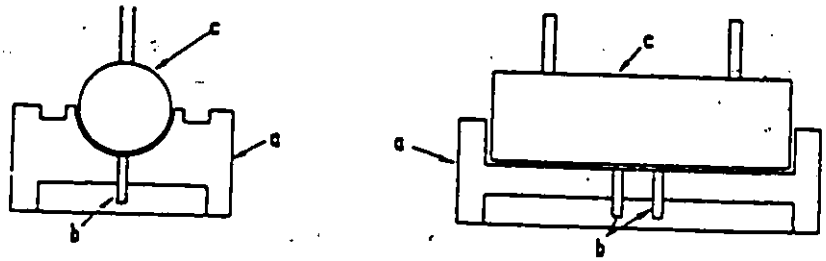

CONSTRUCTION OF FILM THICKNESS CALIBRATION CELL.

A.E.R.E.-R.3921

a- 1.750" Dia. perspex trough
b- Electrodes
c- 1.748" Dia. rod

FIG.8 TWO-ELECTRODE MEASUREMENTS

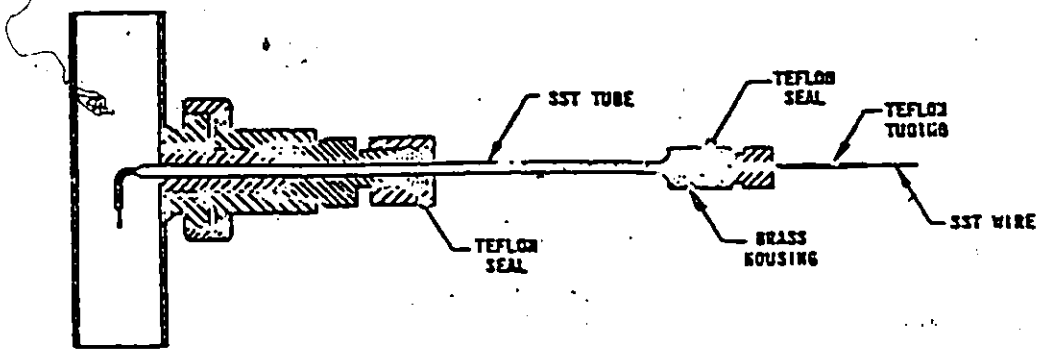

Probe Detail

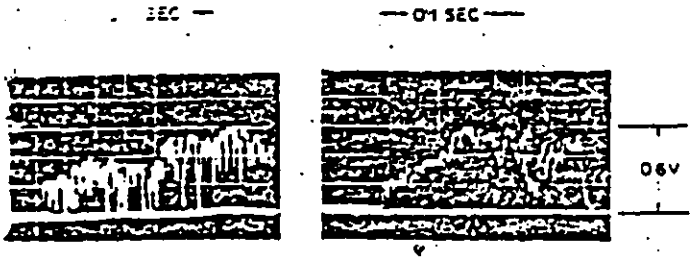

Typical slug-flow traces. Annular flow is simply a straight line on the lower axis

FIG.9 PROBE-TO-WALL MEASUREMENTS

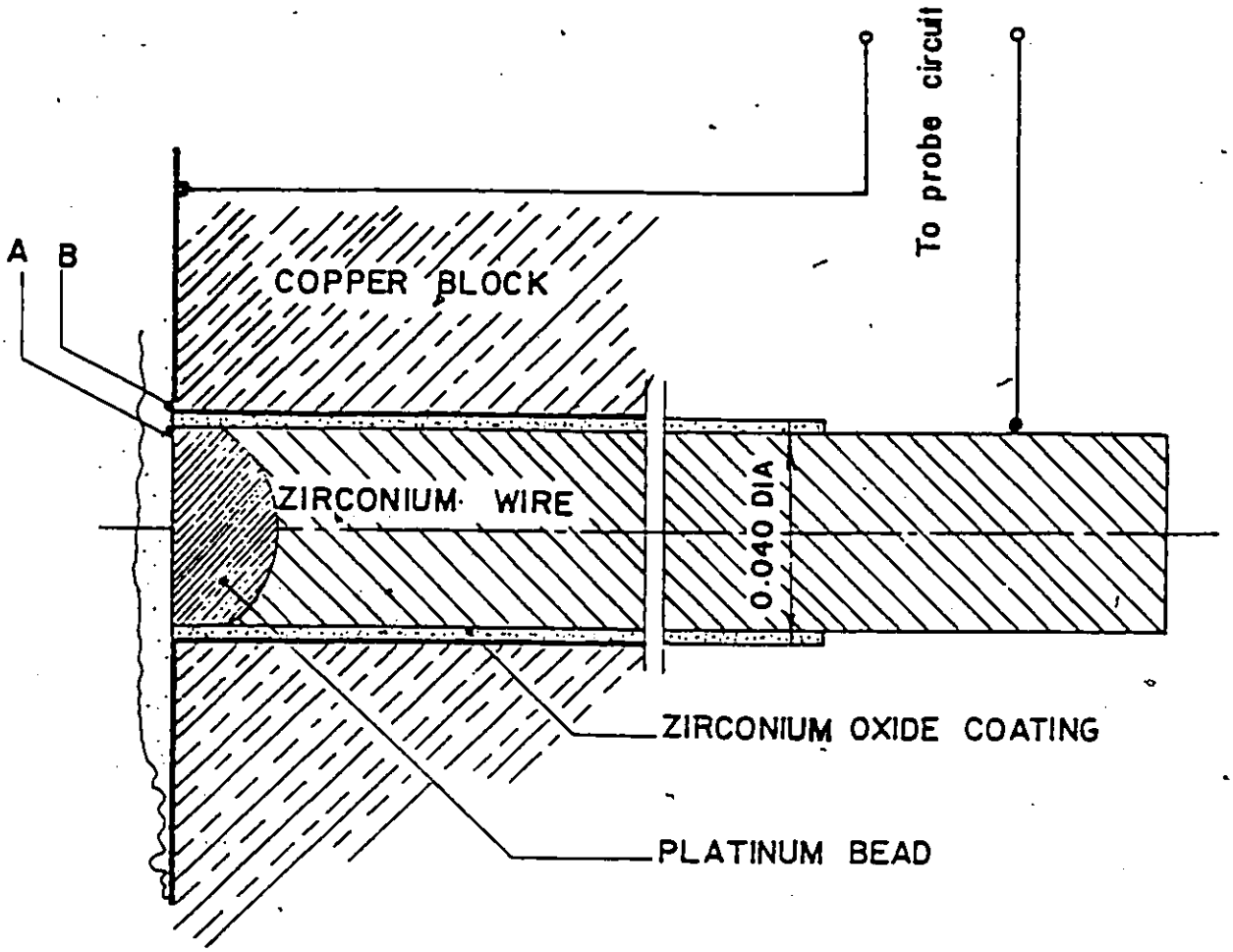

FIG. 10 THE ZIRCONIUM-PLATINUM PROBE

pressure, direct liquid-solid contacts in film boiling were essentially non-existent.

2.2.2 Capacitance Probe

The capacitance probe can measure the void fraction as well as film thickness.

2.2.2.1 Void Measurement

The void measurement method was developed by Bencze and Orbeck [18] to measure void distribution in different geometries. The arrangement and its circuit is shown in Figure 11. There are two concentric or parallel plated electrodes. These electrodes are supplied by a high frequency potential, and the potential is balanced in a bridge circuit while the sensing tip or plate is completely in water. Whenever the sensing electrode contacts with or is very close to a bubble, its electrical capacitance will be altered and the bridge will be thrown off balance. This trigger, an electronic circuit, registers the number of periods of the alternative current during the time that the needle tip is in contact with vapor. In this manner the local void is obtained by the following relation

$$\alpha = \frac{n}{t\, f_o}$$

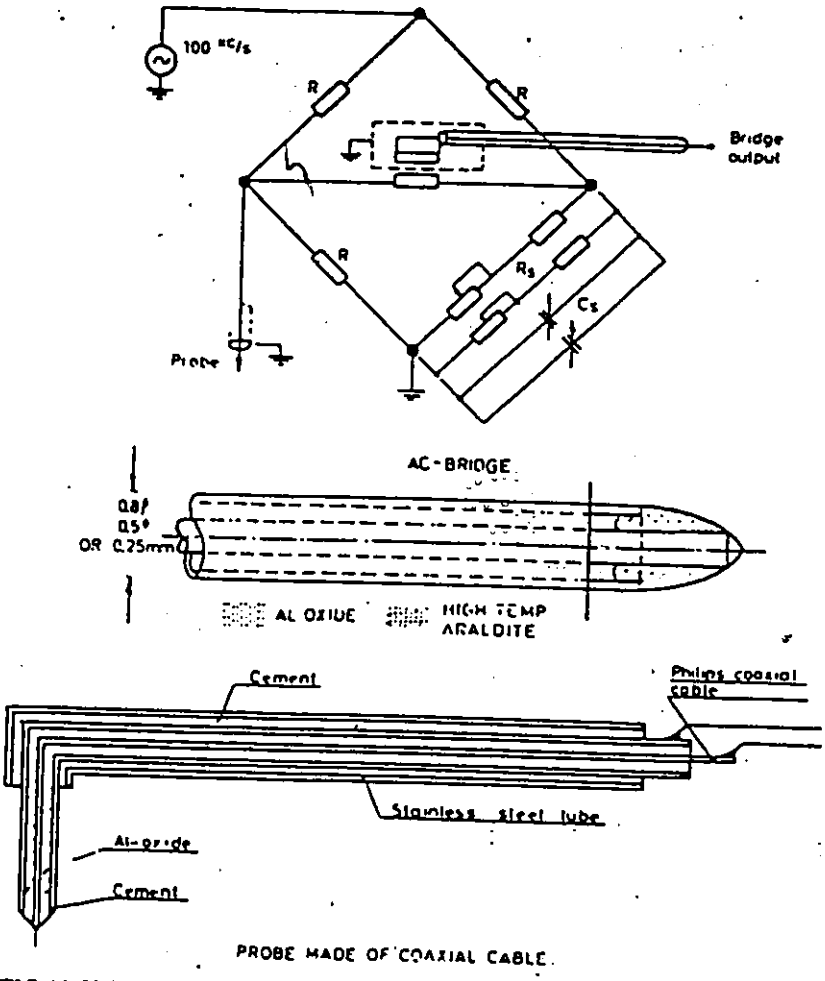

FIG. 11 Void needle with double electrodes and the capacitance measuring circuit

in which n is the total number of pulses registered during time t and f_o is the constant frequency of the supplied potential.

2.2.2.2 Film Thickness Measurement

The method for measuring the film thickness and wave profile of falling films has been used by Dukler and Bergelin [19] and by Tailby and Portalski [20]. The capacitance between the wall and a small parallel plate at a known distance from the wall was determined. The void between the conduction liquid and the small plate could then be computed from the measured capacitance. The average liquid annulus thickness is deduced from the computed gap thickness and total distance between the plate and the wall.

Chapter III

EXPERIMENTAL APPARATUS AND PROCEDURES

3.1 GENERAL

The present project consists of measuring transition boiling in a circular tube under low pressures as well as measuring the rewetting temperature via a probe in single and multi-rod geometries at atmospheric pressure. The experimental procedures and their major components will be described in the following paragraphes.

3.2 PRESSURIZED LOOP FOR TRANSITION BOILING

The transition boiling experiment is conducted in a pressurized containment apparatus which can operate at the pressure up to 1372 kPa. The system is pressurized by argon gas. Figures 12 and 13 are the preliminary and final loop configurations. There were some change as the experiment carried on. In the pressurized loop, the space in the hot tank was too small. Therefore, during quenching the vapour pressure built up in the system. In order to alleviate the pressure build-up, the top of surge tank was connected to the hot tank to provide more space. Another problem of the

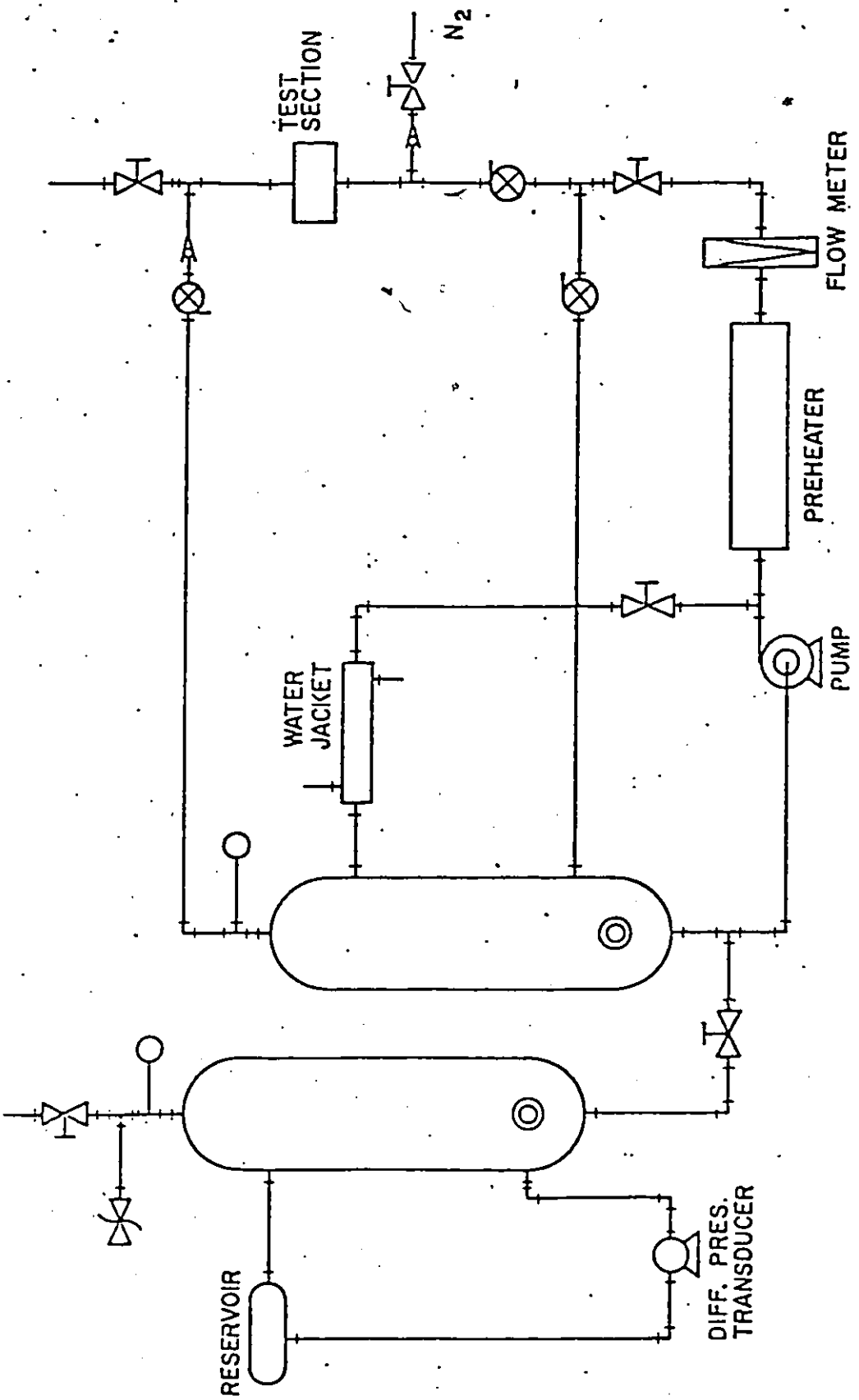

FIG.12 PRELIMINARY DESIGN FOR PRESSURIZED LOOP

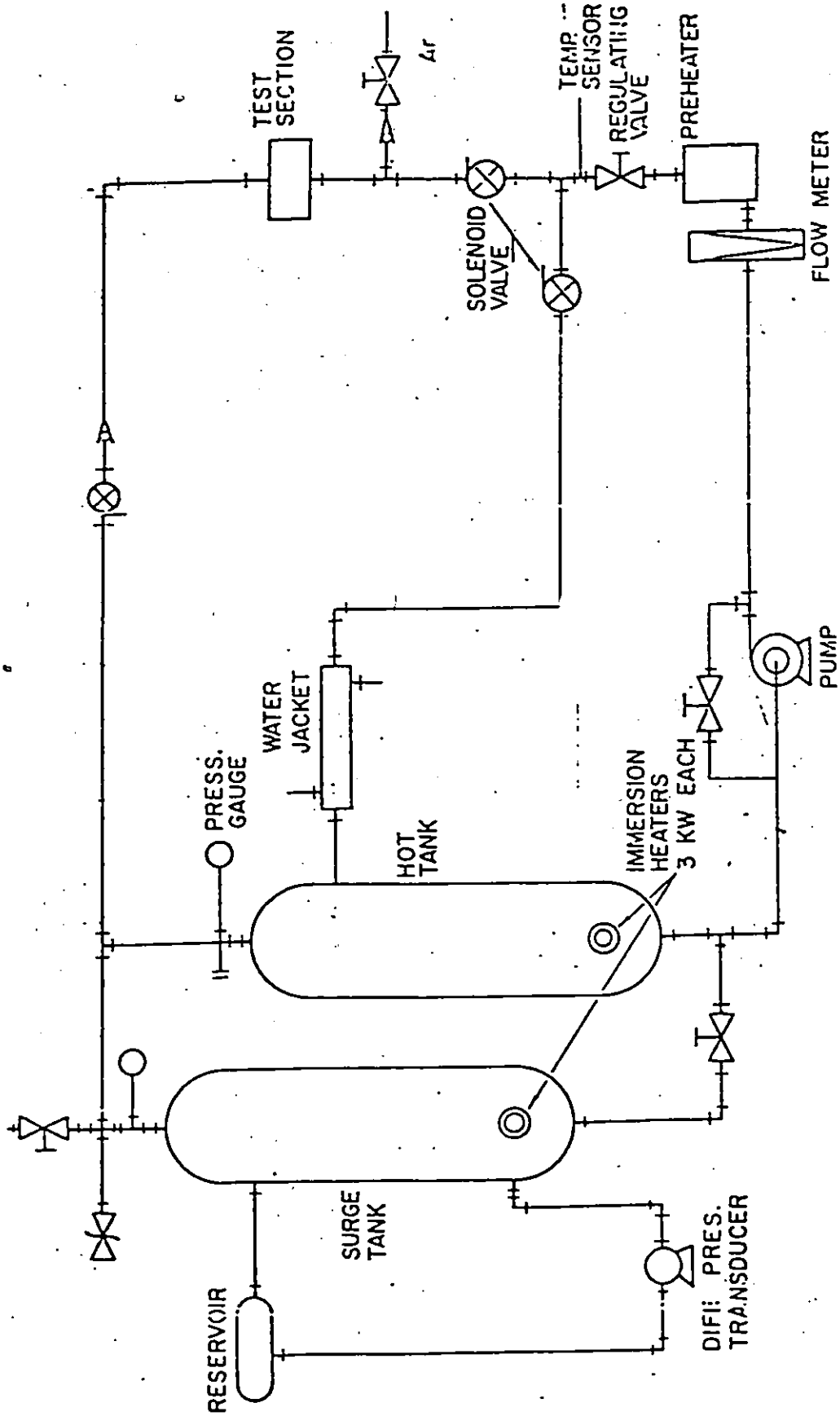

FIG.13 PRESSURIZED LOOP

system in the original design was the oversized preheater. When water was heated, the vapour accumulated inside the preheater. It caused the oscillation which was observed at the flow meter. To correct the problem, the size of preheater was reduced. A water filter was installed to protect the test section from foreign substances which might cause corrosion of test-section surface. Figure 14 to 16 show the general view of the experimental apparatus, test section and control panel, respectively.

3.2.1 Flow Loop

Figure 13 is a schematic flow diagram showing all the important components that complete the test loop. These include a surge tank, hot tank, pressure gauge, pump, preheater, water filter, flow meter, temperature sensor, test section and the associated valves and piping.

The pressure in the system is measured by the pressure gauge which has been calibrated before the experiment was conducted. Two identical stainless steel tanks (surge and hot) are of 5 gallons capacity each. The overall dimensions are about 35" high and 7" in diameter. The hot water tank is powered by a 3-kW immersion heater drawing current via a thermostat that can be adjusted to the desired water temperature.

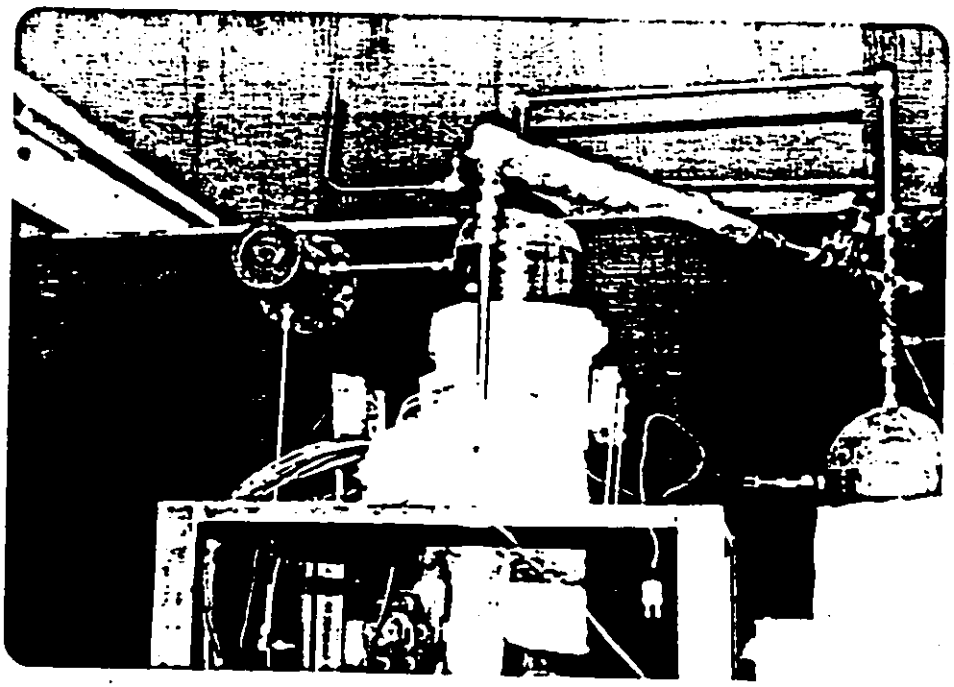

FIG.14 TEST SECTION

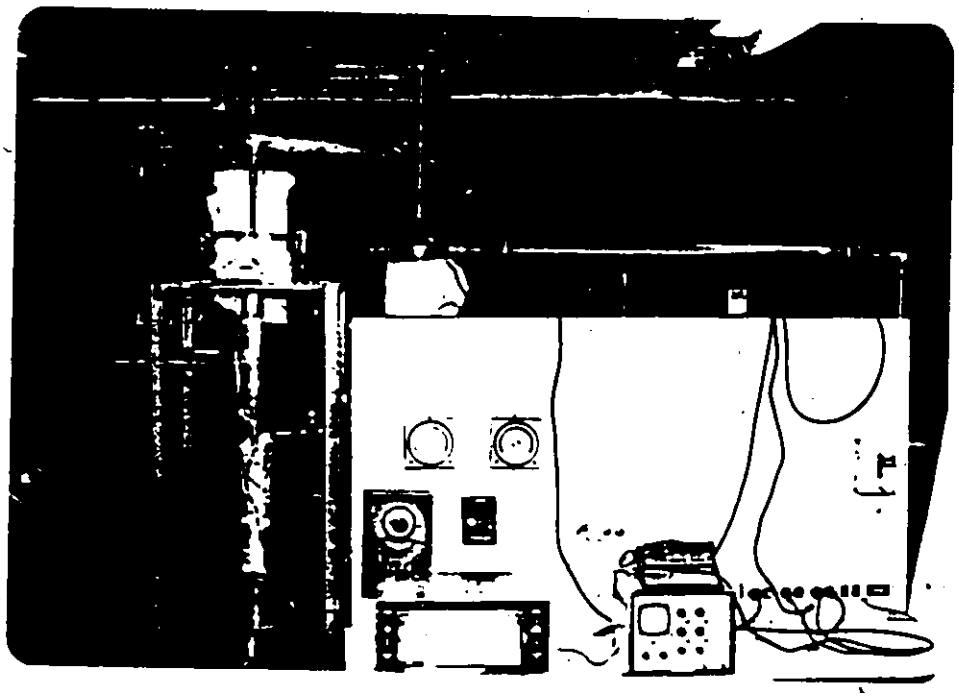

FIG.15 GENERAL VIEW

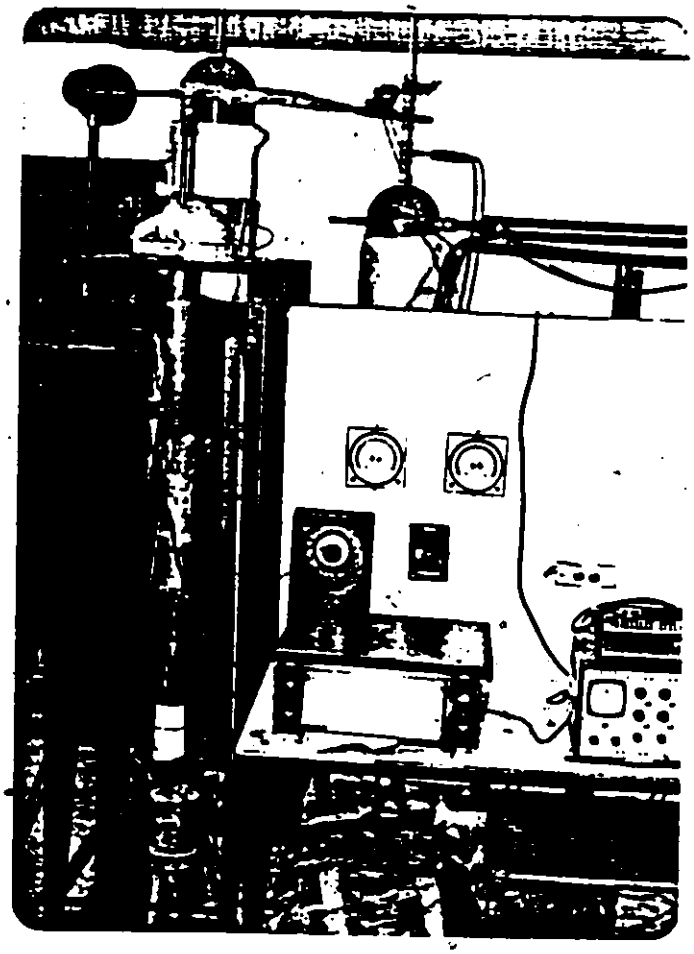

FIG. 16 FLOW LOOP

All the connecting pipings are of 1/2" diameter 304 stainless steel tube with 0.040" thickness and 1" diameter copper pipe of 0.060" thickness. Copper is a good conductor; therefore, it is used in the water jacket heat exchanger. Stainless steel tube is used prior to and after the test section in order to reduce the heat loss of water. In order to accommodate various connection sizes in pump, valves, and flow meter, some reducers and adapters are used in those connections.

Valve and tube fittings are of Swagelok design; Swagelok tube fittings provide a leak-proof, torque free seal at all tubing connections. The seal consists of two (front and back) ferrules. They grasp tightly around the tube, regardless of wall thickness by ferrules interaction. Since this interaction moves along the tube axially instead of a rotary motion, (free of torque that might otherwise impact onto tubings), ferrules provide a leak-proof seal under pressure up to the burst of the tubing. Valves and fitting are all rated by manufacturer to a higher limit than the present operating condition.

Water is circulated by a 1/4 HP centrifugal pump from the hot tank passing through by-pass or test section and drained back to the tank. The flow rate is measured by a rotameter and controlled by a regulating valve. There are two by-pass

loops, namely, pump by-pass and test section by-pass. The pump by-pass is to stabilize the flow when the regulating valve is adjusted. The test section by-pass is to have water passing through it instead of test section in order to check the required inlet water temperature and to maintain the flow rate. Along the test section and its by-pass loop, there are two Solenoid ON/OFF valves. They are controlled by one switch. Either the test section valve is open or by-pass valve is open. These valves are also one-way valves to guarantee no back flow.

3.2.2 Test Section

A typical Inconel-copper or stainless steel-copper composite test section as shown in Figure 17 consists of a long Inconel or stainless steel tube and a copper block. The copper block is used in this experiment because of its high thermal capacity for energy storage, and because of its high thermal conductivity. It is able to minimize thermal gradients in the test section, thus ensuring that the boiling heat flux at the surface is not limited by conduction within the test section. Physical dimensions of the test section along with the thermocouple locations are given in Figure 13. The tube (Inconel or stainless steel) with 1/2" outside diameter is soldered into 0.514" diameter center bore of copper block with silver solder (melting

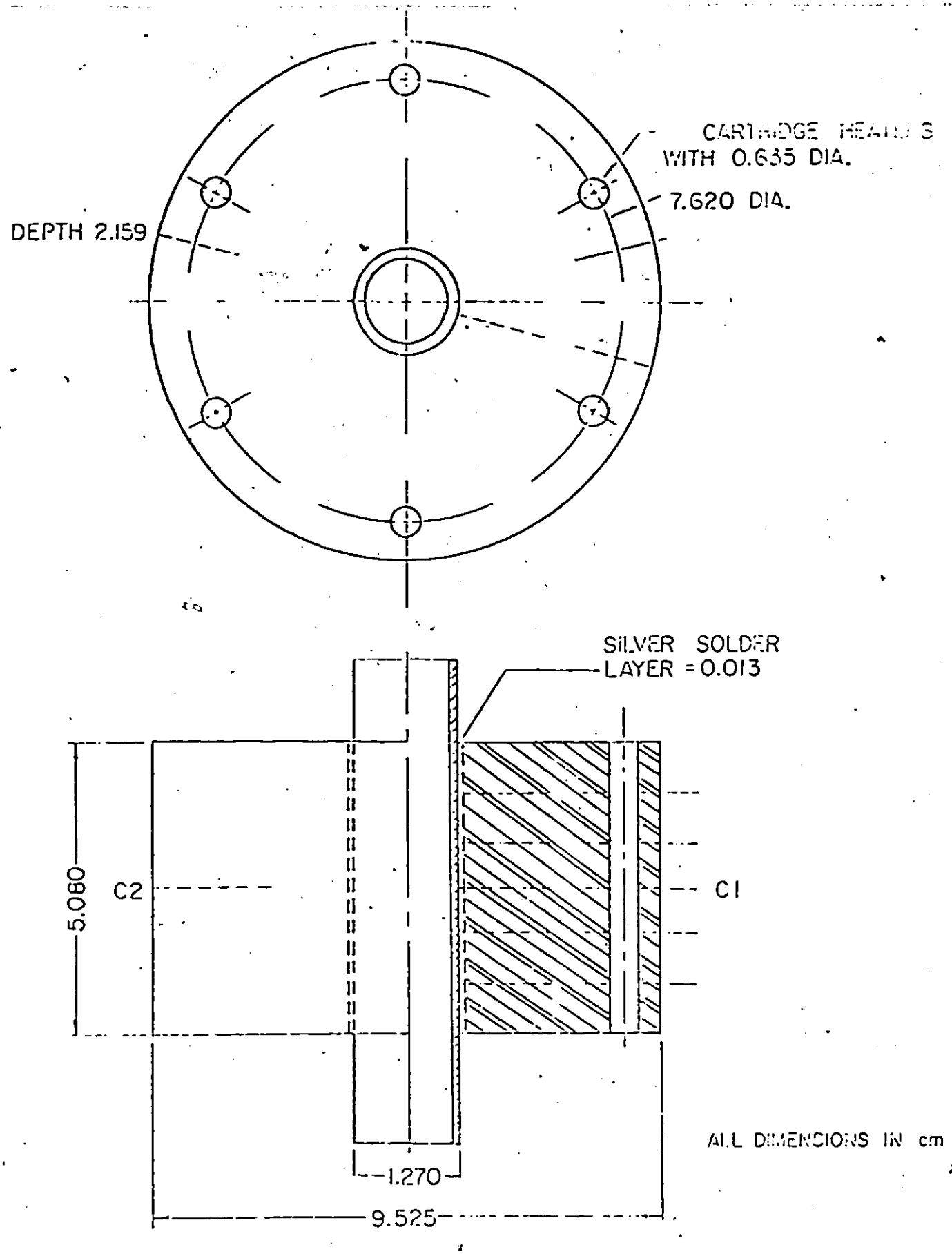

FIG.17 TEST SECTION

temperature 680°C). Heating of the test section is accomplished by using six cartridge heaters (1/4" diameter and 250 W). Two thermocouples are soldered on the outer surface of the tube 180° apart passing through the copper block. The entire test section is insulated with high temperature ceramic fiber.

3.2.3 Experimental Procedure

1. The system is first pressurized up to 90% of the desired operating pressure by introducing argon gas.
2. Water in the hot tank is heated to the required testing temperature by an immersion heater which is thermostatically controlled. As the water temperature rises the pressure in the system increases slightly.
3. The pump is turned on to circulate water around the flow loop and the flow rate is adjusted. The flow is passed through the test section by-pass and drained back to the hot tank.
4. The preheater, which is also thermostatically controlled, is set to the required inlet water temperature.
5. The test section is heated to about 600°C with cartridge heaters in the copper block. During heating, a small amount of argon gas is introduced to minimize the oxidating of the inner wall of test tube.

6. The system pressure is rising to the targeted operating value because of steps 2 and 5. As a self checking procedure, before the quenching test starts, the system pressure, flow rate, and the inlet water temperature are checked to make sure that they are at the operating conditions.
7. The thermocouples at the wall of tube are connected to the Fluke B2340 data logger and a chart recorder.
8. The solenoid valve switch is turned to the ON position for the flow passing through test section; automatically the flow to the by-pass would be OFF.
9. The data logger and the chart recorder have been already operated at the beginning of each test.

3.3 PROBE EXPERIMENT FOR REWETTING TEMPERATURE

The experimental investigation of quenching by an electric resistance probe in a single rod (annulus test-section) and 3-rod test sections is conducted at atmospheric pressure.

3.3.1 Flow Loop for Probe Study

Figure 18 is a schematic flow diagram which is slightly modified from the previous pressurized loop. Instead of surge and hot tanks, a large supply tank is used, therefore,

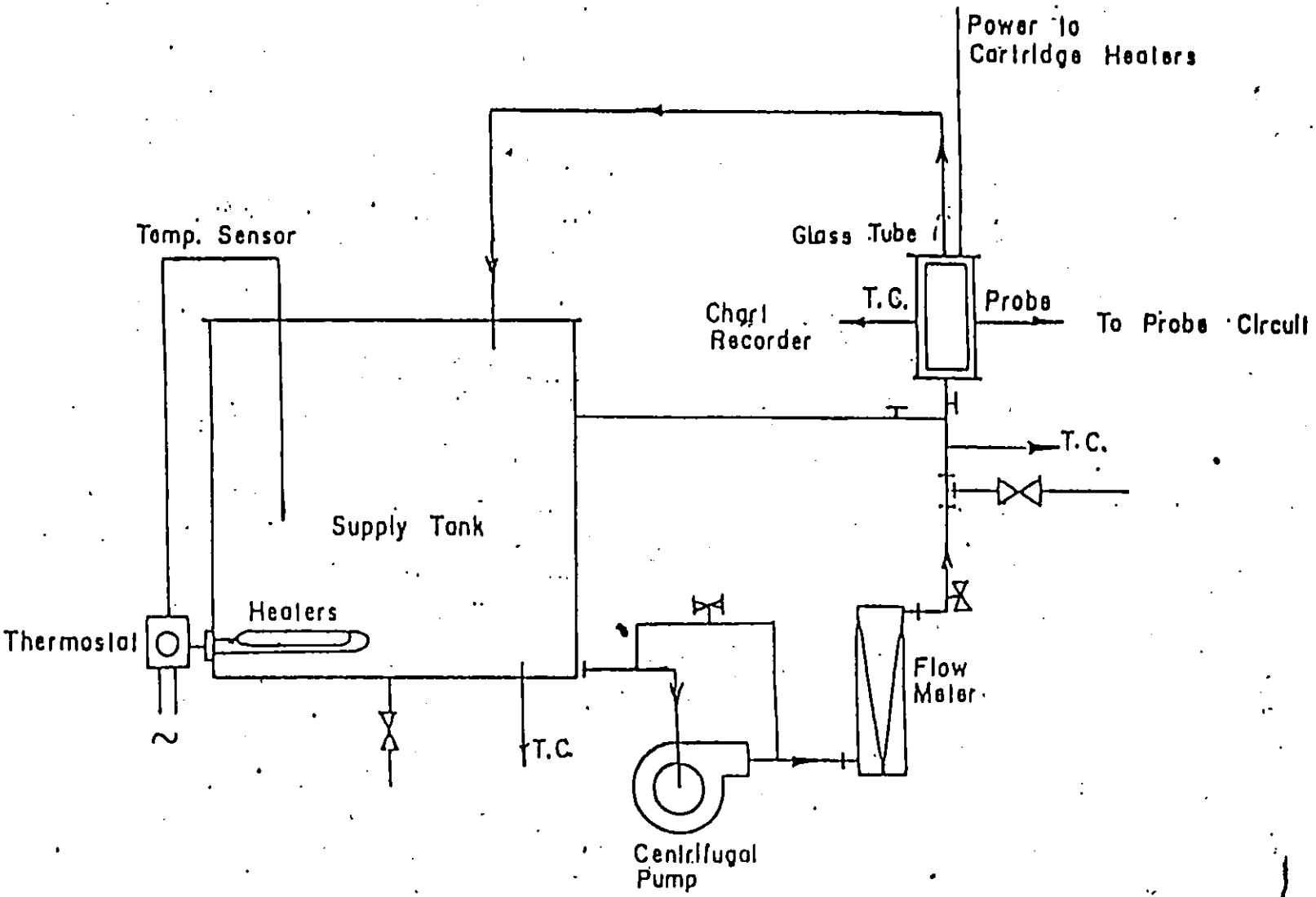

FIG.18 SCHEMATIC DIAGRAM OF FLOW LOOP

the heat exchanger is not necessary. There are three 3-kW immersion heaters to heat the water in supply tank. The rest of components are similar to the pressurized loop.

3.3.2 Single Rod Test Section

The annulus transparent section assembly is shown in Figure 19. The test section consists of a 3/4" diameter pyrex tube and a 1/2" diameter copper rod which are arranged in a concentric manner. Two data thermocouples are embedded length-wise in the copper rod to a depth of 0.020", with extension leads coming out at the top end of the copper rod via an Inconel tube. The method of mounting the copper rod is shown in Figure 20. The supporting end of the copper rod is threaded to a stainless steel tube which is also the cartridge heater leads outlet. The whole test-section assembly with Inconel and stainless steel tubes attached to top and bottom ends, respectively, is Swagelok mounted.

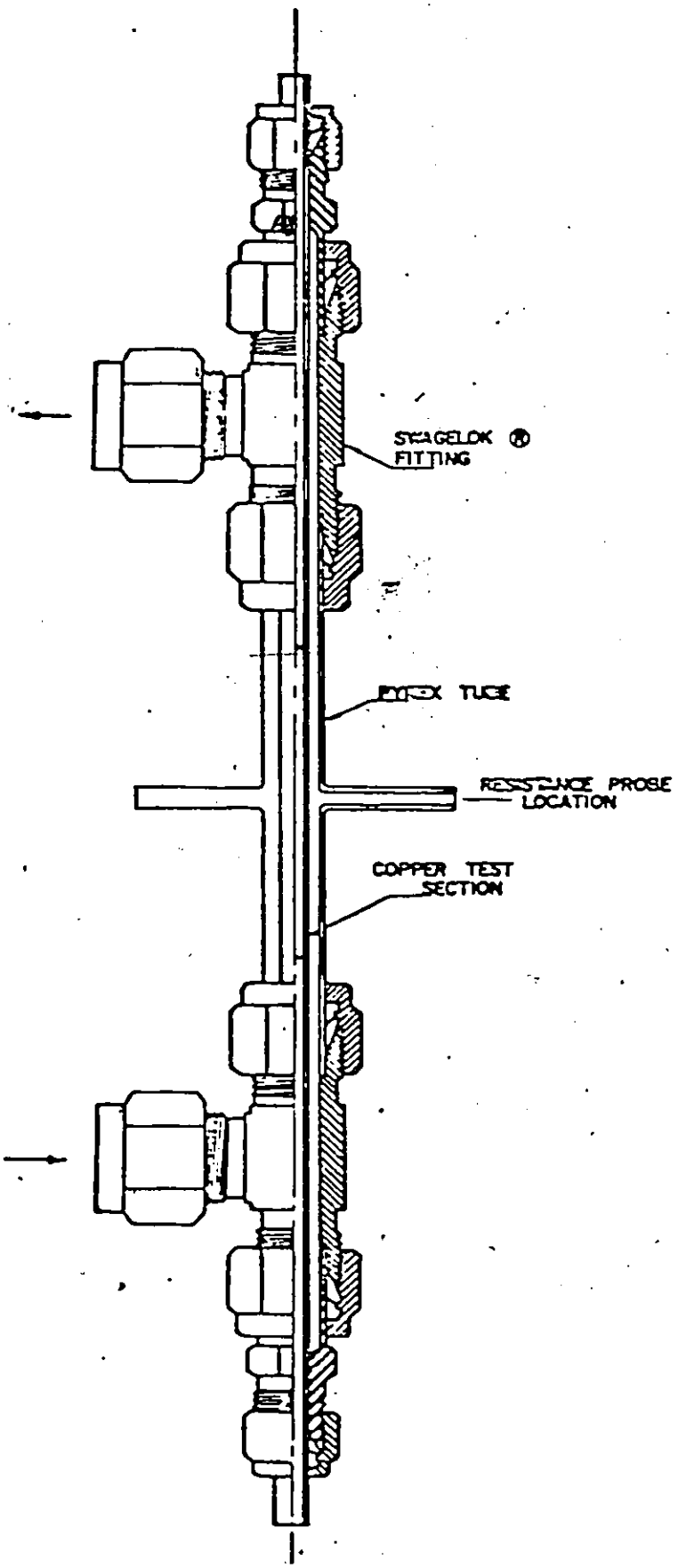

FIG.19 ANNULAR TRANSPARENT TEST-SECTION

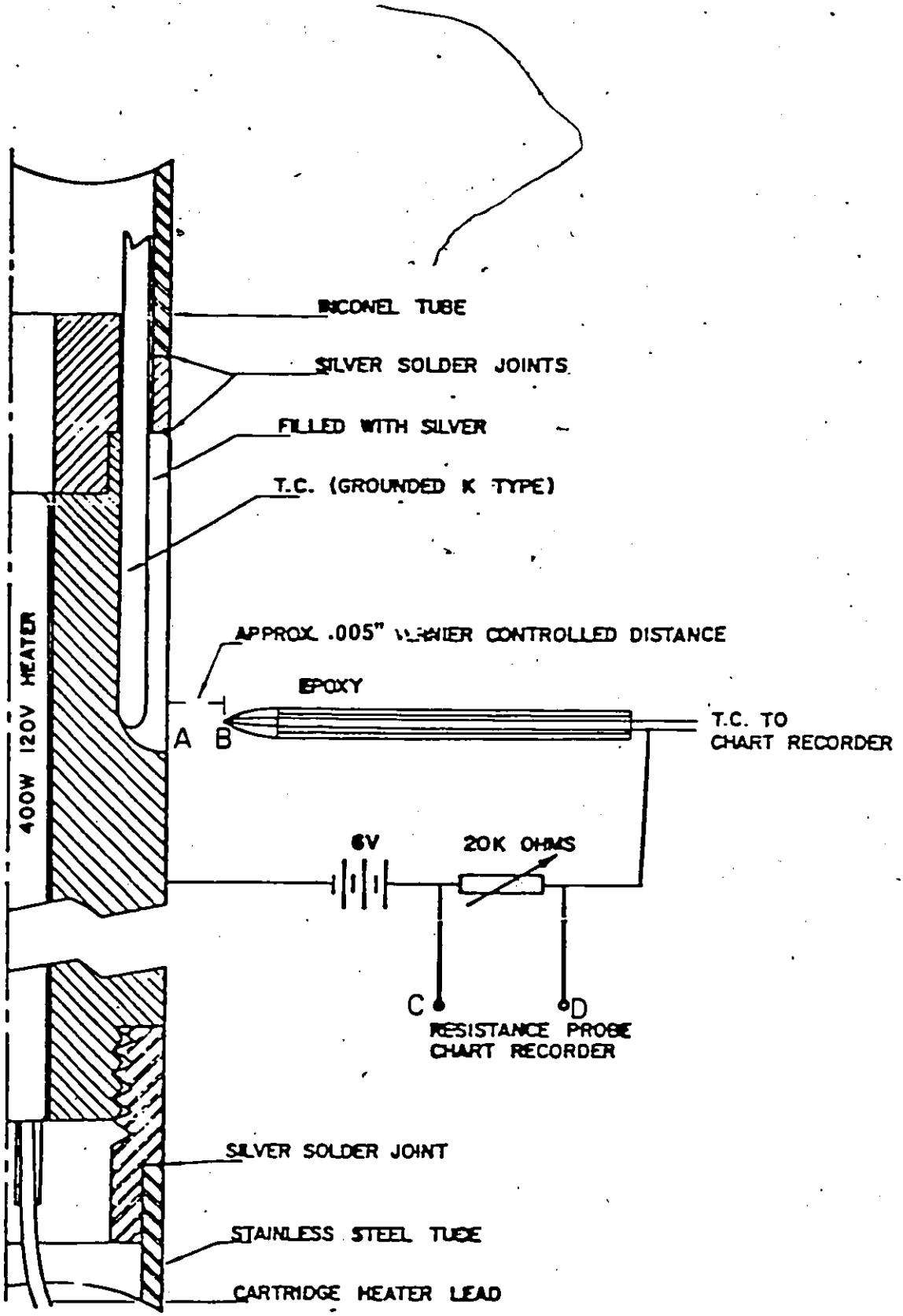

FIG. 20 PROBE CONFIGURATION

3.3.3 3-Rod Bundle Test Section

This test section consists of three single rods which are made in the same way as single rod test-section. Three rods are placed on a special end connections shown in Figures 21, 22 and 23. At the bottom end of connection, a cone-shaped end connector is designed in order to minimize the entrance effect.

3.3.4 Probe and its Circuit

Electrical connection of the electric resistance probe is shown schematically in Figure 20 and it is placed directly opposite to the data thermocouple. For the 3-rod bundle, one probe is placed at the smallest gap between pyrex tube and one of the rods; the other is placed at 180° from the first one. These are called inside probe and outside probe, respectively (see Figure 24). The probe itself is made up of thermocouple wire with sheath stripped off. Welded junction and exposed wires are encapsuled by epoxy for added strength. The probe circuit is shown in Figure 20 which includes a 6-V battery and 20 K ohm resistor. The probe measures the electric resistance between the tip of probe and the wall of the rod. If the wall is dry, the resistance across A B is infinite and a small voltage drop will registered across C D. Similarly, if the wall is wet, the resistance is finite and a large voltage drop across C D is noticed.

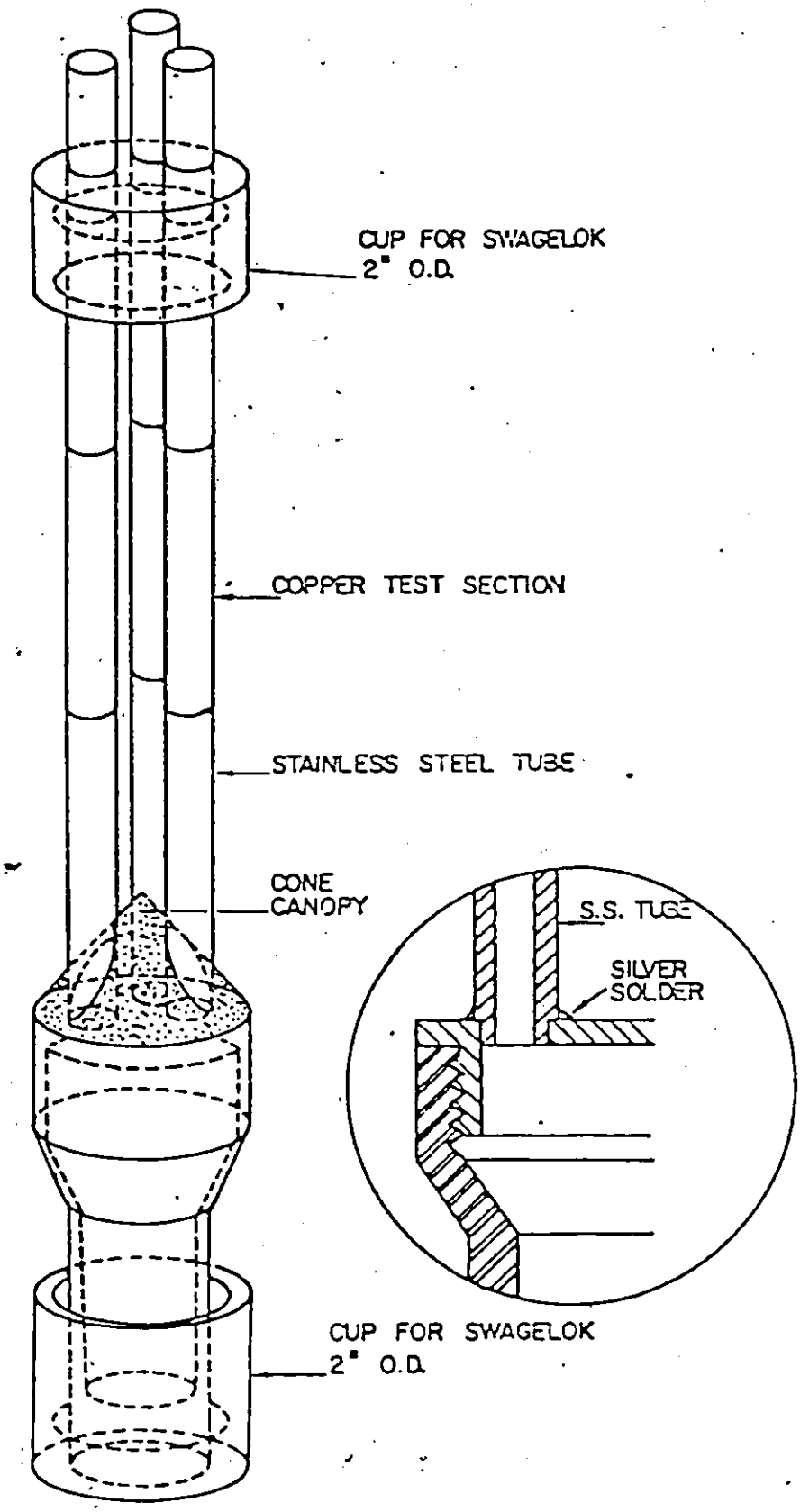

FIG.21 3-BUNDLE ASSEMBLY

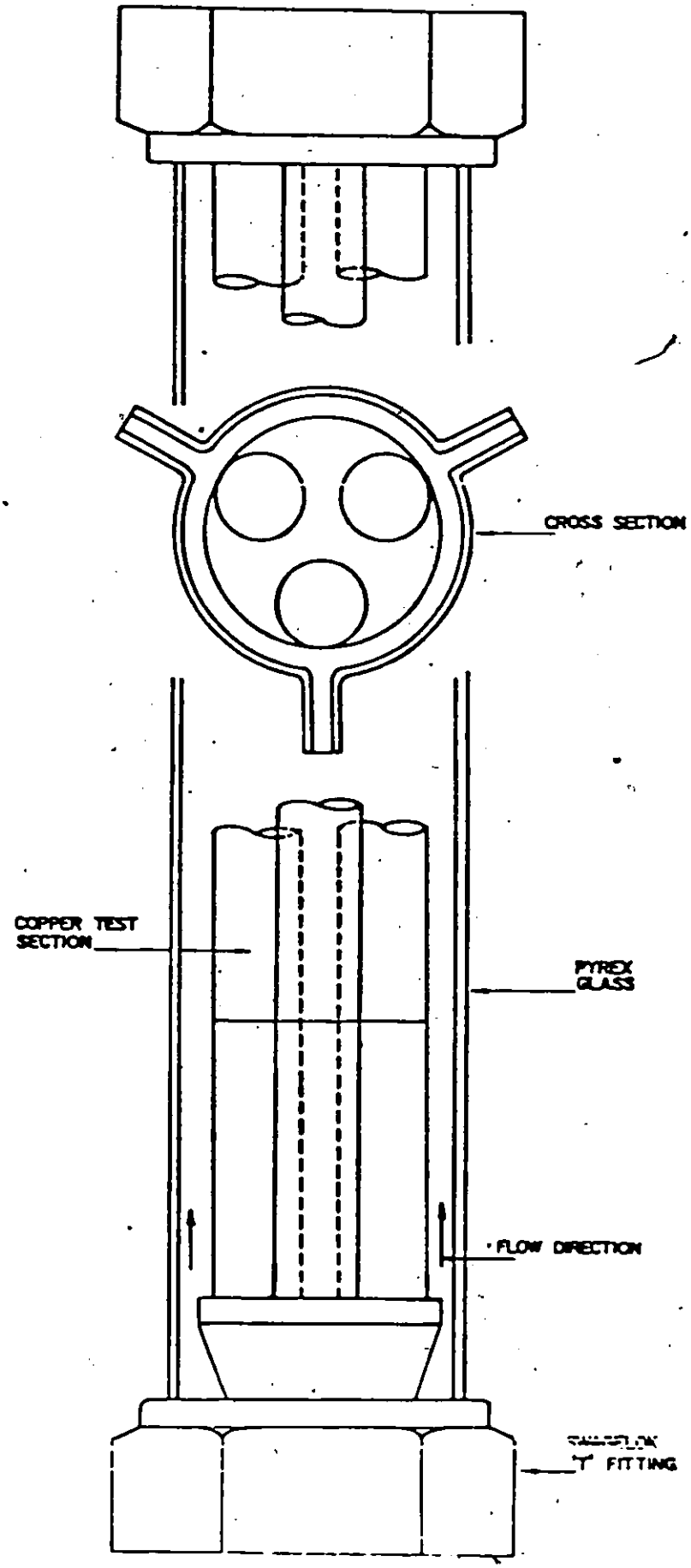

FIG. 22 3-ROD BUNDLE TEST SECTION

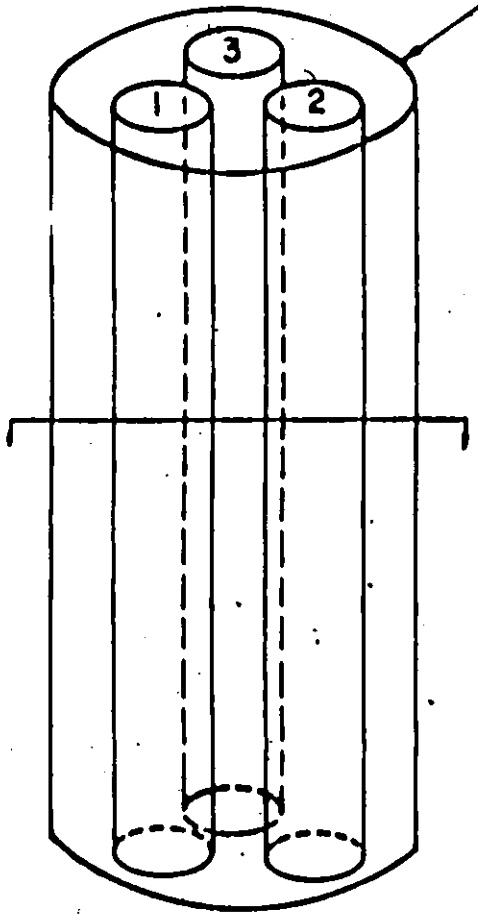

a. TEST SECTION

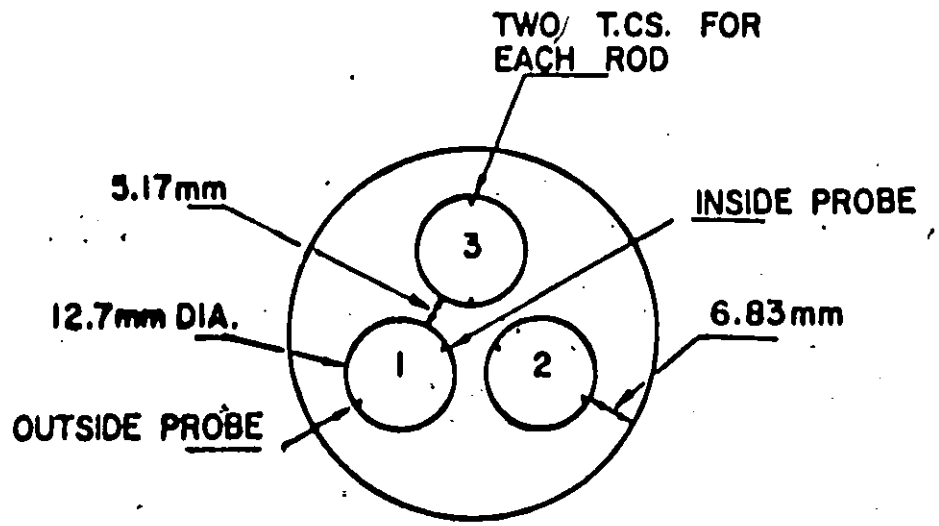

b. TEST SECTION CROSS-SECTION

FIG. 23 DIMENSIONS OF 3-ROD BUNDLE

3.3.5 Experimental Procedure for Probe Study

1. Water in the supply tank is heated to the desired temperature by immersion heaters which are controlled by a thermostat.
2. Lower and upper voltage levels of the probe output signal are checked by a chart recorder. Low voltage level representing the air resistance is determined under no flow conditions. By passing water in the test section for a few seconds, voltage level representing the water resistance is registered. A suitable span is chosen to incorporate these two points.
3. The pump is turned on for circulation and adjustment of the flow rate. The inlet water temperature is also checked from the test section by-pass.
4. The test section is heated by the cartridge heater in the rod. During heating a small amount of argon gas is passed through to prevent oxidation of test section surface.
5. When the temperature of rod (or rods) reaches about 500°C, the heaters and argon gas are turned off. The flow is diversed to the test section by switching the appropriate valves.
6. Chart recorders for tracing the probe signal, data thermocouple and probe temperature are already running at the beginning of every run.

Chapter IV

EXPERIMENTAL RUNS AND DATA REDUCTION

4.1 GENERAL

Experimental runs consist of four test series, they are :

1. 5400 series using the stainless steel tube and the copper block as the test section, with runs conducted under five different pressures (101, 206, 344, 550, and 686 kPa).
2. 5700 & 5800 series using the Inconel tube and the copper block as the test section, with runs conducted under five different pressures (101, 206, 344, 550, and 686 kPa), three different mass fluxes (68, 136, and 203 $kg/m^2sec.$), and two different degree of subcoolings.
3. 6000 series using the electric resistance probe in the single rod test section, with runs conducted for three different mass fluxes and two different degree of subcoolings.
4. 8000 series using the resistance probe in the 3-rod bundle test section.

In 5000 series, the temperature history of data thermocouple (Figures 24 and 25) and the system pressure are recorded on a two-channel chart recorder. The data thermocouple temperature is also recorded by the Fluke B2340 data logger with desired time interval.

In 6000 and 8000 series, two 2-channel chart recorders are used. The resistance probe signal trace, recorded through one channel, provides the information of the flow in the space between the wall and the probe. The data thermocouple trace, recorded through the other channel on the same recorder, gives the temperature history during the quenching process. The other chart recorder gives the trace of probe signal and probe temperature. The probe temperature indicates the fluid temperature, which can be vapour temperature during film boiling, vapour or liquid temperature for transition boiling, and liquid temperature during nucleate boiling.

4.2 SIGNAL RECORDED FROM THERMOCOUPLE FOR PRESSURIZED LOOP.

Figures 24 and 25 show a typical wall temperature history at a given system pressure. The temperature dropped gradually at the beginning. This indicates the film boiling region and it is confirmed by the boiling curve. A sudden drop of temperature then occurs, which indicates the change

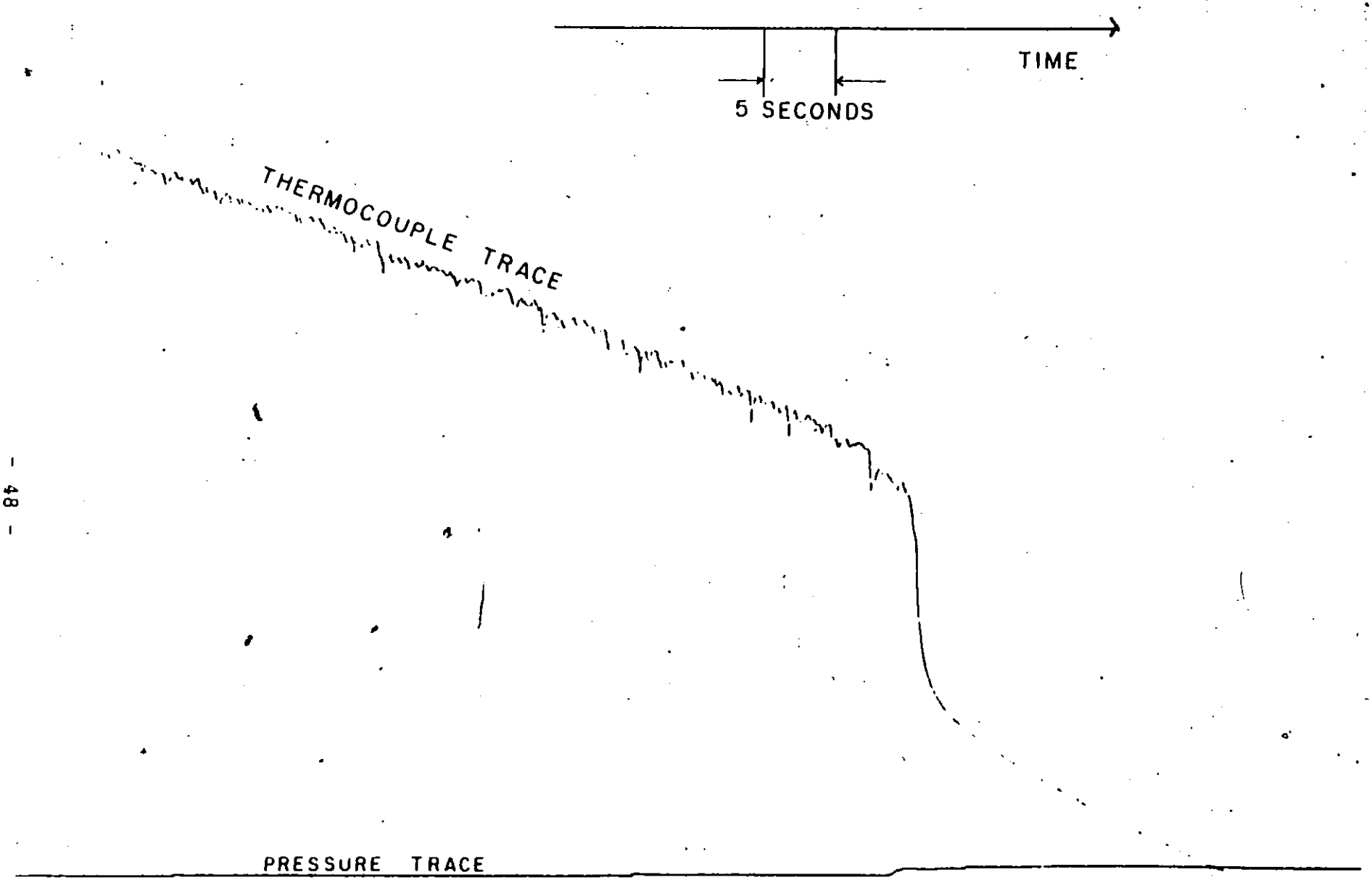

FIG. 24 TEMPERATURE HISTORY FOR 30 PSIA SYSTEM PRESSURE

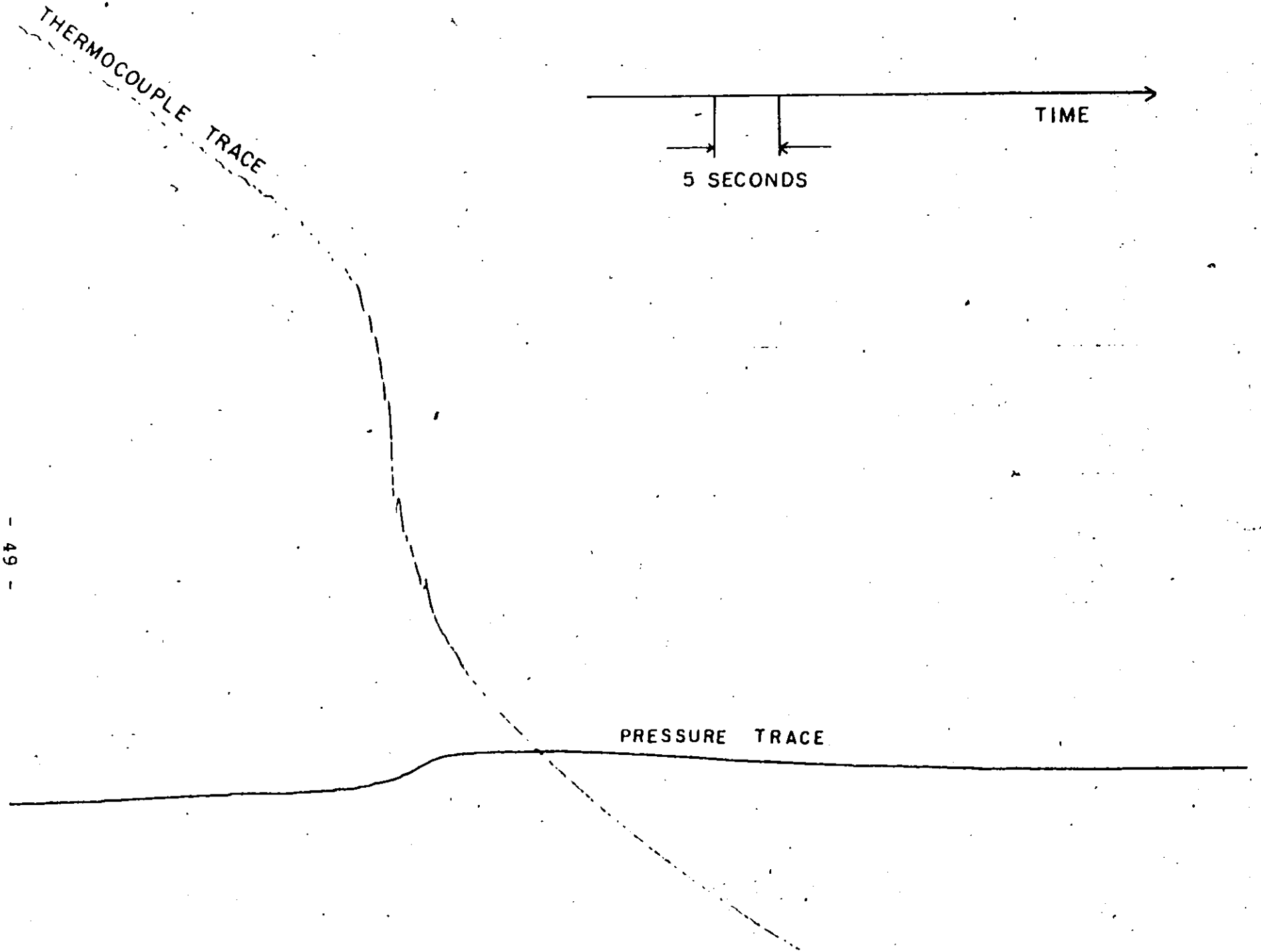

FIG. 25 TEMPERATURE HISTORY FOR 50PSIA SYSTEM PRESSURE

to the transition boiling region on the test section. At this period, the system pressure increases about 5-10% which can be observed clearly in Figure 25. For the same mass flux and inlet subcooling, the drop of temperature during quenching is steeper as the system pressure increases.

4.3 SIGNAL RECORDED FROM PROBE EXPERIMENT

Two chart recorders (each with two channels) record the experimental results for the single rod experiment. Figure 26 shows an example of the probe signal and the data thermocouple signal (the thermocouple tip is located about 0.040" from the wall) for a typical rewetting run. The distance between the probe tip and the surface of the wall is 0.005". Different gap sizes between the probe tip and the wall ranging from 0.003" to 0.030" have been tested. The result of test indicated that the 0.005" gap size gave the most consistent experiment results.

The data thermocouple signal provides the temperature history, and the probe signal indicates the resistance between the probe and test section during the experiment. The probe temperature signal and the probe signal are presented in Figure 27 for the same run. The probe temperature signal gives the temperature of fluid around the probe. For the 3-rod bundle, both chart recorders are used

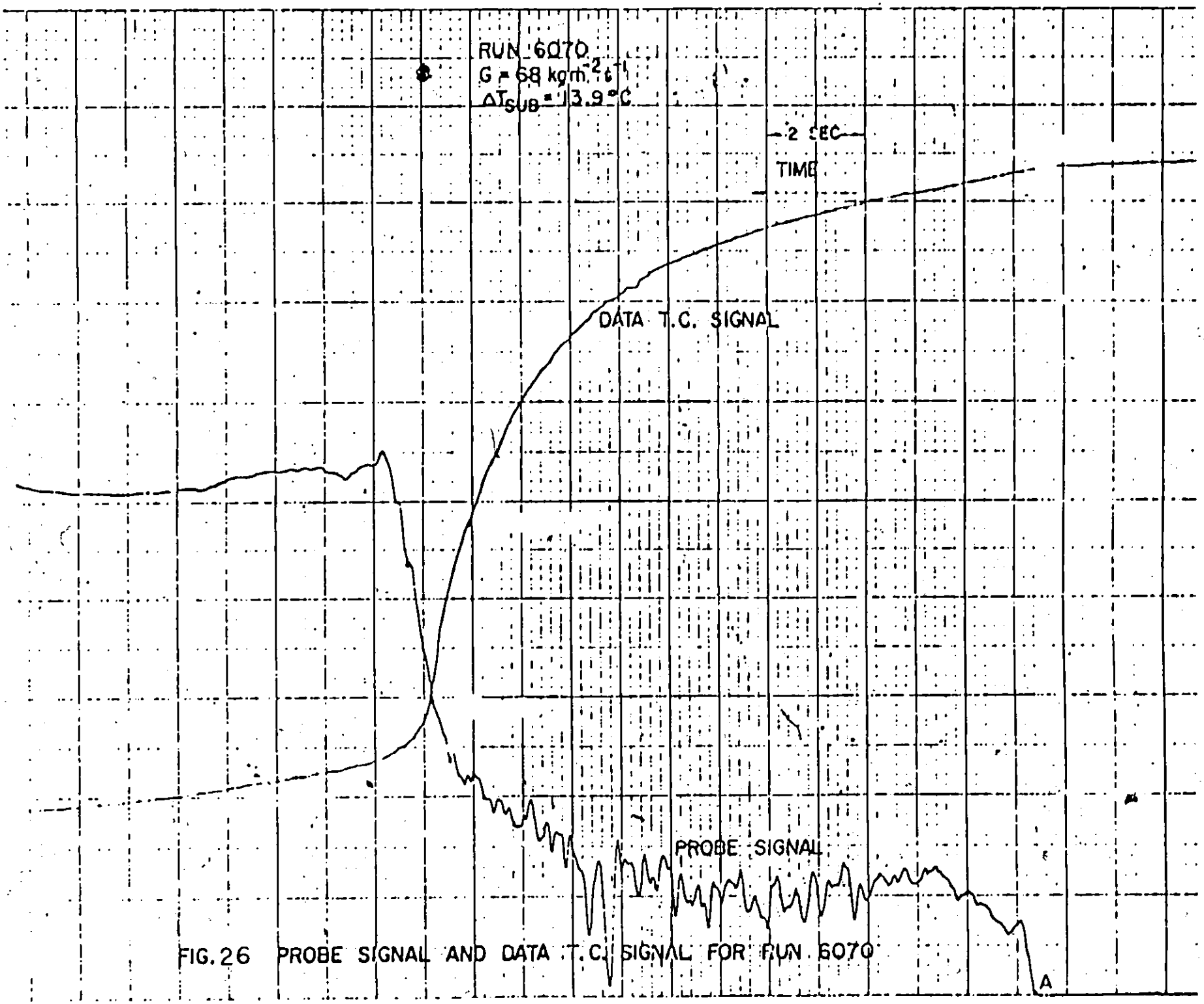

FIG. 26 PROBE SIGNAL AND DATA T.C. SIGNAL FOR RUN 6070

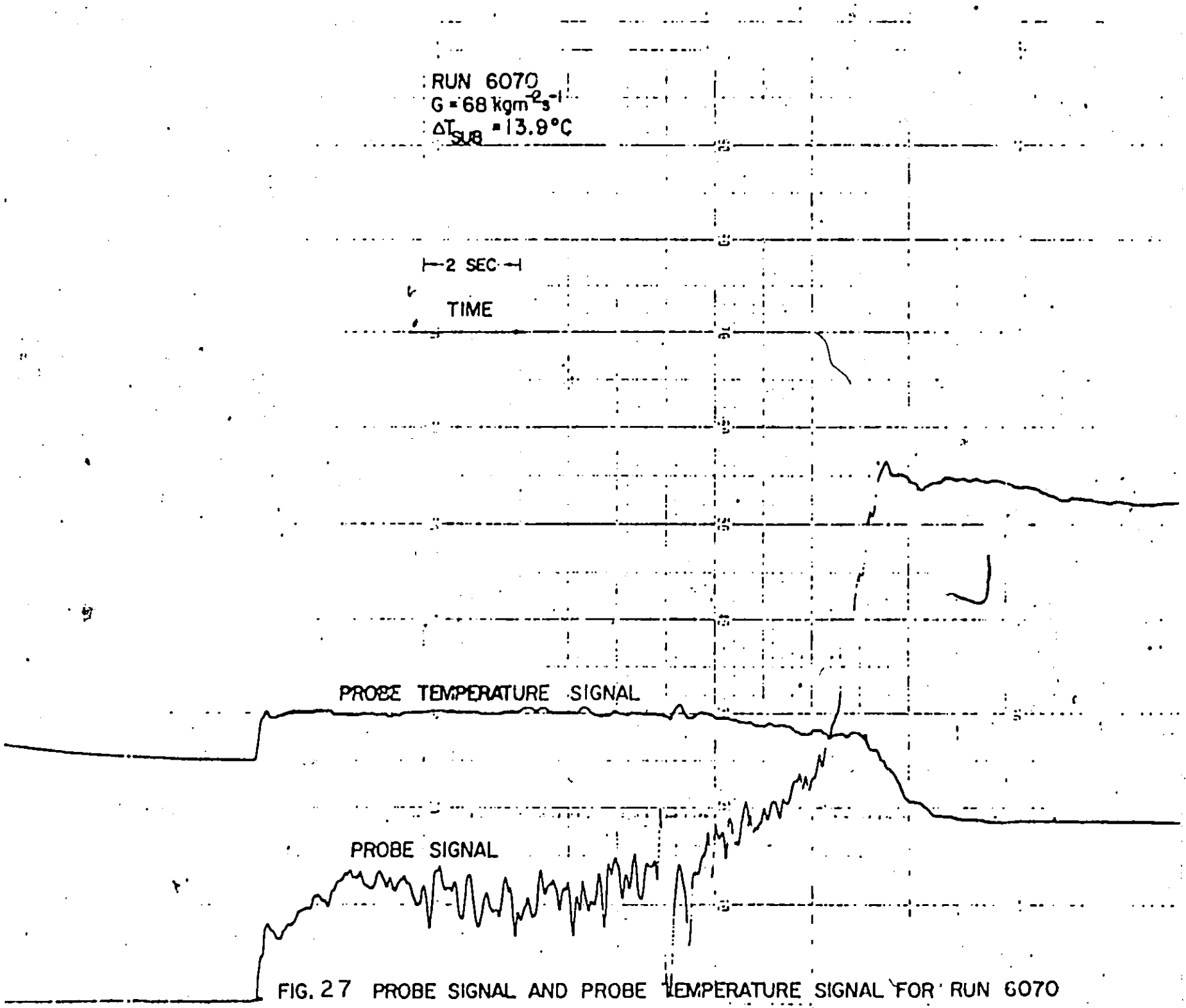

FIG. 27 PROBE SIGNAL AND PROBE TEMPERATURE SIGNAL FOR RUN 6070

for recording the outside probe signal (see Figure 24) and data thermocouple, as well as the inside probe signal and its corresponding data thermocouple.

4.4 DERIVATION OF 1 D MODEL FOR COMPOSITE TEST SECTION

The boiling curve (heat flux vs $\Delta T_w = T_w - T_{sat}$) is obtained from the temperature history of the thermocouple, which is located at the outer wall of tube for the composite test section. Both the chart recorder and data logger record only the outside wall temperature at the certain time intervals. Therefore, a mathematic model and computational technique is necessary for the construction of the boiling curve.

A modified one dimensional model technique developed by Cheng et al[21] is used for constructing the boiling curve for the composite test section. For a hollow cylinder test section insulated on the outer surface and both ends, heat transfer from the test section to the fluid between time 0 to t is assumed equal to the change in heat content Q inside the cylinder mimus heat loss through the outer wall during the same time interval. Q can be expressed as

$$Q(t) = \rho c_p L \int_{r_{in}}^{r_{out}} 2\pi r T(r,t) dr \qquad 4.1$$

where L represents the length of the test section. The function T(r,t) is obtained as the solution to the one-dimensional Fourier equation in cylindrical coodinates :

$$\frac{\partial T}{\partial t} = \alpha\left(\frac{\partial^2 T}{\partial r^2} + \frac{1}{r}\frac{\partial T}{\partial r}\right) \qquad 4.2$$

and is subjected to the following initial and boundary conditions :

1. $T = T(r,0)$ 4.3

   In general, at t=0, the temperature across the test section is assumed to be constant through the block.

2. $T(r_0, t) = T_0$ 4.4

   r_0 and T_0 are the location and recording of thermocouple respectively.

3. $$-k\frac{\partial T}{\partial r}\Big)_{r=r_{out}} = h(T_n - T_{amb}) \qquad 4.5$$

   h is the heat transfer coefficient at the outer wall.

The solution of Eq. (4.2) can be obtained by reducing it to a system of linear first order differential equation in t. This is achieved by discretizing along the r-direction (Figure 28), using the approximation :

$$\frac{\partial T}{\partial r}\Big|_{r=r_i} = \frac{T_{i+1}(t) - T_{i-1}(t)}{2\,\Delta r} \qquad 4.6$$

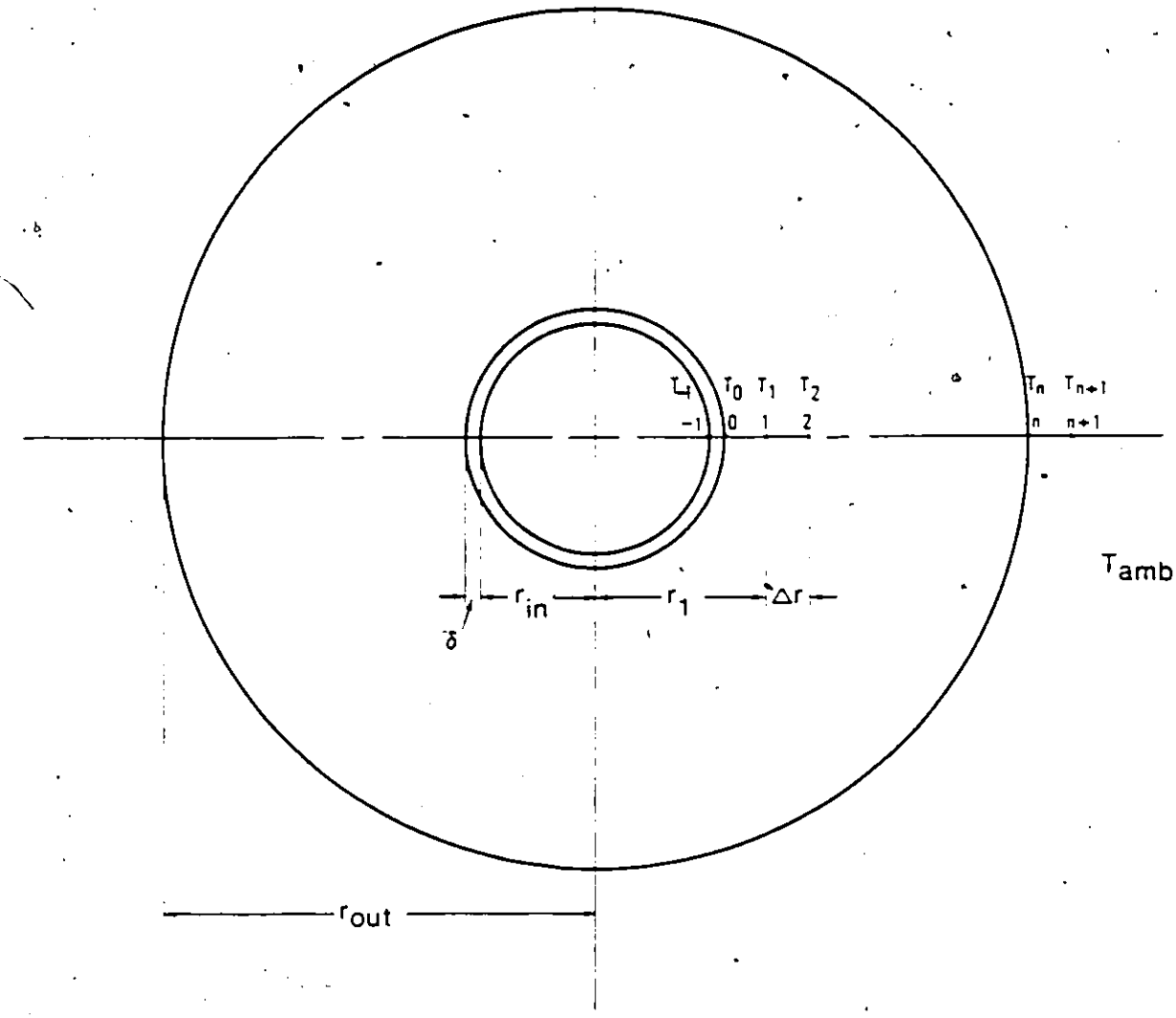

FIG. 28 NODAL POINTS DISTRIBUTION FOR

COMPOSITE TEST SECTION

and

$$\left.\frac{\partial^2 T}{\partial r^2}\right|_{r=r_i} = \frac{T_{i-1}(t) - 2T_i(t) + T_{i+1}(t)}{(\Delta r)^2} \qquad 4.7$$

where $T_i(t)$ represents the temperature at the ith nodal point $(1 <= i <= n+1)$.

Using Eqs. 4.6 and 4.7 along with initial and boundary conditions, the following system of equations can be inferred from Eq. 4.2,

$$\frac{\partial T_i}{\partial t} = \alpha\left[\frac{T_{i-1} - 2T_i + T_{i+1}}{(\Delta r)^2}\right] + \frac{\alpha}{r_i}\left[\frac{T_{i+1} - T_{i-1}}{2\Delta r}\right] \qquad 4.8$$

where $r_i = r_{in} + \delta + i\Delta r \qquad 1 \leq i \leq n$

$$\frac{-k}{2}\left(\frac{T_n - T_{n-1}}{\Delta r} + \frac{T_{n+1} - T_n}{\Delta r}\right) = h\,(T_n - T_{amb}) \qquad 4.9$$

Eq. (4.9) is a direct consequence of Eq. 4.5. Furthermore, T_{n+1} in Eq. 4.8 can be eliminated by using Eq.(4.9).

Eq.(4.8) contains a system of n equations with n unknowns in T_i. Once T_1 up to T_n have been solved and dT_o/dt determined experimentally, the inner wall temperature T_{-1} can then be calculated in the following Fourier equation based on the nodal point $i = 0$

$$\frac{[r_o^2 - (r_o - \delta/2)^2]\rho_t c_t + [(r_o + \Delta r/2)^2 - r_o^2]\rho_c c_c}{(r_o + \Delta r/2)^2 - (r_o - \delta/2)^2}\frac{dT_o}{dt}$$

$$= \frac{k_c(T_1 - T_o)/\Delta r - k_t(T_o - T_{-1})/\delta}{(\Delta r + \delta)/2} + \frac{1}{2r_o}\left[\frac{k_c(T_1 - T_o)}{\Delta r} + \frac{k_t(T_o - T_{-1})}{\delta}\right] \qquad 4.10$$

Eq.(4.1) expressed in terms of summation, becomes

$$Q = 2\pi\delta\rho_t c_t L \left[0.5T_{-1} r_{in} + 0.5T_o(r_{in} + \delta)\right] +$$

$$+ 2\pi\Delta r\rho_c c_c L \left[0.5T_o(r_{in} + \delta) + \sum_{i=1}^{n-1} T_i r_i + 0.5T_n r_n\right] \qquad 4.11$$

The expression of net heat transfer to the fluid, q, in terms of Q and heat loss is

$$q = \frac{-dQ}{dt} / A_{in} - h A_{out} (T_n - T_{amb}) / A_{in}$$

$$= \frac{-1}{2\pi r_{in} L} \frac{dQ}{dt} - h \frac{r_{out}}{r_{in}} (T_n - T_{amb}) \qquad 4.12$$

where A_{in} and A_{out} represent the inner and outer test section areas, respectively.

All calculations are performed via the CSMP computer package [22]. Due to its flexibility, power, relative ease of use and plotting capability, CSMP has gained wide acceptance recently in solving differential equations [23]. The Runge-Kutta fixed-step size method has been used in numerical integration with selection of n = 8 and t = 0.1 second and its convergency checked. NLFGEN (nonlinear function generation) capability of CSMP is used to generate T_o from experimental data and Derio (derivative) module used

to compute dT_o/dt from T_o and dQ/dt from Q. A complete program has been established starting with T.C. recording (temperature vs time) as input, and at the end q vs the wall temperature printed and plotted (for a sample program, see Appendix I).

4.5 DERIVATION OF 1 D MODEL FOR ROD

In order to construct the boiling curve for single and 3-rod test sections, a model for rod has been derived. Based on Figure 29, the one-dimensional Fourier equation in cylindrical coordinates for a rod can be expressed as

$$\frac{\partial T}{\partial t} = \alpha \left(\frac{\partial^2 T}{\partial r^2} + \frac{1}{r} \frac{\partial T}{\partial r} \right) \qquad 4.13$$

and is subjected to the following initial and boundary conditions :

1. $T(r,0) = T$ 4.14

   where T is the initial temperature.

2. $T(r_o,t) = T_o$ 4.15

   where r_o and T_o are the location and the recording of the data thermocouple.

3. $\left.\frac{\partial T}{\partial r}\right|_{r=0} = 0$ 4.16

   assuming the temperature distribution is axially symmetrical.

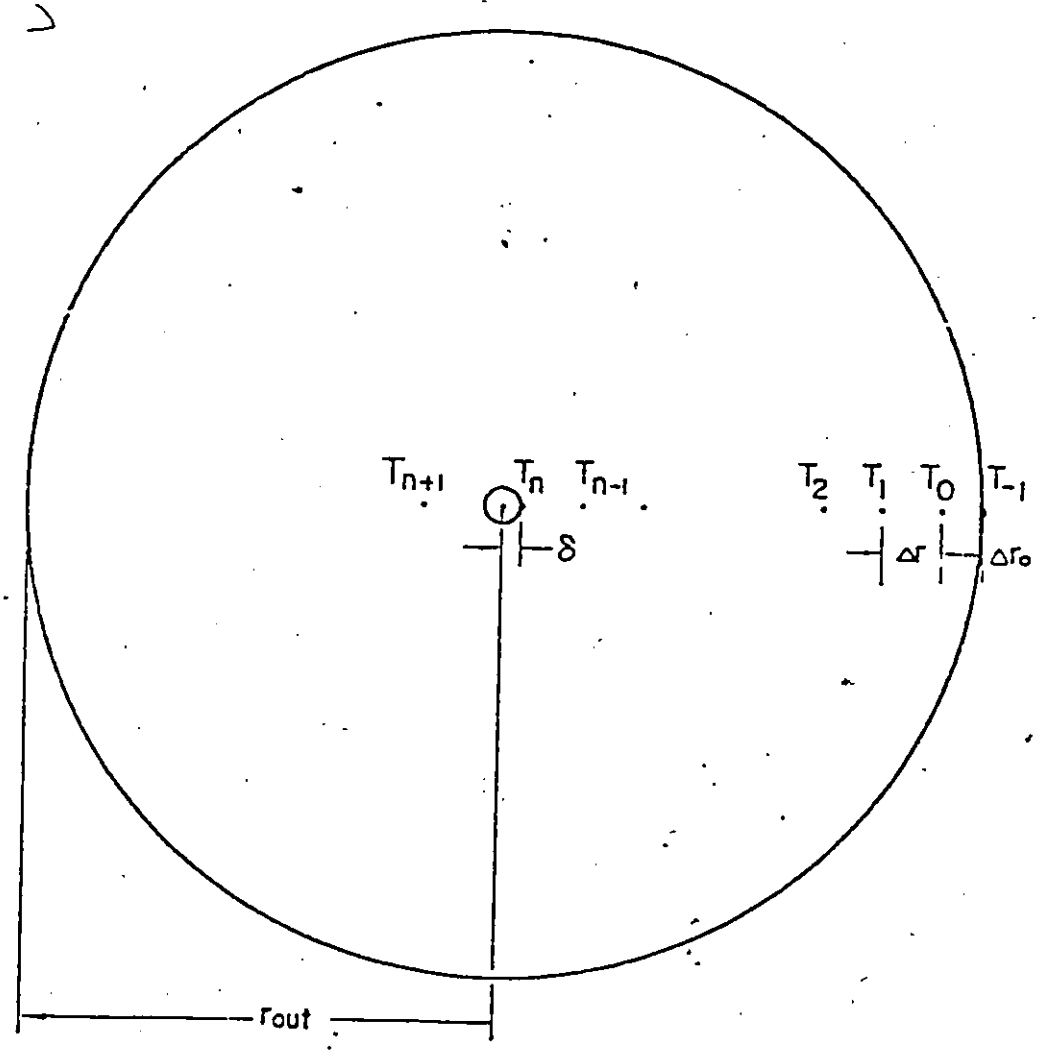

FIG. 29 NODAL POINTS DISTRIBUTION

The solution of Eq.(4.13) can be obtained by reducing it to a system of linear first-order differential equations in t. This is achieved by discretizing along the r-direction using the approximation

$$\frac{\partial T}{\partial r} = \frac{T_{i-1}(t) - T_{i+1}(t)}{2\Delta r} \qquad 4.17$$

and

$$\frac{\partial^2 T}{\partial r^2} = \frac{T_{i-1}(t) - 2T_i(t) + T_{i+1}(t)}{(\Delta r)^2} \qquad 4.18$$

where $\Delta r = (r_{out} - \Delta r_o - \delta)/n$.

Eq.(4.13) becomes

$$\frac{dT_i}{dt} = \alpha \left[\frac{T_{i-1} - 2T_i + T_{i+1}}{(\Delta r)^2} \right] + \frac{\alpha}{r_i} \left(\frac{T_{i-1} - T_{i+1}}{2\Delta r} \right) \qquad 4.19$$

where $r_i = r_{out} - \Delta r_o - i\Delta r$

Substituting the third boundary condition (Eq.(4.16)) into Eq.(4.17), one obtains

$$T_{n+1} = T_{n-1} \qquad 4.20$$

T_{n+1} in Eq.(4.19) is to be eliminated from Eq.(4.20).

Eq.(4.19) contains a system of n equations with n unknowns in T_i and are readily to be solved. Theoretically, T_n is located at the center with r = 0, thus it becomes a singular point. To circumvent this difficulty, T_n is

arbitrarily moved away from the center point with δ. Once T_1 up to T_n solved and dT_o/dt determined from experimental data, the outer wall temperature T_{-1} can be calculated from the following Fourier equation based on the nodal point at i = 0

$$\frac{dT_o}{dt} = \alpha \frac{(T_{-1} - T_o)/\Delta r_o - (T_o - T_1)/\Delta r}{(1/2)(\Delta r + \Delta r_o)} + \frac{\alpha}{r_o}\left(\frac{T_{-1} - T_1}{\Delta r + \Delta r_o}\right) \qquad 4.21$$

where $r_o = r_{out} - \Delta r_o$

The heat content of the rod now can be expressed as

$$Q = 2\pi\rho c_p L\left[0.5\, T_{-1}\, r_{out}\, \Delta r_o + 0.5\, T_o(r_{out} - \Delta r_o)\Delta r_o + 0.5\, T_o(r_{out} - \Delta r_o)\Delta r + \sum_{j=1}^{n-1} T_i r_i\, \Delta r\right] + \pi\left[(\delta + 0.5\Delta r)^2 - \delta^2\right]L\rho c_p T_n + \pi\delta^2 L\rho c_p T_n \qquad 4.22$$

and heat flux as

$$q = -\frac{dQ}{dt}/A_{out}$$

$$= -\frac{1}{2\pi r_{out} L}\frac{dQ}{dt} \qquad 4.23$$

In our computation, for a rod of 0.5 in. O.D., n = 5 and δ = 0.01" are used with sufficient accuracy.

Starting with data from the thermocouple as input, using the model computed via CSMP (Appendix II), the boiling curve can be constructed.

Chapter V

RESULTS AND DISCUSSION

5.1 PRESSURIZED TRANSITION BOILING HEAT FLUX

The transition boiling data produced from the experiment using the method mentioned in the previous chapter are tabulated in Appendix III. These data are also plotted on the following figures. Figure 30 to 33 show the trend due to the pressure effect under constant subcooling and mass flux, while Figure 34 to 37 show the mass flux effect under constant subcooling and pressure. In all figures the standard units are used; for example, G in kg/m^2s, P in kPa and ΔT_{sub} in degree C. Normally ΔT_{sub} refers to degree subcooling at the inlet, however T_{sub} is used instead of ΔT_{sub} in Figure 30 to 37.

5.1.1 Effect of the Initial Temperature

The initial temperature of the test section has no obvious effect on the actual transition heat flux results. However, in order to construct boiling curve, stable film boiling in the test section must be established at the beginning of each test. As a consequence, the initial

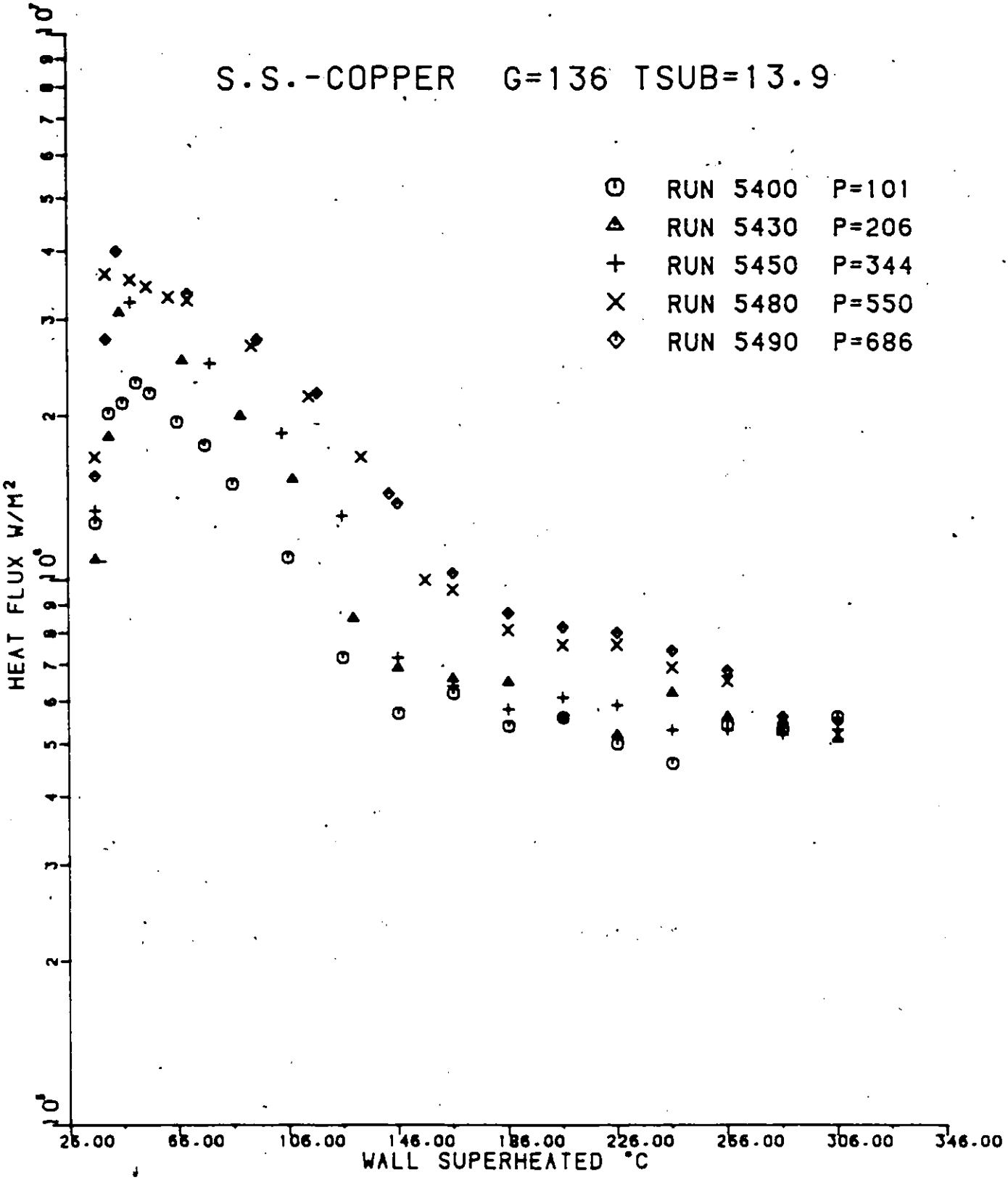

FIG.30 EFFECT OF PRESSURE ON TRANSITION BOILING HEAT FLUX OF 5400 SERIES

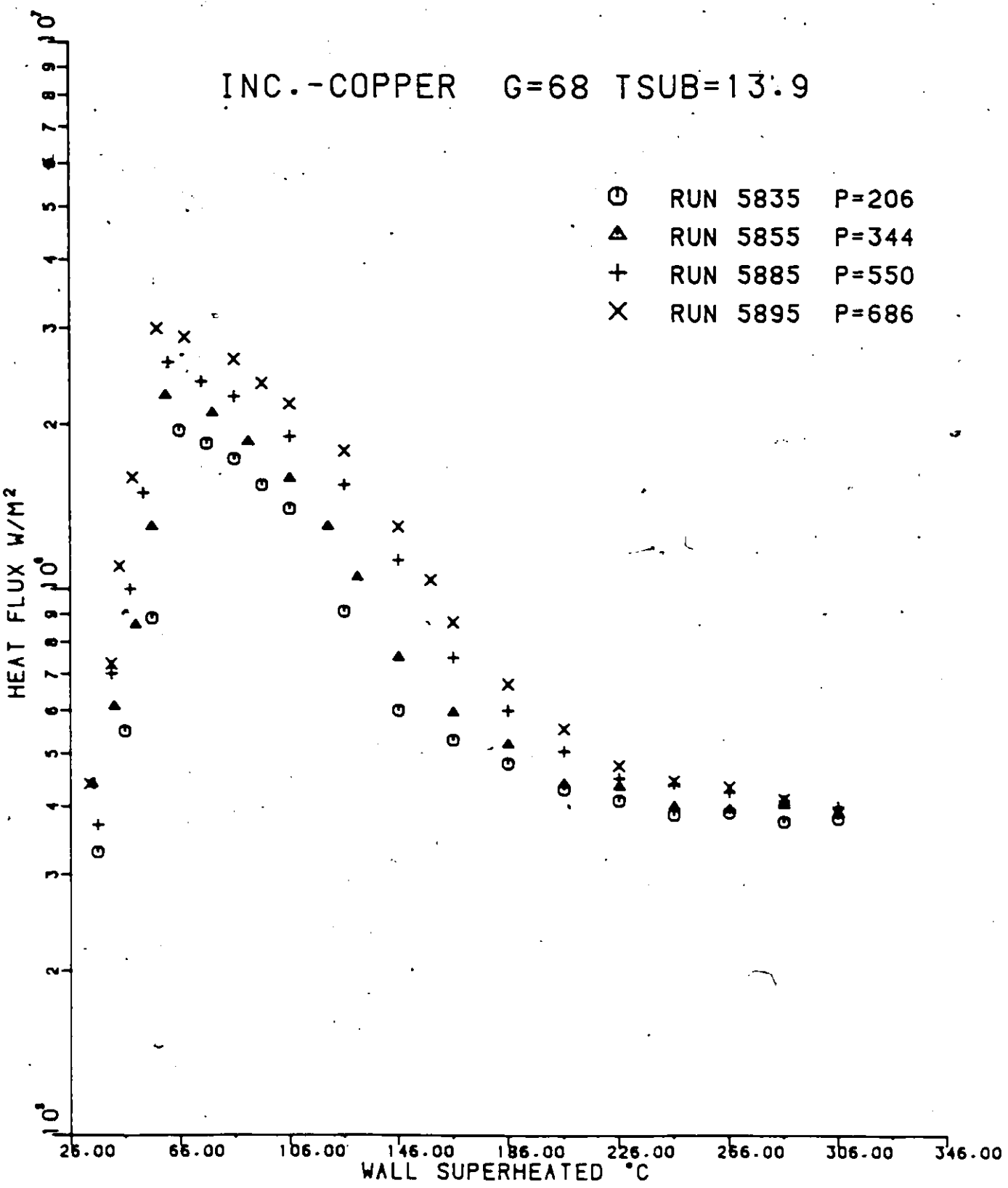

FIG.31 EFFECT OF PRESSURE ON TRANSITION BOILING HEAT FLUX FOR G=68

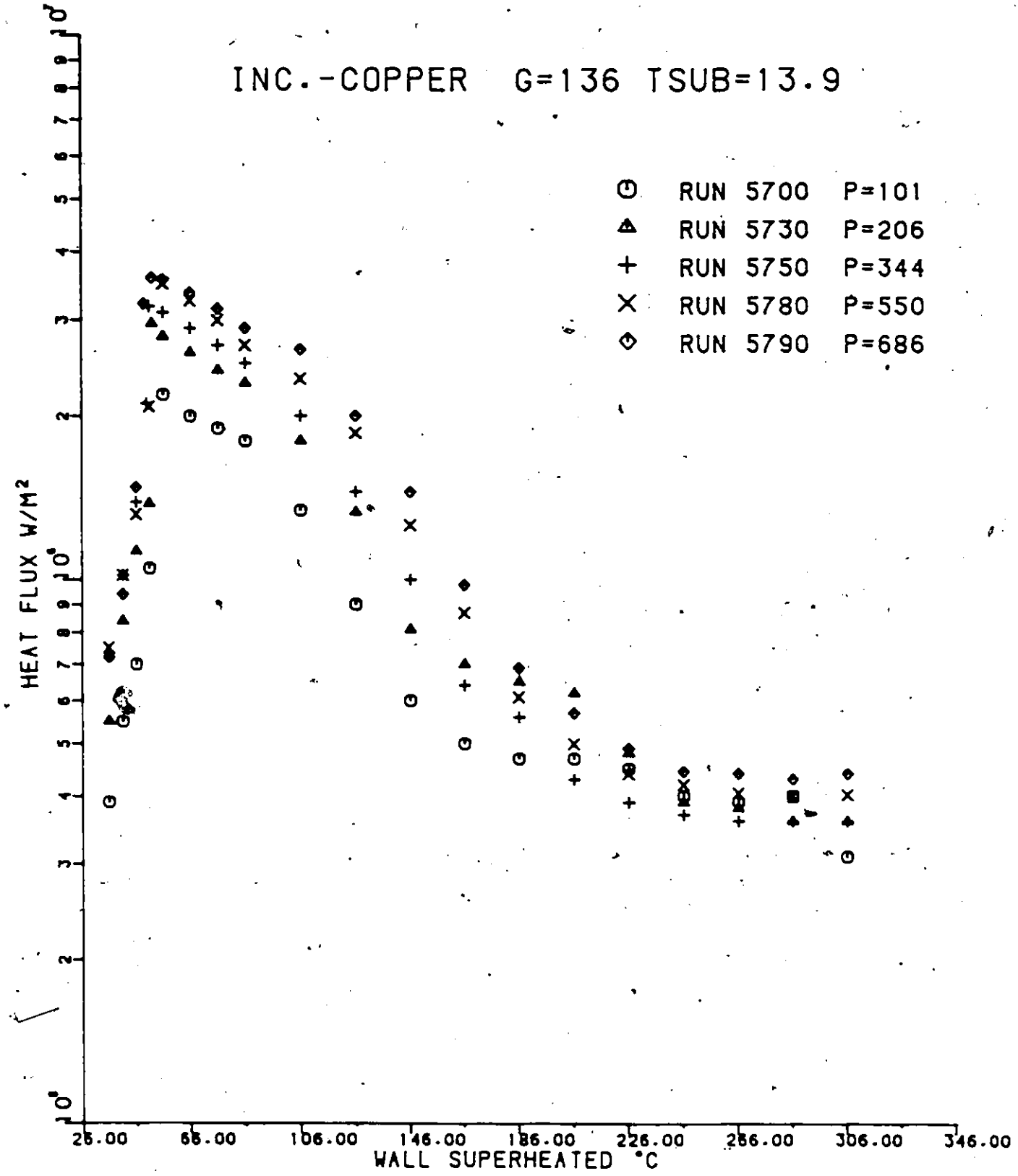

FIG.32 EFFECT OF PRESSURE ON TRANSITION BOILING HEAT FLUX FOR G=136

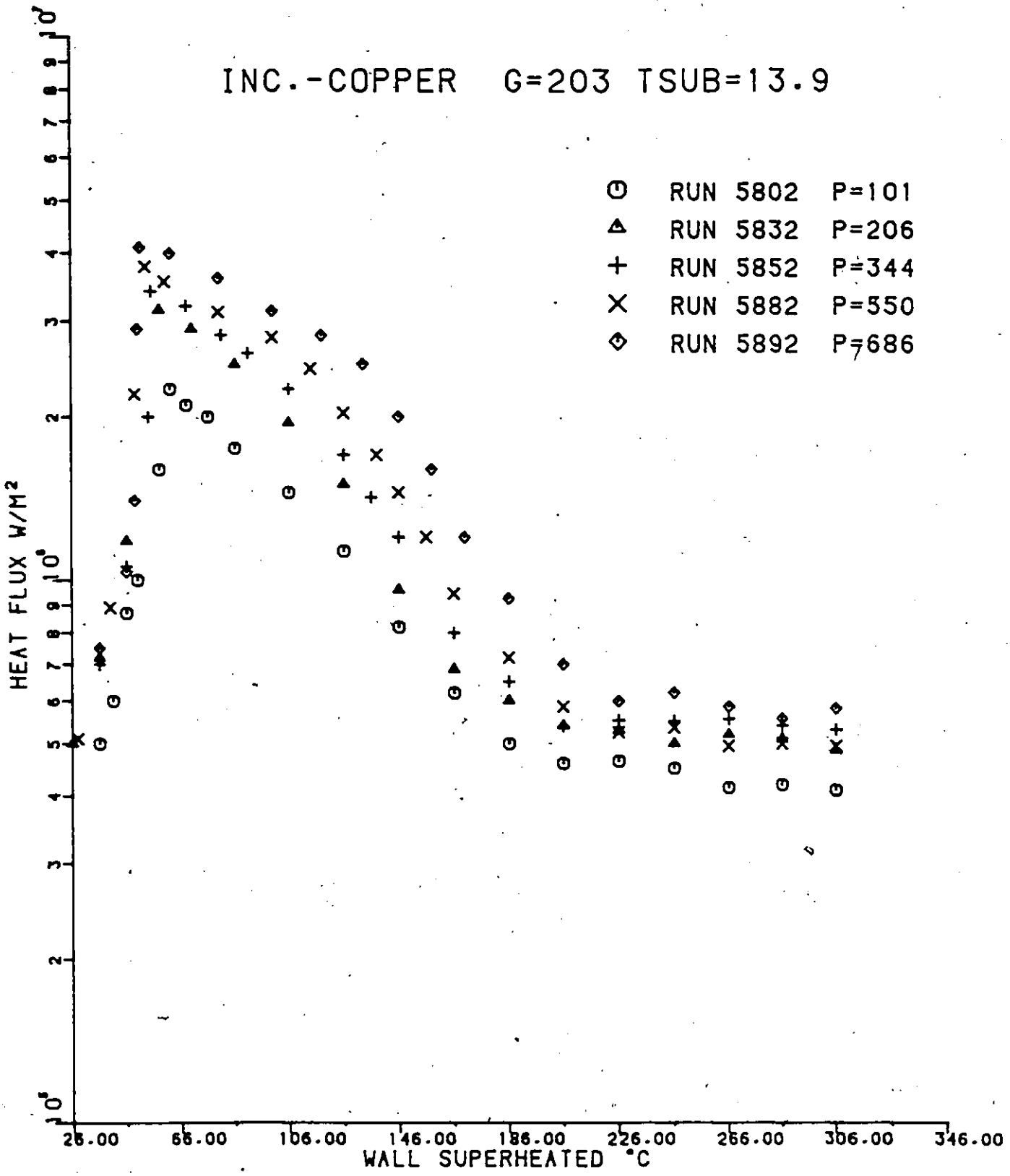

FIG.33 EFFECT OF PRESSURE ON TRANSITION BOILING HEAT FLUX FOR G=203

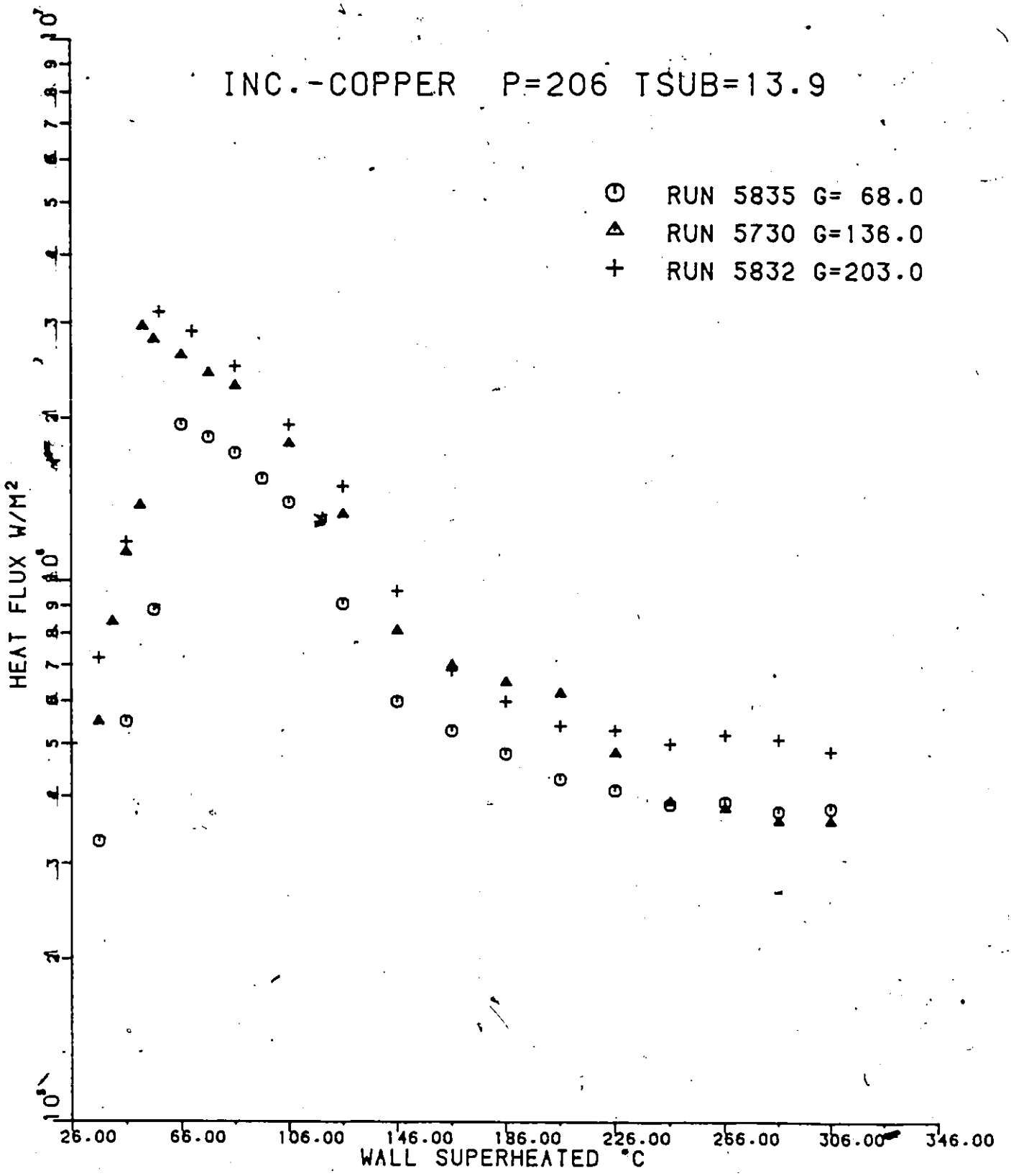

FIG.34 EFFECT OF MASS FLUX ON TRANSITION BOILING HEAT FLUX FOR P=101 Kpa

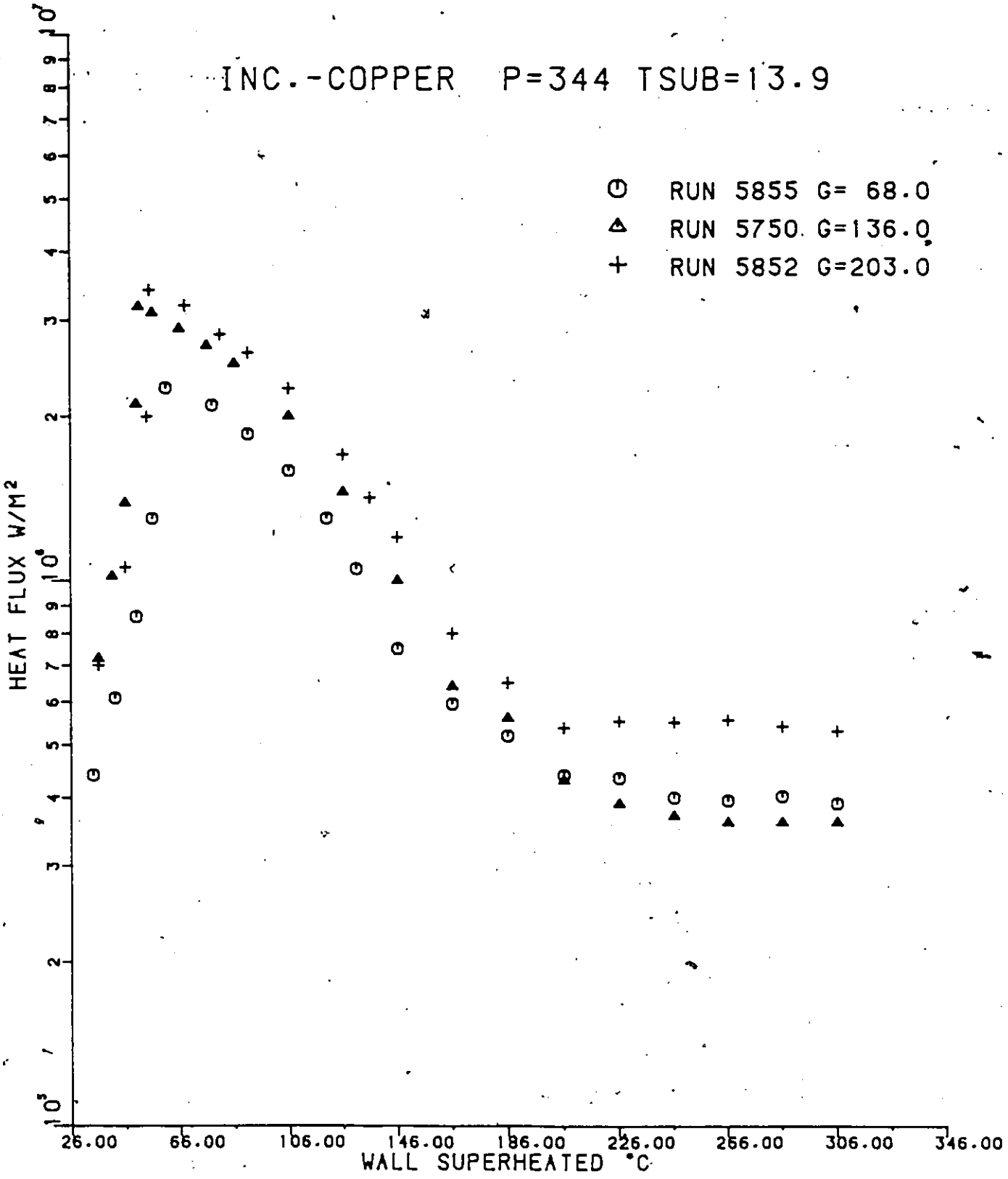

FIG.35 EFFECT OF MASS FLUX ON TRANSITION BOILING HEAT FLUX FOR P=344 Kpa

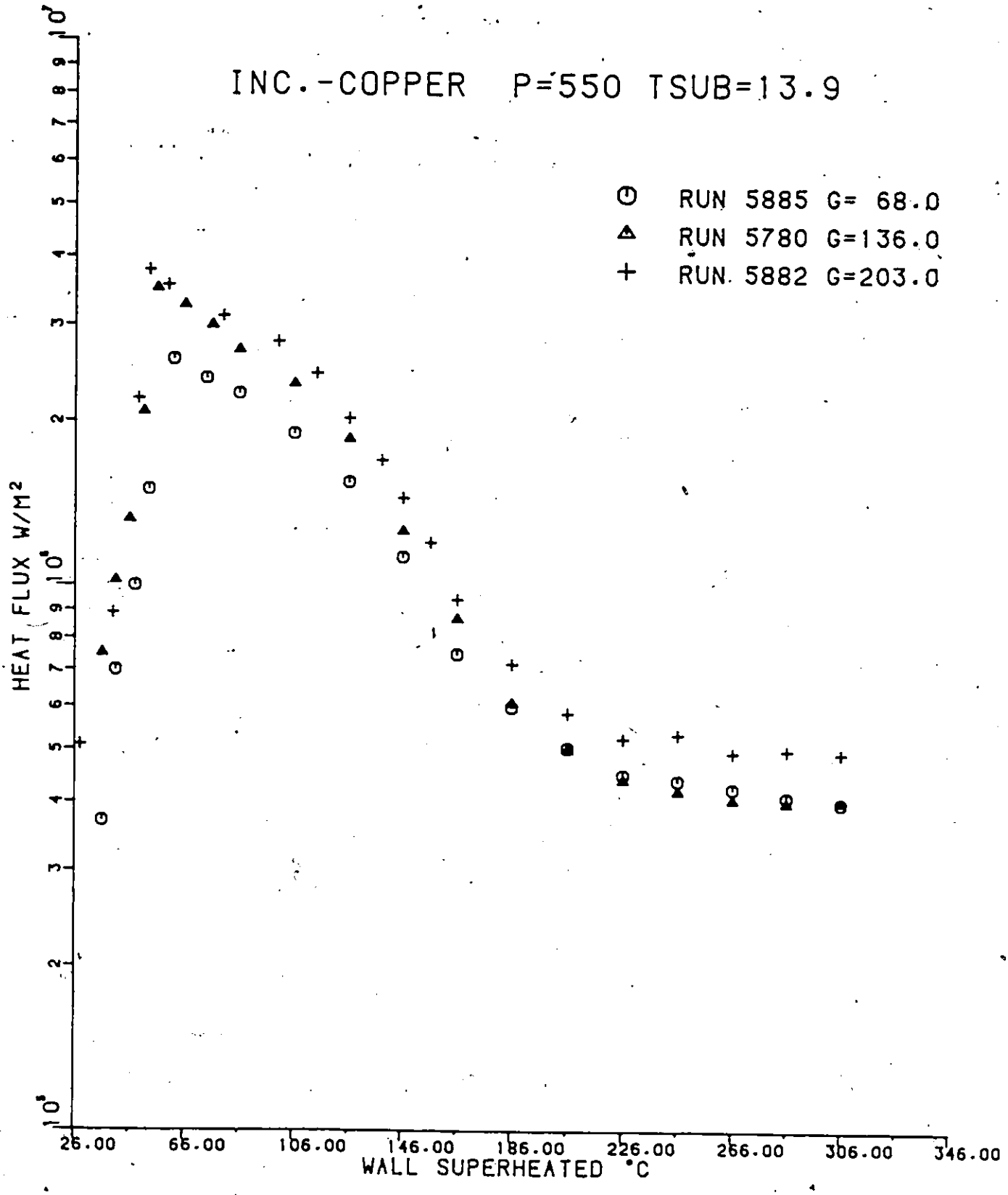

FIG.36 EFFECT OF MASS FLUX ON TRANSITION BOILING HEAT FLUX FOR P=550 Kpa

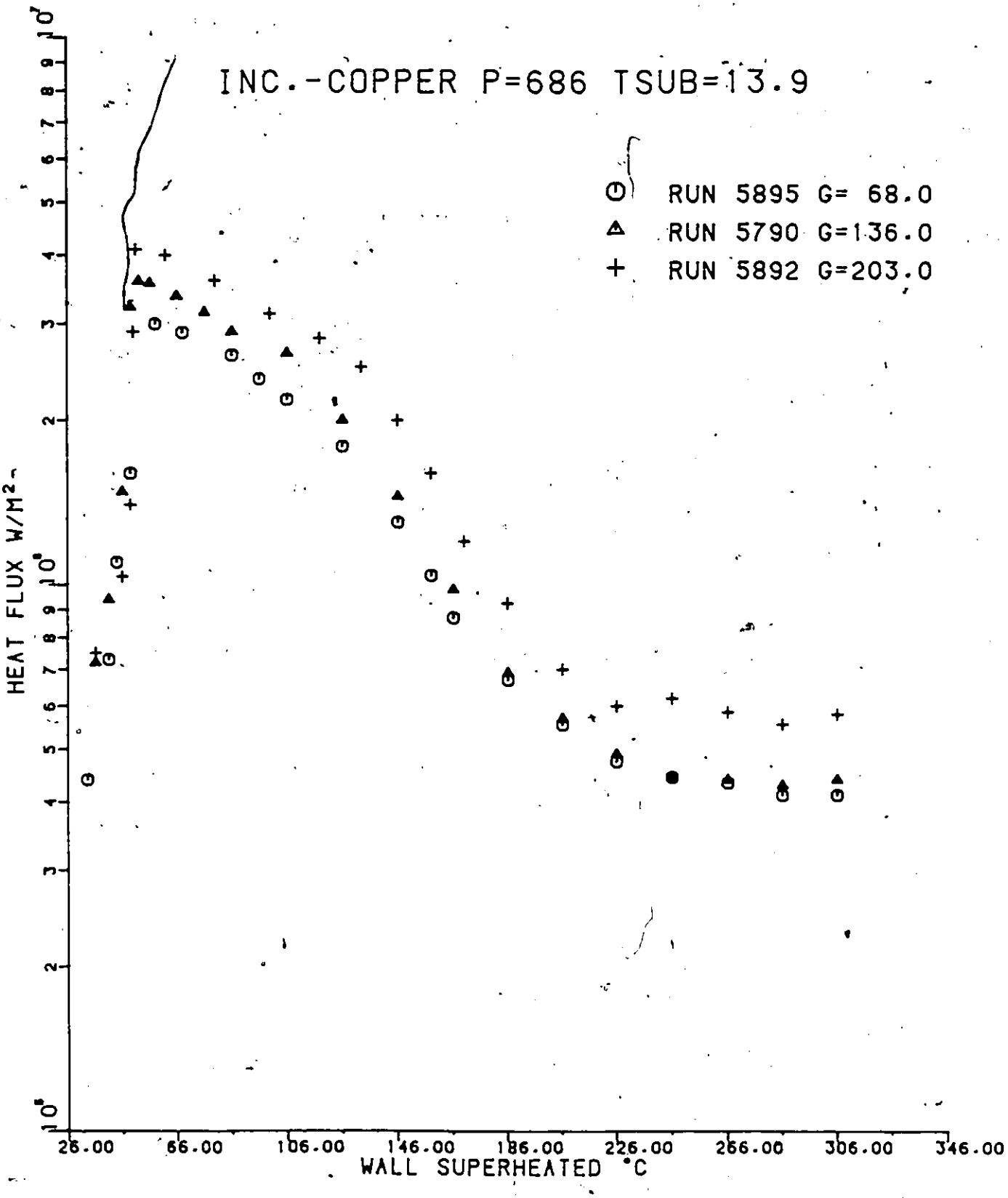

FIG.37 EFFECT OF MASS FLUX ON TRANSITION BOILING HEAT FLUX FOR P=686 Kpa

temperature should be high enough to meet this requirement. Generally the initial temperature is about 400°C higher than the saturation temperature of water. Since the saturation temperature of water increases with pressure, the initial temperature for 686 kPa is about 600°C. Hence, for most runs the initial temperature is set at 600°C.

5.1.2 Effect of Inlet Subcooling

The range of inlet water temperature in this experiment is restricted due to following reasons. Firstly, when the water temperature reaches the saturated temperature, the pressure in the system is very unstable; hence, it should be avoided in the experiment. Secondly, if the water temperature is too low, stable film boiling requires a much higher initial temperature to establish. Furthermore, for low inlet temperature, a violent vibration is observed during transition boiling. Thus, only two different subcooling conditions have been performed (i.e. 13.6 and 27.8°C). The effect due to the inlet subcooling at these two values for transition boiling is almost negligible, which contradicts the results obtained by Cheng et al [24] for atmospheric pressure. The reason for this can be explained by the fact that the heat flux is very much affected by the pressure through the change of water properties, rather than the inlet subcooling effect.

5.1.3 Effect of Mass Flux

Figure 34 to 37 illustrate the effect of mass flux on transition boiling heat flux at a fixed inlet subcooling and pressure. The transition boiling heat flux increases slightly with mass flux. Transition boiling is an intermediate heat transfer mode occurring between CHF and minimum film boiling. Since both the CHF and minimum film boiling heat flux increase with mass flux, it is expected that transition boiling heat flux also increases with mass flux. The observed increase in transition boiling heat flux is attributed to: (i) more efficient removal of bubbles around the tube because of the higher flow, (ii) improved convective heat transfer during film boiling, and (iii) improved wall liquid interaction due to a higher turbulence level of flow.

5.1.4 Effect of Pressure

The experiment was conducted at the range of 101 kPa to 686 kPa which is a relatively low pressure compared to most available sources [8, 25, 26]. Figure 30 to 33 show that the transition boiling heat flux increases with increasing pressure (i.e., the heat flux moves upward at the same degree of wall superheat) for fixed inlet water subcooling and mass flux on tests performed for both stainless steel-

copper and Inconel-copper test sections. The CHF points also move upward and to the left with the increase of pressure. CHF increase with pressure when the pressure is less than 25% of critical pressure, which has been cited in the literature. In this experiment the pressure is much lower than 0.25 P_{cr}. In general the effect of pressure on film boiling heat transfer in the neighbourhood of minimum film boiling point follows the same trend. Yet in some cases, for example run 5750 in Figure 32, the effect of pressure is not clear.

As mentioned before, the transition heat flux is a combination of unstable film boiling and unstable nucleate boiling. The region of transition boiling for the quenching process starts at point D and ends Point C, as shown in Figure 1. The heat flux of unstable film boiling and unstable nucleate boiling in the transition region is related to minimum heat flux and critical heat flux points, respectively. The transition boiling curve will shift up slightly with pressure since both the minimum heat flux and CHF increase with pressure.

In boiling heat transfer, physical properties of fluid play an important role. Since the physical properties of water are affected by the pressure, the boiling heat flux will be affected by pressure. Experimental data for physical

properties of water along the saturation line have been generalized [27], namely, latent heat of vaporization and surface tension (Figure 38), viscosity, thermal conductivity, specific heat and density of water (Figure 39), viscosity, thermal conductivity, specific heat and density of vapour (Figure 40). From these figures it can be seen that as pressure increases, specific heat of water, thermal conductivity, specific heat, and density of vapour increase, but all other physical properties decrease. It is obvious that the increase in thermal conductivity, density, and specific heat of vapour, and specific heat of water and the decrease in surface tension, viscosity of liquid and vapour will improve boiling heat transfer. The decrease in latent heat of vaporization, thermal conductivity, and density of liquid will decrease boiling heat transfer. The overall effect of properties due to the pressure variation reflects each individual property effect; thus it is very difficult to analyze. Most correlations are based on actual experimental results to form an empirical or semi-empirical correlation.

In most phenomenal correlations, many of these physical properties are important terms in the prediction of transition boiling, e.g.,

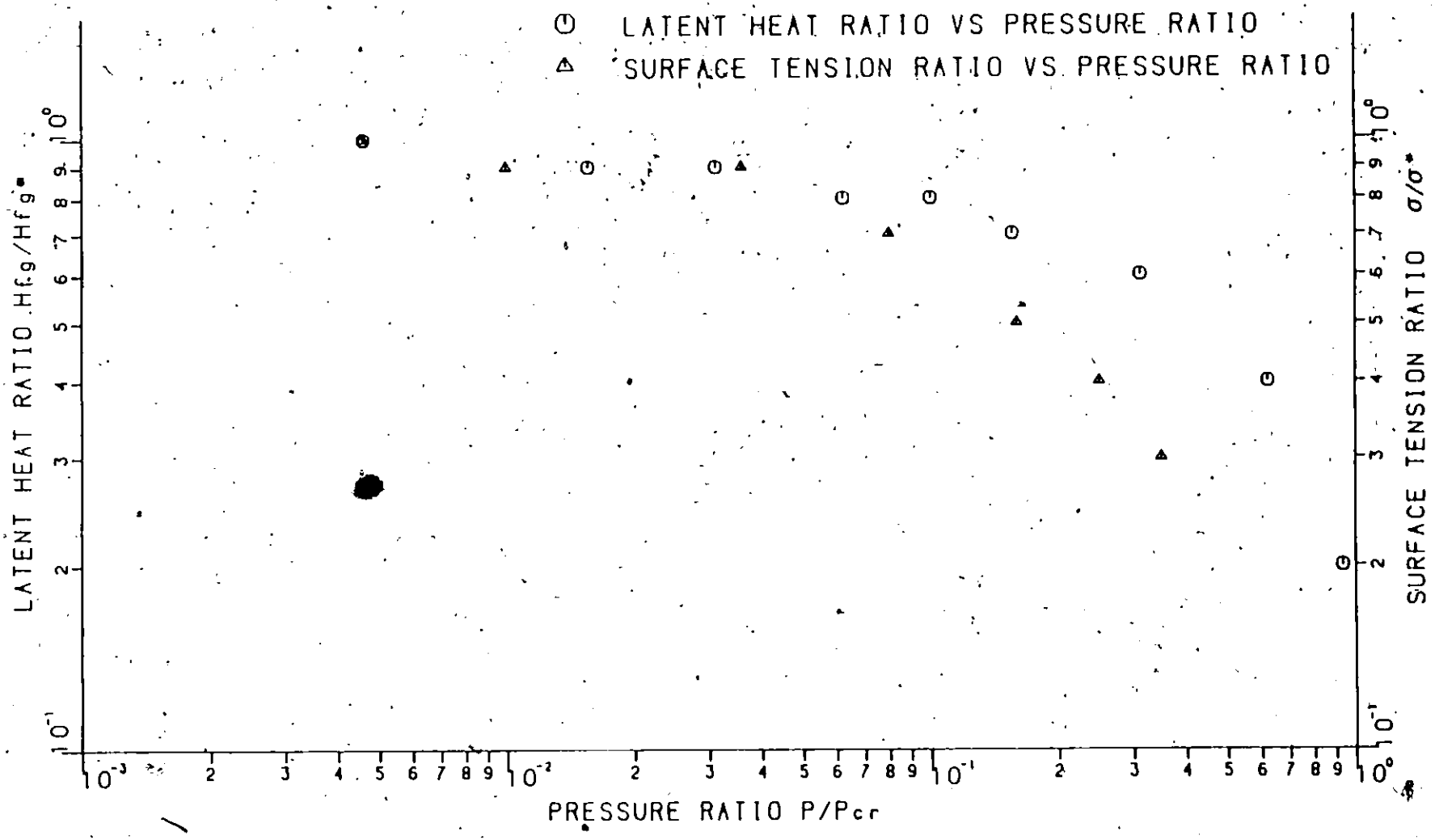

FIG.38 CORRELATION OF DATA FOR THE LATENT HEAT OF VAPORIZATION AND SURFACE TENSION OF WATER

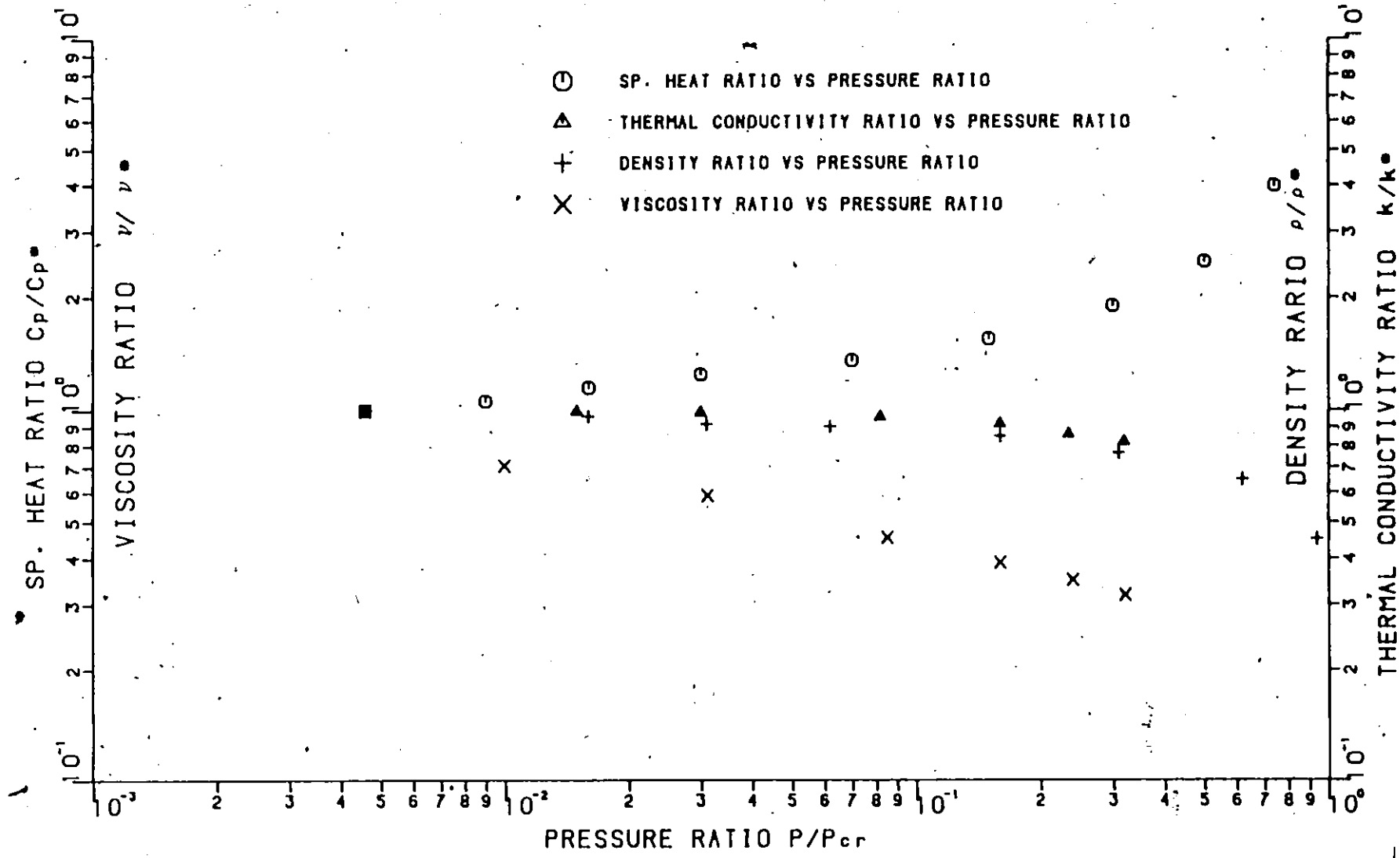

FIG.39 CORRELATION OF DATA FOR THE PHYSICAL PROPERTIES OF SATURATED LIQUID

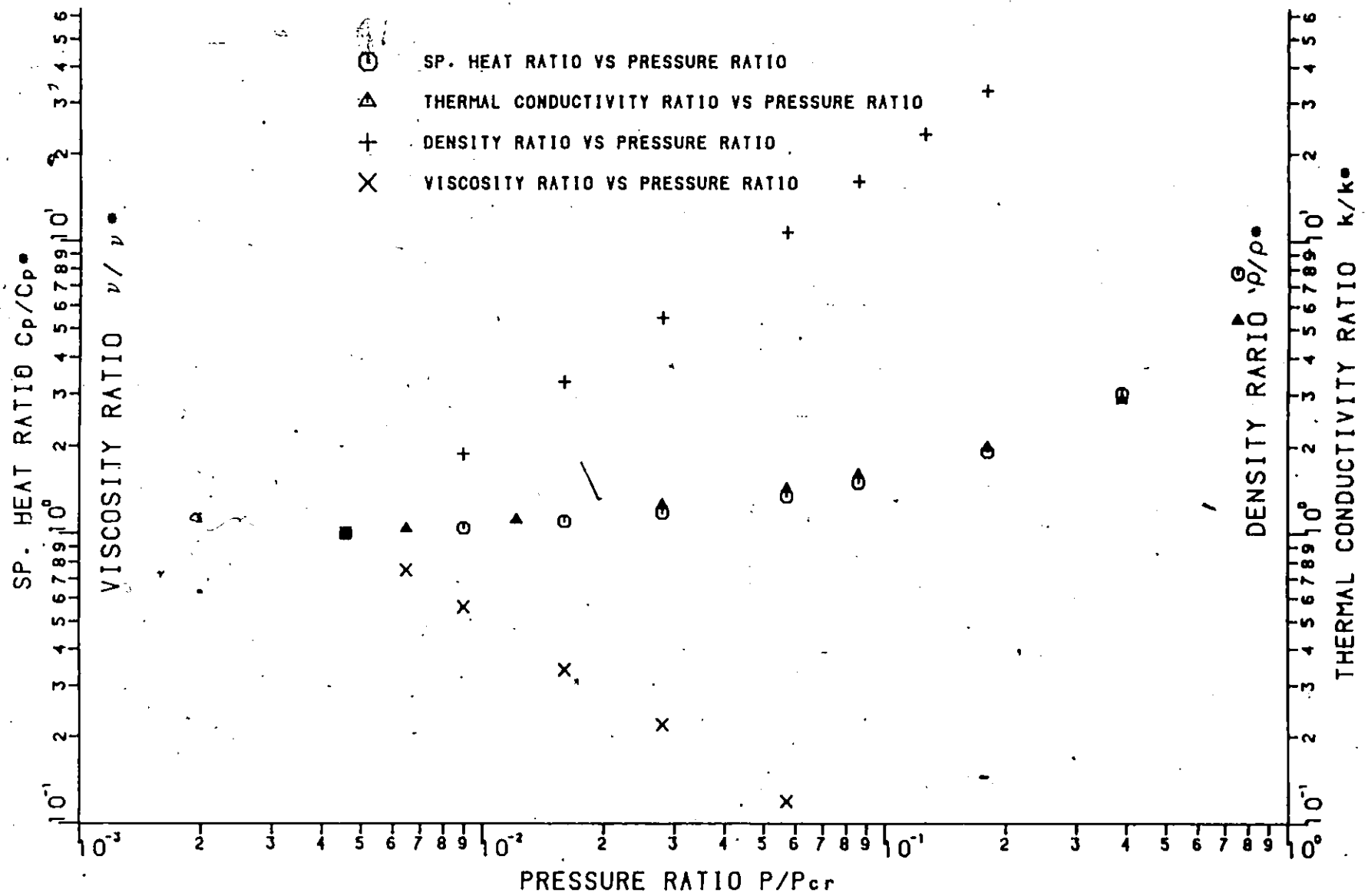

FIG.40 CORRELATION OF DATA FOR THE PHYSICAL PROPERTIES OF SATURATED VAPOUR

Tong's correlation [25]:

$$h_{TB} = 7000 \exp(.0082 T_{sat}) + .023 \frac{k_f}{D_e} \exp\left[-\frac{100}{T_{sat}}\right]\left[\frac{C_p \mu}{k}\right]_f \left[\frac{D_e G}{\mu_f}\left\{x_e \frac{\rho_f}{\rho_g} + (1-x_e)\frac{\rho_f}{\rho_l}\right\}\right]^{.8}$$

Weisman's correlation [7]:

$$h_{TB} = .5\, h_{CHF}\left[\exp\{-.0078(T_w - T_{CHF})\} + \exp\{-.698(T_w - T_{CHF})\}\right] + .023 \frac{k_g}{D_e}\left[\frac{\mu_g}{\mu_v}\right]^{.14}\left[\frac{C_p \mu}{k}\right]_g^{1/3}\left[\frac{G D_e x_e}{\mu_g}\right]^{.8}\left[1 + \frac{1-x_e}{x_e}\left[\frac{\rho_g}{\rho_l}\right]^{2/3}\right]$$

Hsu's correlation [26]:

$$h_{TB} = .62\left[\frac{g k_v^3 \rho_v (\rho_l - \rho_v) h_{fg}}{\Delta T_{sat} \mu_v} \frac{1}{2\pi}\sqrt{\frac{g(\rho_l - \rho_v)}{\sigma}}\right]^{1/4} + A \exp(-B\, \Delta T_{sat})$$

$$A = 1456\, P^{-.558} \qquad B = 3.758 \times 10^{-3}\, P^{-.1733}$$

as well as the Cheng et al (see 5.1.6).

5.1.5 Effect of Wall Properties.

The influence of the thermal properties of heating wall on the transition boiling heat flux was studied by Cheng et al [28] who reported the transition boiling data of water with copper, stainless steel, brass and Inconel surfaces at atmospheric pressure. Their results show that transition heat flux decreases with the increasing of $k\rho C_p$ of wall. In this experiment, only stainless steel and Inconel tubes are used. Since $k\rho C_p$ of both materials are very close, the effect of wall properties is not noticeable.

The roughness of surface has some effect on transition heat flux, but in this experiment all the tubes used are smooth surface ($\frac{\epsilon}{d} < 0.004$), hence, no conclusion can be made for this effect.

5.1.6 Correlation and Comparision

In this section, the measured transition boiling data are correlated, and compared with the applicable correlations and available data. The data for pressurized experiment can be correlated in the form of

$$\phi = \phi_a \left(\frac{P}{P_a} \right)^c \qquad 5.1$$

where ϕ heat flux at the pressure p

ϕ_a heat flux at the atmospheric condition

P pressure

P_a atmospheric pressure

c constant

The constant in Eq. (5.1) was determined based on experimental data by the SPSS program (Appendix IV) to be 0.3126. ϕ_a in Eq. (5.1) can be obtained from Cheng's general empirical correlation [22]:

$$\phi = 9.267 \times 10^7 (\Delta T_{sat})^{-1.18910 - 0.22599 \times 10^{-5} \sqrt{k\rho c_p}} \exp(0.02012\ \Delta T_{sub} + 0.00393 \cdot G + \frac{5770}{\sqrt{k\rho c_p}})$$

Figures 41 and 42 show the predicted pressurized boiling curves using Eq. (5.1) with the experimental results and good agreement is observed.

Groeneveld [29] concluded that the agreement between transition boiling correlation and experimental data was poor due to the scarcity of experimental data. Furthermore, these available data covered only a very limited range of conditions. It is difficult to find experimental data from available literature for comparison. The work done by Weisman et al is one of the very few studies on the effect of pressure on transition boiling. The results of Weisman and those of present experiment are shown in Figure 43. Since both experiments are not conducted under the same conditions, the results of the closest conditions are used for comparison.

From Figure 43, it is observed that the present experimental results are higher than Weisman's. This is because Weisman's results were obtained via a steady state method with the hot liquid metal circulating outside the test tube and water flowing in the tube, and the present experiment uses a transient method. Normally it is expected that the boiling heat flux measured by the transient method

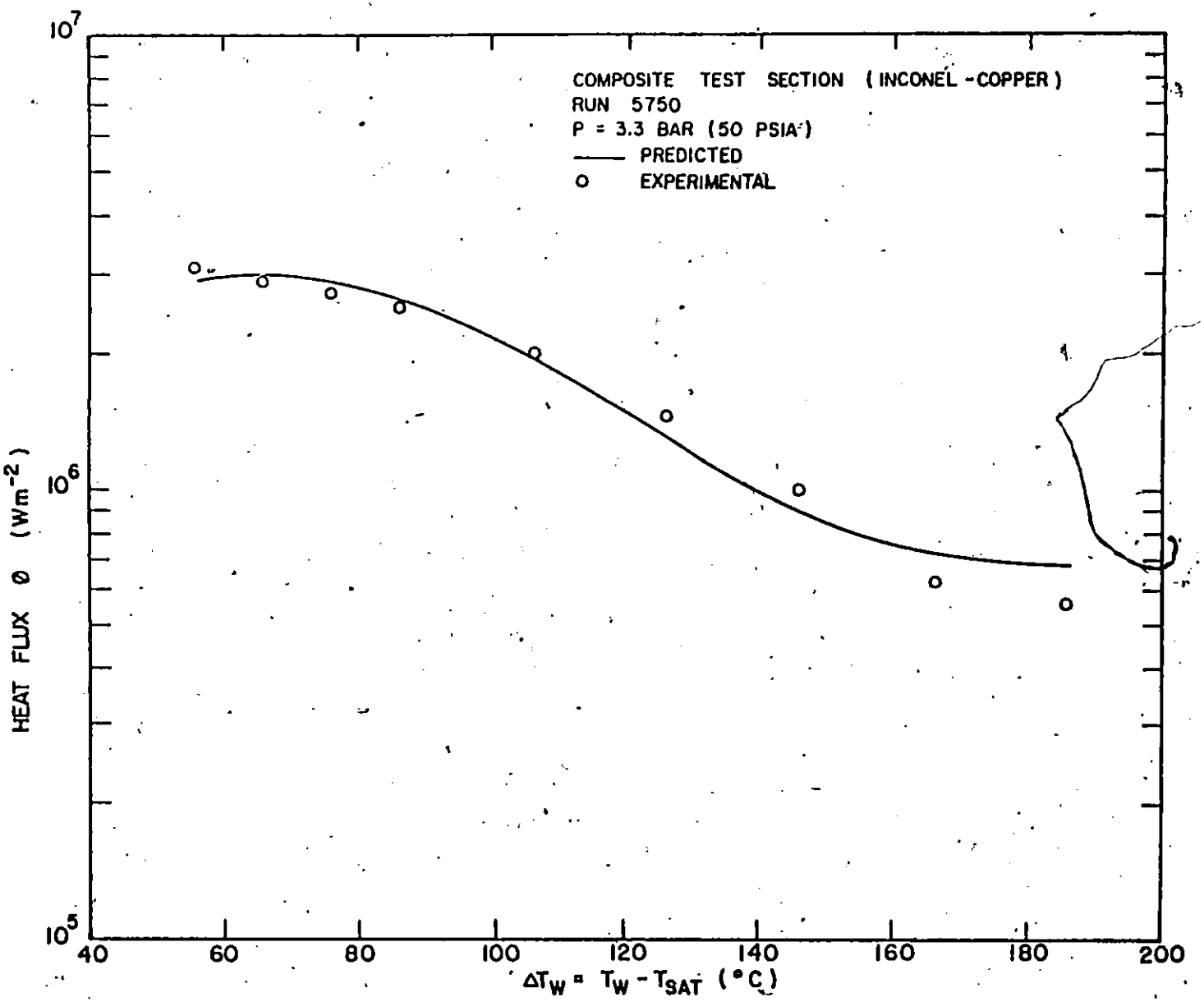

FIG.41 COMPARISON OF PREDICTED PRESSURIZED BOILING CURVE WITH EXPERIMENTAL DATA, 5700 RUN SERIES FOR P = 3.3 BAR, G = 136 $kgm^{-2}s^{-1}$ AND ΔT_{SUB} = 13.9°C

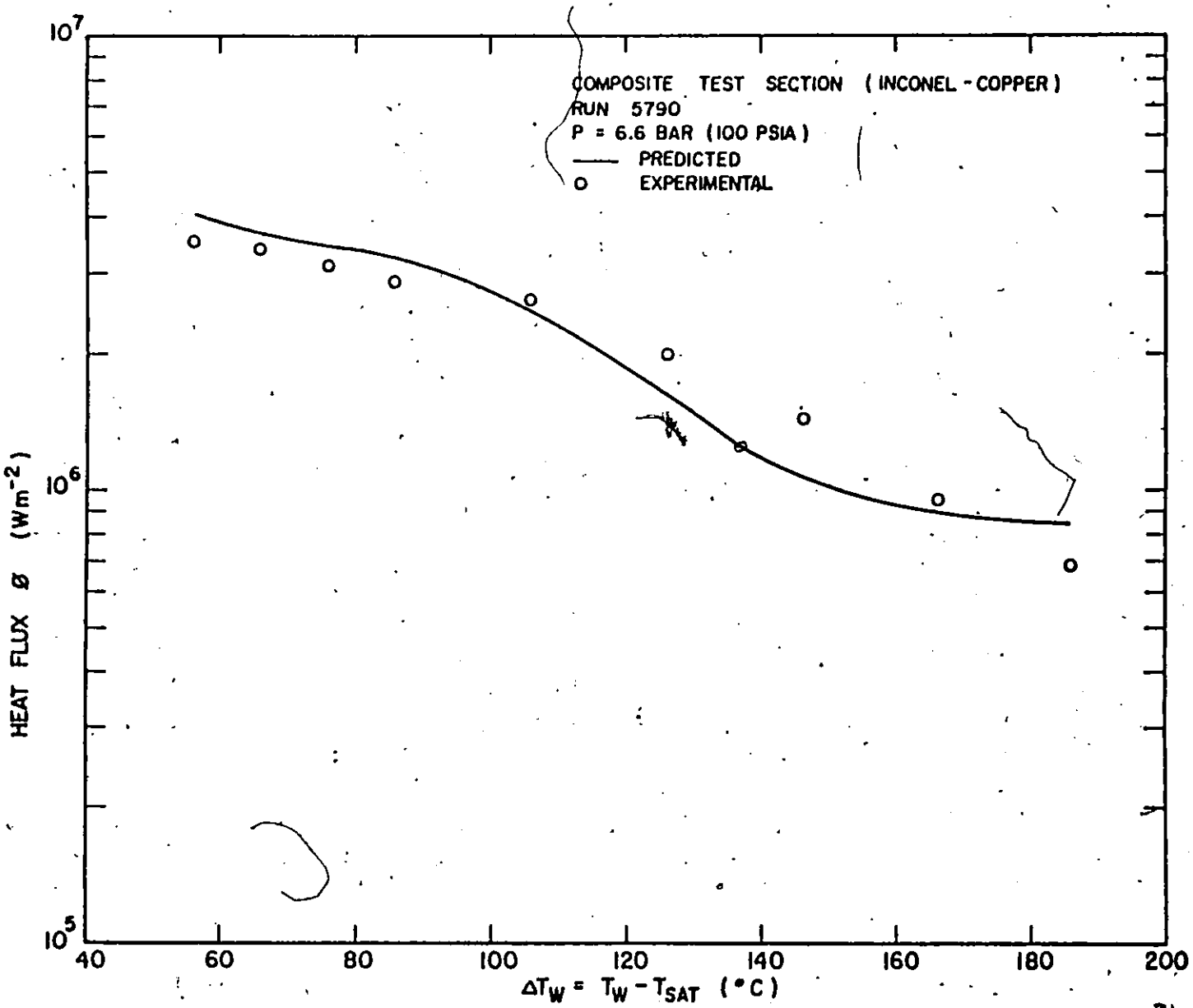

FIG.4 2 COMPARISON OF PREDICTED PRESSURIZED BOILING CURVE WITH EXPERIMENTAL DATA, 5700 RUN SERIES FOR P = 6.6 BAR, G = 136 $kgm^{-2}s^{-1}$ AND ΔT_{SUB} = 13.9 °C

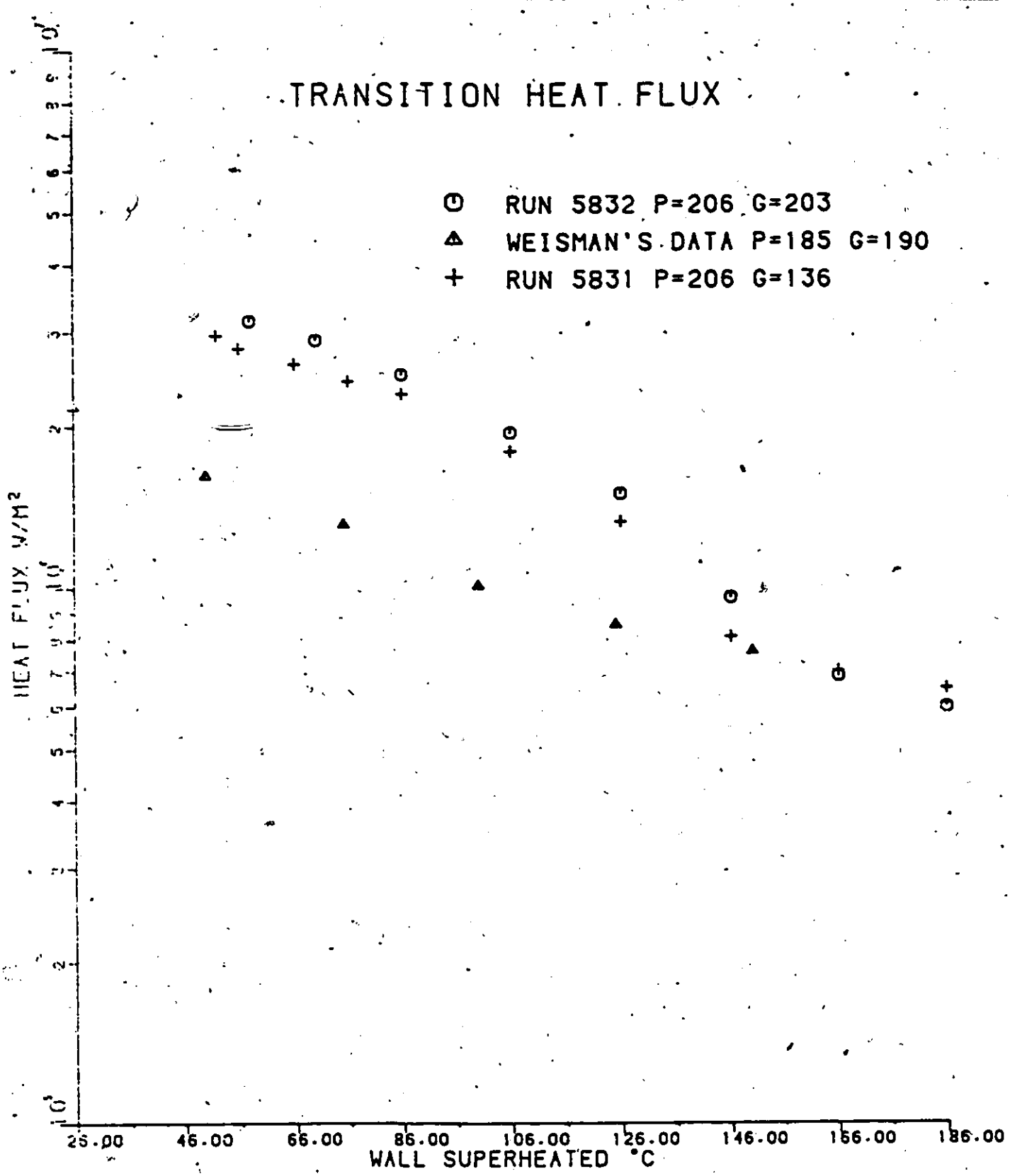

FIG.43 COMPARISION WITH WEISMAN'S DATA
BOILING HEAT FLUX FOR G=203

is higher than by the steady state method. One possible explanation is due to the fact that during the transient experiment the flow is not fully established, thus more mixing occured. This will result more efficient heat transfer, which is similar to the entrance flow region.

A correlation was derived by Hsu based on post CHF FLECHT data[26]. The correlation is reproduced here

$$h_{TB} = .62\left[\frac{gk_v^3 \rho_v (\rho_l-\rho_v)h_{fg}}{\Delta T_{sat}\,\mu_v}\;\frac{1}{2\pi}\sqrt{\frac{g(\rho_l-\rho_v)}{\sigma}}\right]^{1/4} + A\exp(-B\,\Delta T_{sat})$$

$$A = 1456\ P^{-.558}$$

$$B = 3.758\times10^{-3}\ P^{.1733}$$

Hsu's correlation does not depend on quality, but depends on pressure. The predicted results of Hsu's correlation and present experimental data are shown in Figure 44. Hsu's prediction is higher. This may be due to the fact that the FLECHT tests was conducted on a rod bundle. However, it shows the correct pressure trend in transition boiling region.

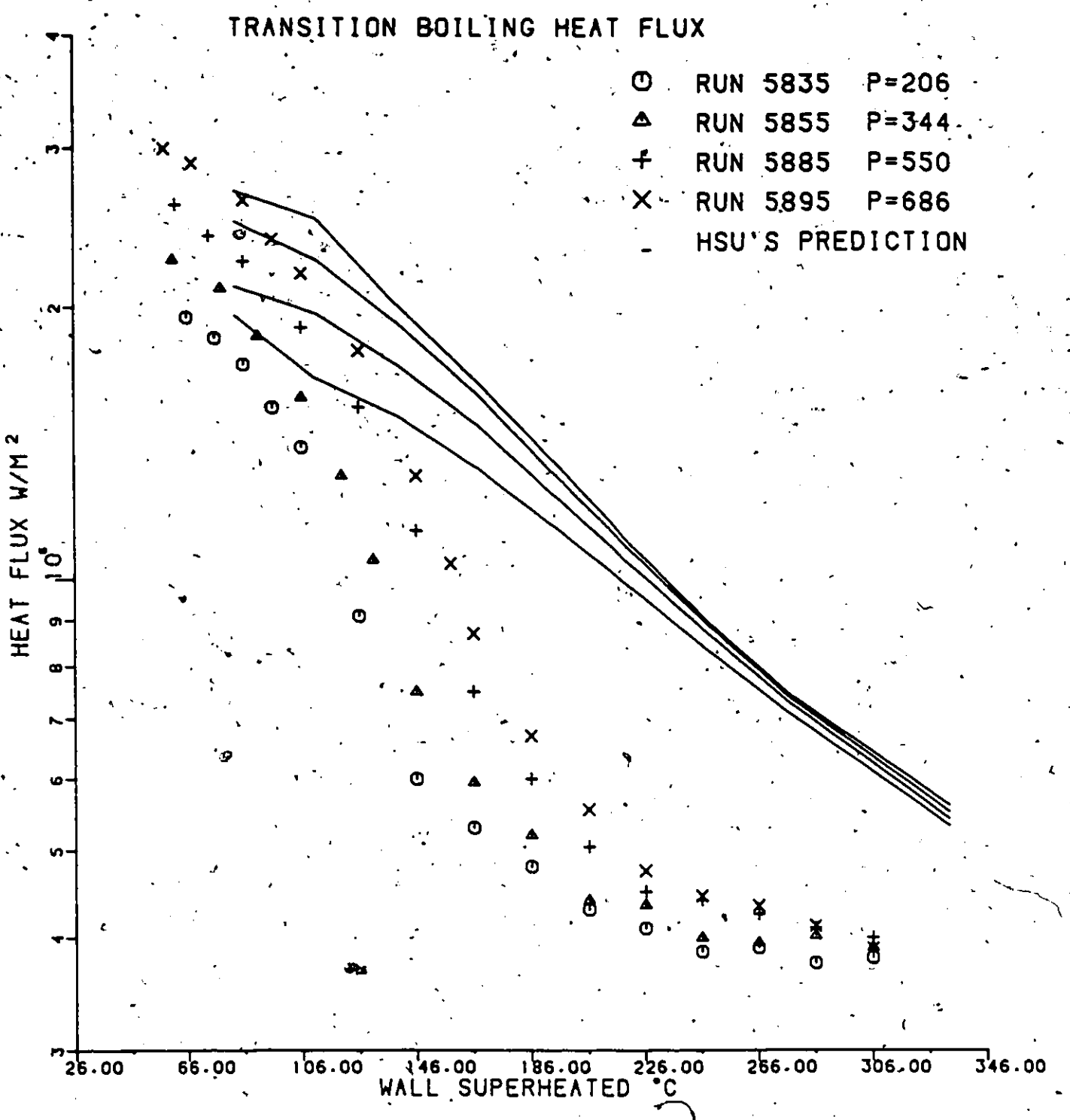

FIG.44 COMPARISION WITH HSU'S CORRELATION

5.2 PROBE STUDY

The probe measurement technique can detect rewetting and maximum heat flux points, as well as provide some knowledge on boiling phenomena during quenching.

5.2.1 Single Rod Results

The results and observation of probe experiment and their corresponding boiling curves for single rod runs are shown in Figure 45 to 56. The region AB in Figure 45 for Run 6022 representing film boiling shows a gradual rise of voltage with momentary dry collisions of liquid droplets with wall, as this is apparent from fluctuations of the voltage trace. Jackson and Jen [30], Petruckhov et al [31], and Van Stralen and Cole [32] all discovered that there was film layer thickness fluctuation during the film boiling on a vertical plate or cylinder.

Iida, Y. [33] found that the thickness of film layer over a flat copper surface is quite small, with less than 0.05 mm in pool boiling. If it is true in pool boiling, it is expected, with the introducing of the velocity component in flow boiling, that this thickness will be thinner and the collisions of the liquid droplets with wall becomes possible. The region AB of Figure 45 does indicate the liquid droplets momentarily hitting the dry wall and causing

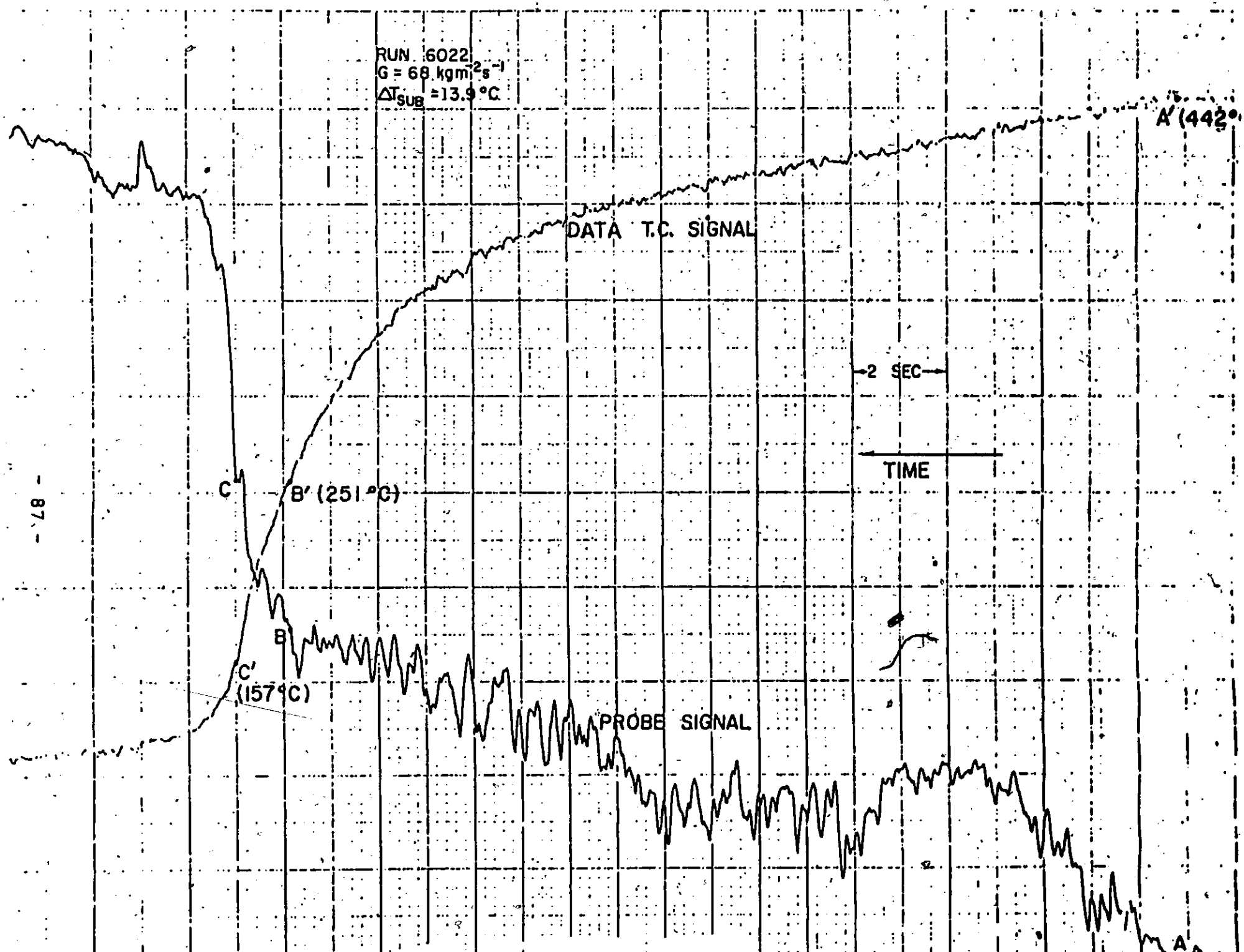

FIG 4.5 PROBE SIGNAL AND DATA T.C. SIGNAL FOR RUN 6022

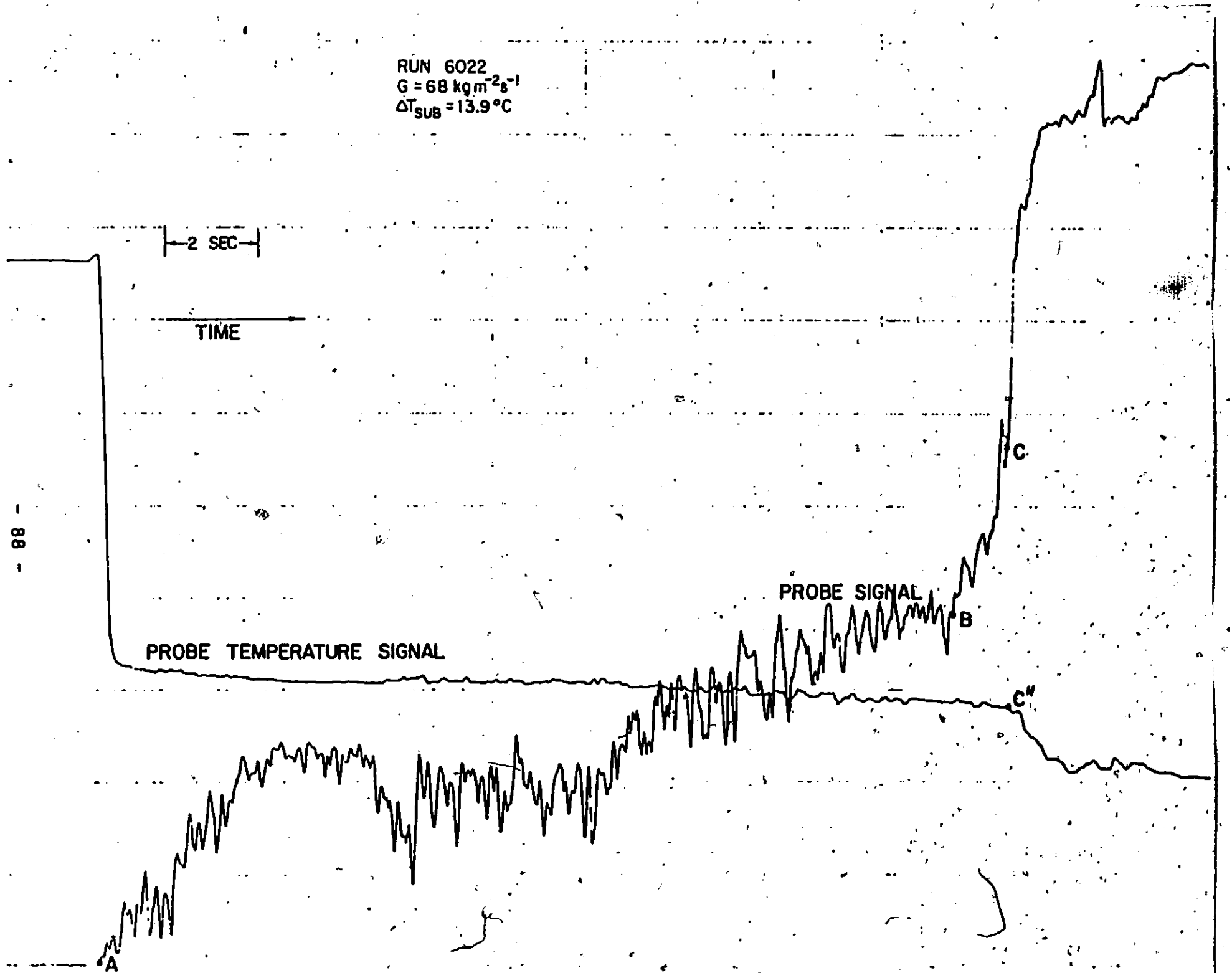

FIG. 46 PROBE SIGNAL AND PROBE TEMPERATURE SIGNAL FOR RUN 6022

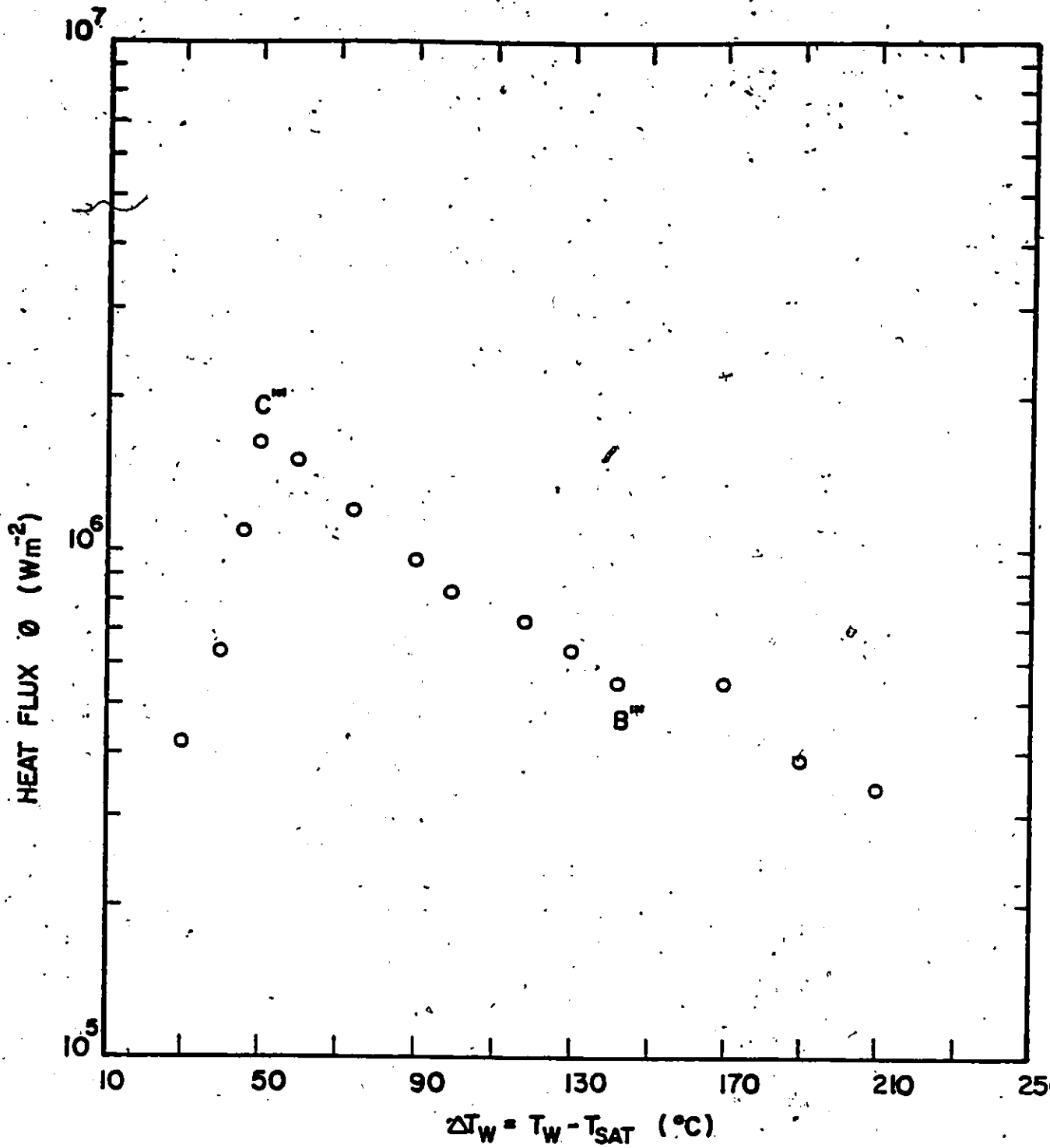

FIG. 47 BOILING CURVE OF DISTILLED WATER FOR RUN 6022 AT $G = 68\ kgm^{-2}s^{-1}$ AND $\Delta T_{SUB} = 13.9°C$

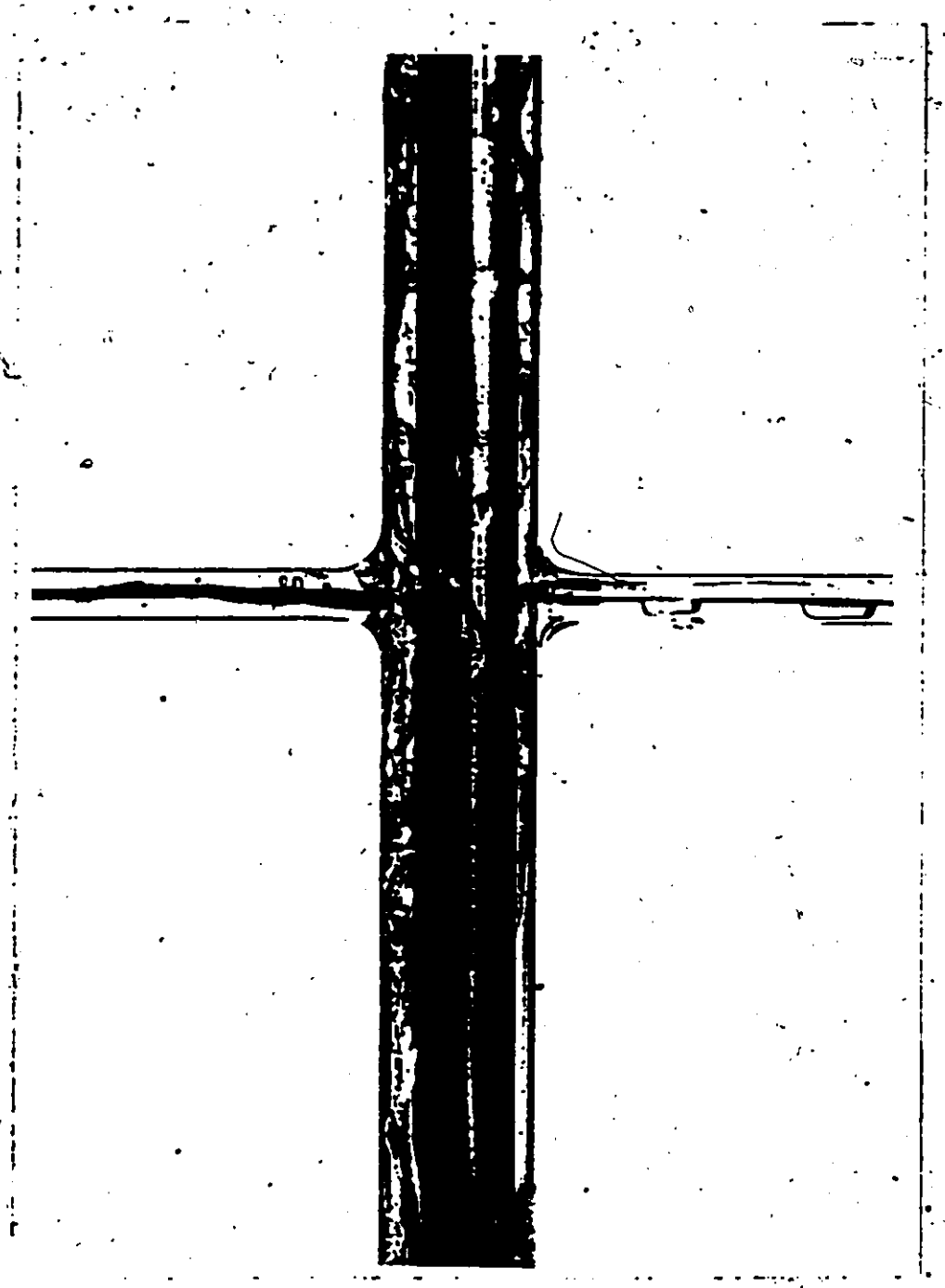

FIG. 48: Flow Region Before Initiation of Quench Front

FIG. 4 9 Quench Front Located at One Inch Below Probes

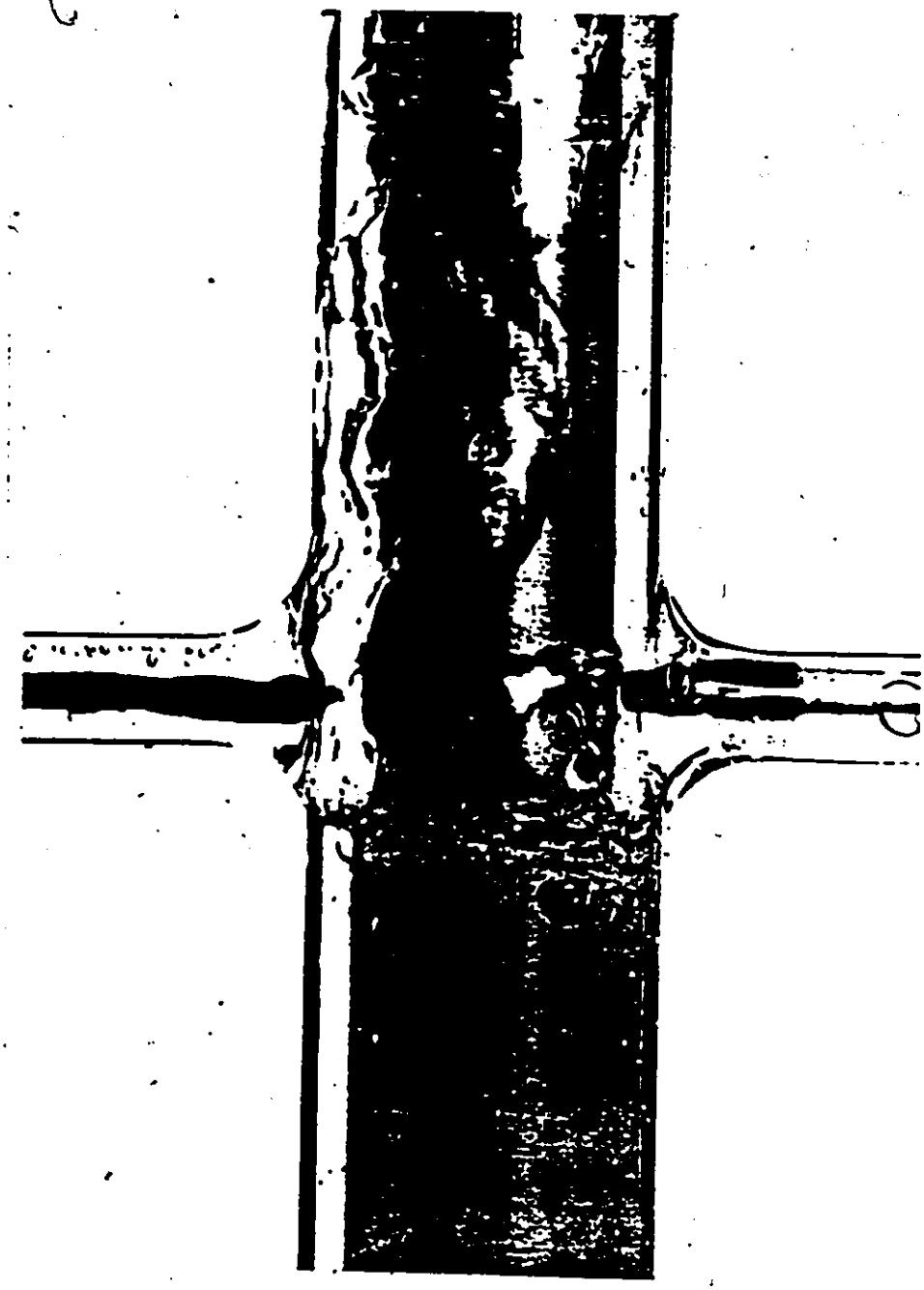

FIG.50 Quench Front Located Just Below Probes

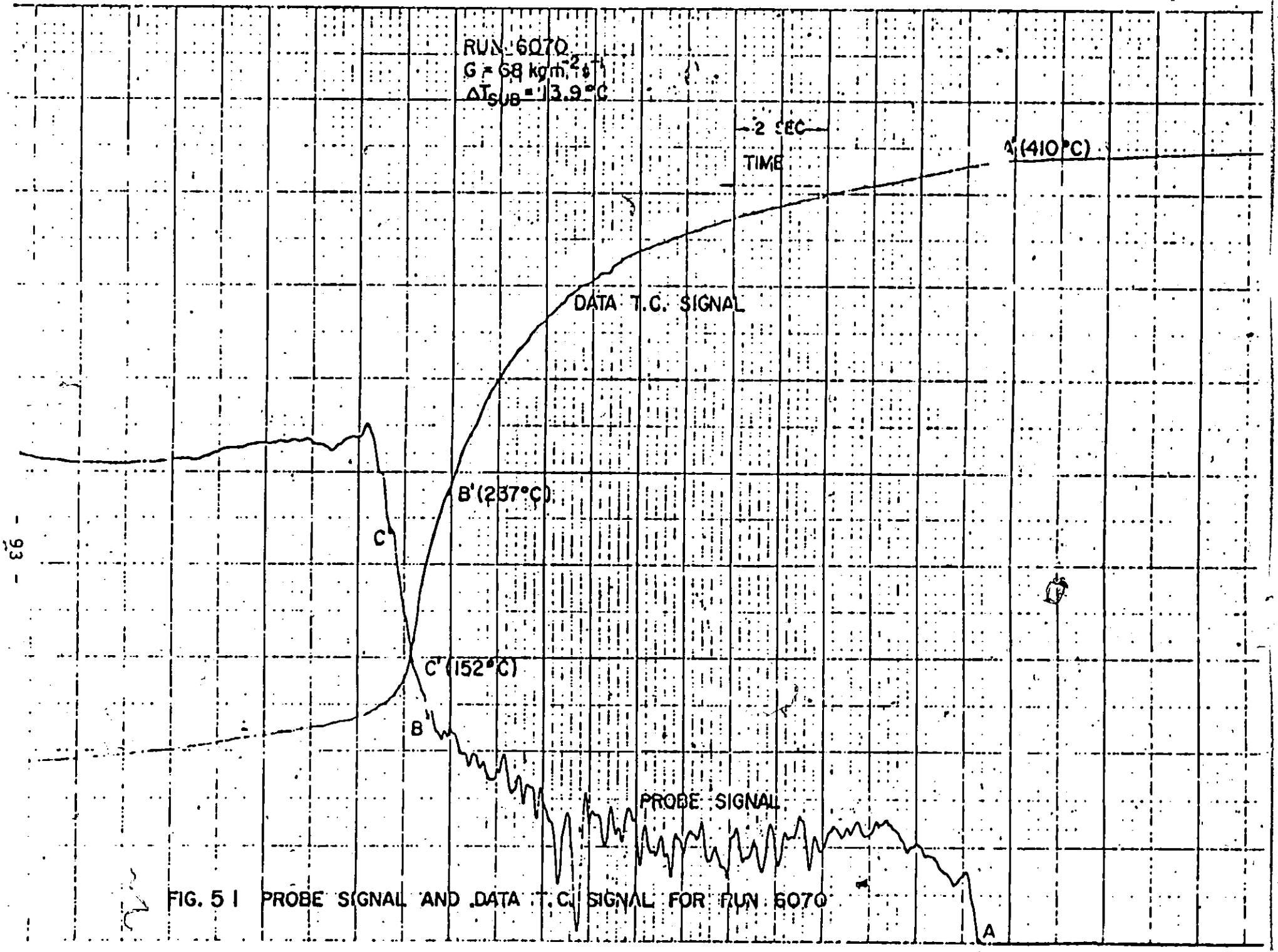

FIG. 5 I PROBE SIGNAL AND DATA T.C. SIGNAL FOR RUN 6070

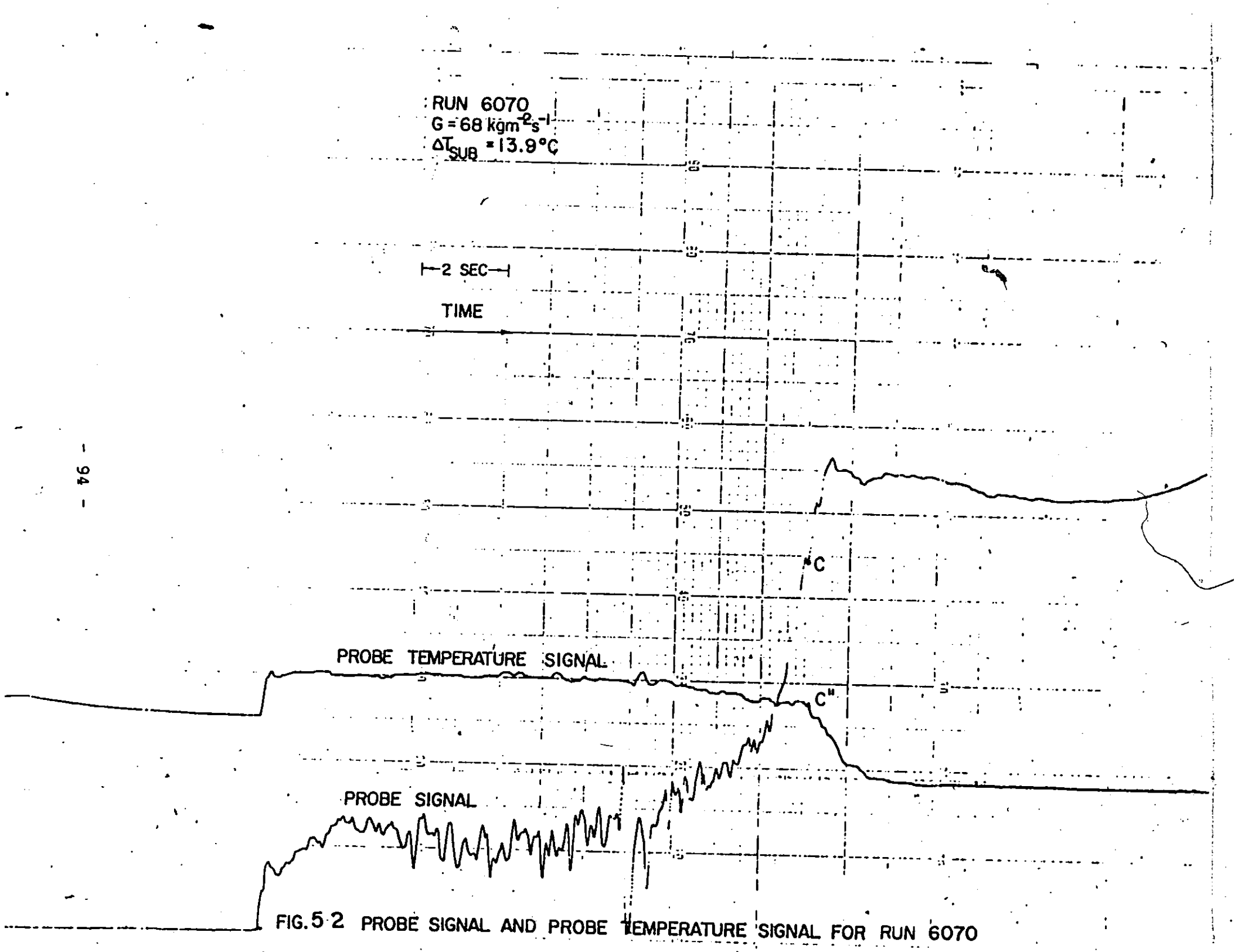

FIG. 5·2 PROBE SIGNAL AND PROBE TEMPERATURE SIGNAL FOR RUN 6070

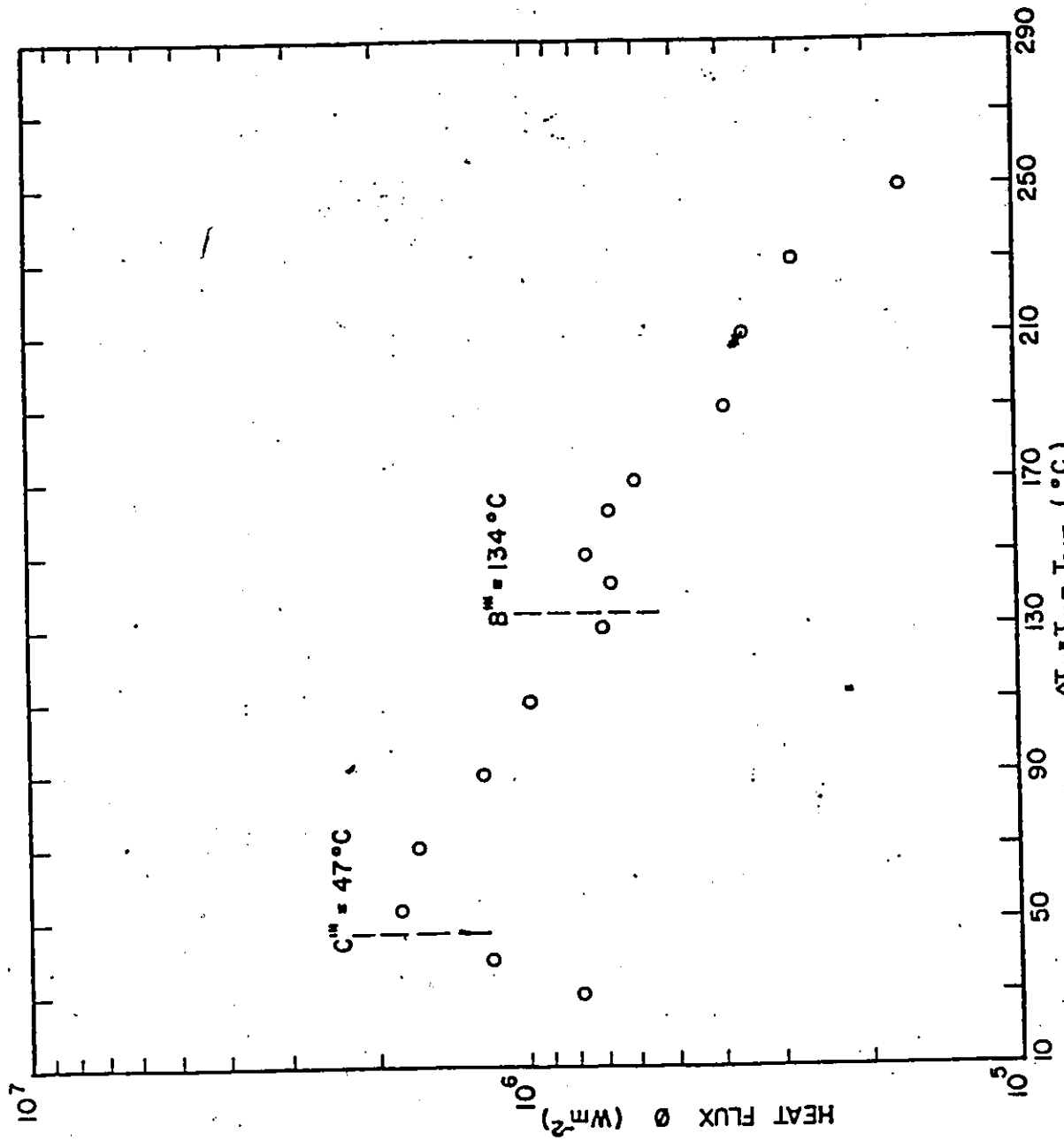

FIG. 53 BOILING CURVE OF DISTILLED WATER FOR RUN 6070 AT
$G = 68\ kgm^{-2}s^{-1}$ AND $\Delta T_{SUB} = 13.9$ °C

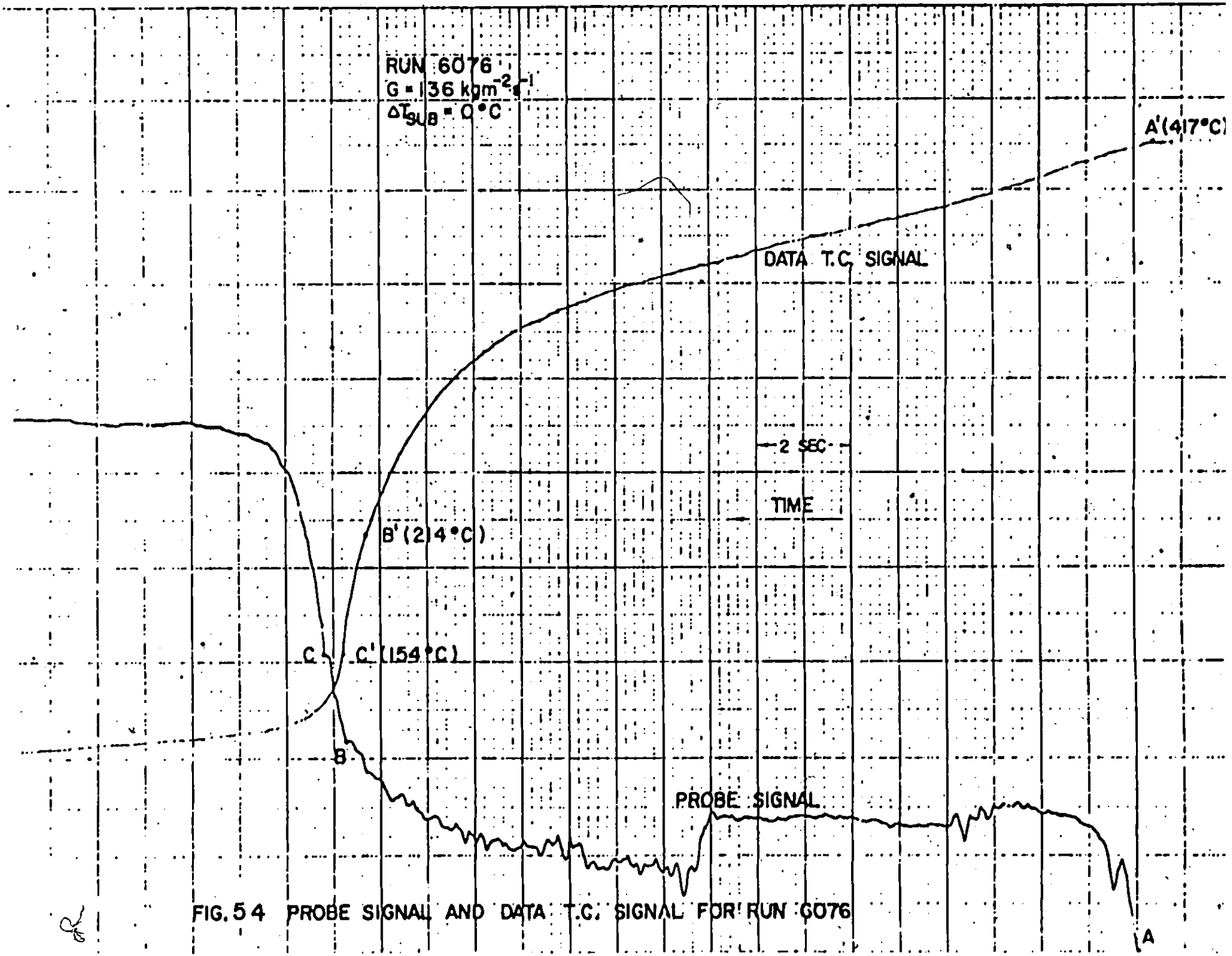

FIG. 54 PROBE SIGNAL AND DATA T.C. SIGNAL FOR RUN 6076

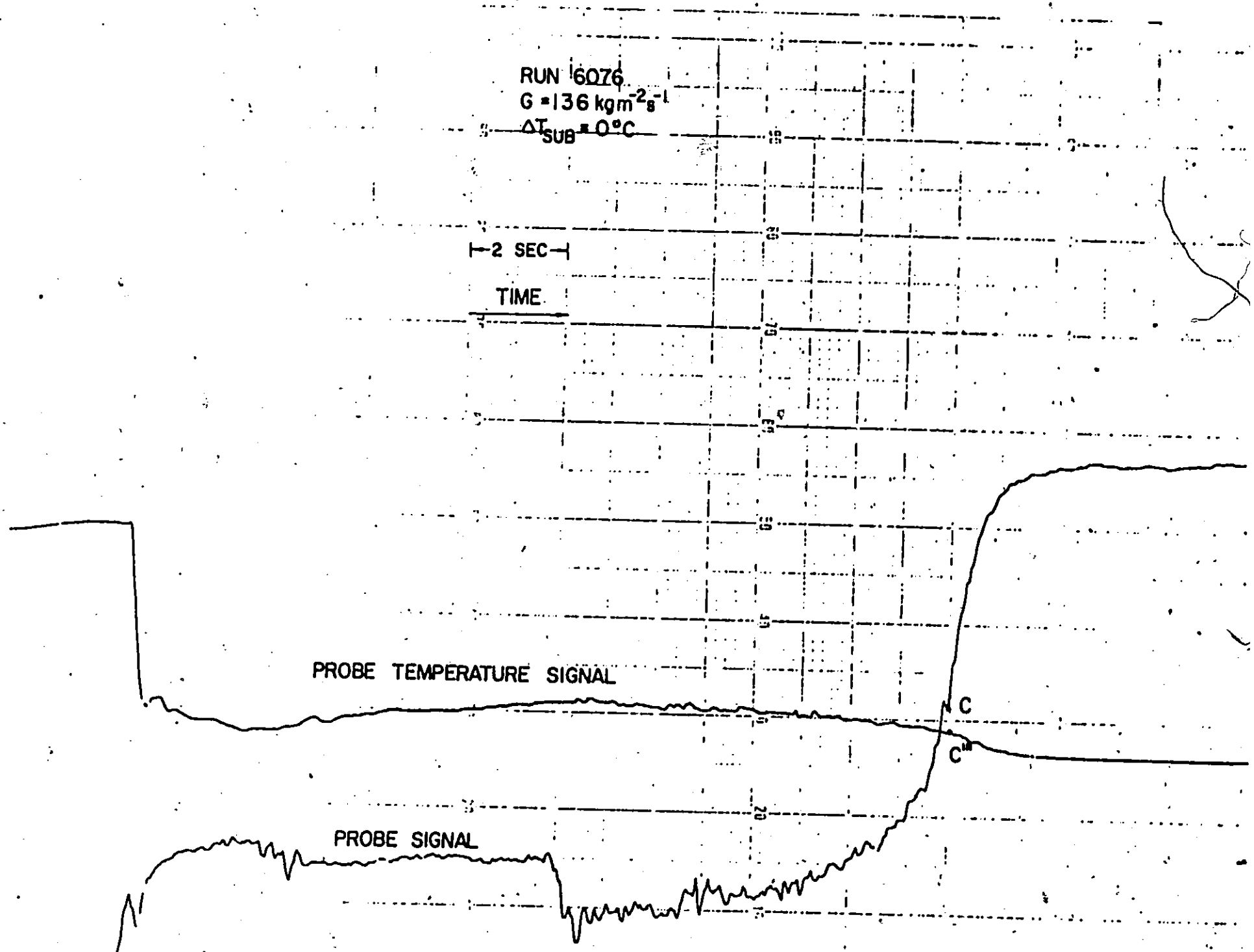

FIG. 55 PROBE SIGNAL AND PROBE TEMPERATURE SIGNAL FOR RUN 6076

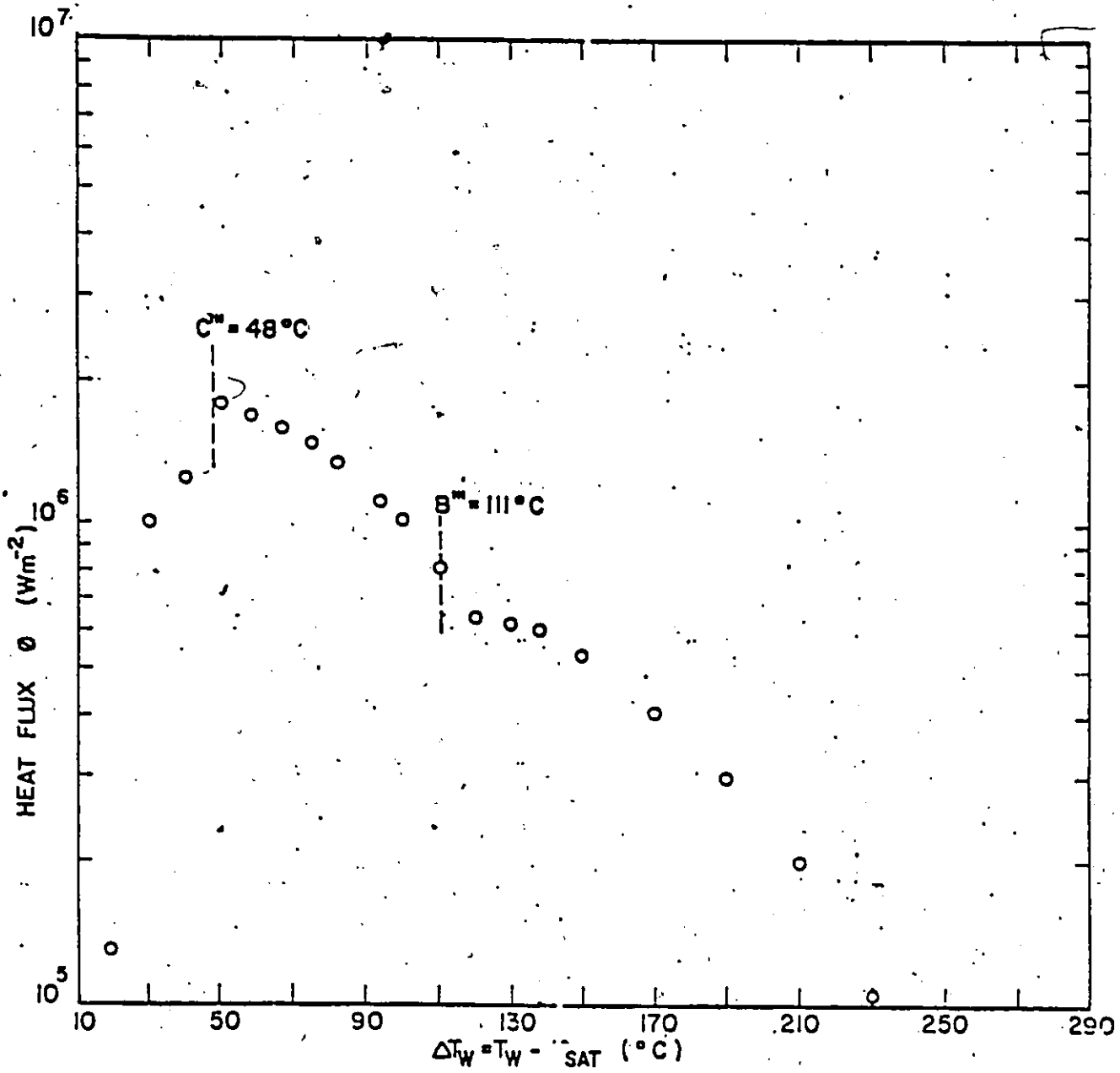

FIG.5.6 BOILING CURVE OF DISTILLED WATER FOR RUN 6076 AT $G = 136\ kgm^{-2}s^{-1}$ AND $\Delta T_{SUB} = 0°C$

the probe signal to increase and decrease again. This is the reason that the signal of region A B is fluctuating.

The region BC characterizes transition boiling with a sharp rise of voltage starting from point B. It is also observed visually (Figure 48) that at point B the rewetting front reaches the probe station. Point C is the CHF point as witnessed by a steep rise of voltage. In addition, point C also signifies a rapid drop of probe temperature as seen from point C" of Figure 46. The duration for transition boiling in this annulus flow lasts only a few seconds.

Points A', B' and C' are the corresponding points A, B and C on data thermocouple trace in the Figure 45. Its significance can be explained in conjunction with the resulting boiling curve of that particular run. The mathematical model presented in Chapter IV is used for the construction of boiling curve. From the boiling curve (Figure 47) the minimum point B''' occurs at T_w = 243°C and the corresponding data thermocouple reading from the computer program is 246°C as compared with B' value of 251°C. Similarly, CHF point C''' occurs at T_w = 150°C and corresponding data thermocouple reading from the computer program is 157°C, which is of the same value as C'. The results of rewetting and CHF points from probe signal are very close to those of boiling curve. Notice that in Figure

47, the film boiling heat flux at ΔT_w greater than 170°C does not follow the expected trend. This is due to the experimental system transient effect, hence this portion of the boiling curve should be ignored.

Run 6070 is the repetition of Run 6022. The results are shown in Figure 51 to 53. Notice that point B''' and C''' in Figure 53 represent the wall temperature at the minimum and CHF point, respectively, based on the probe study after the correction for the distance of thermocouple and the wall. Since the probe has been changed, the probe tip size might not be exactly the same as the previous one. As a result, the tracings of Runs 6022 and 6070 are not identical. In analyzing the Point A', B', and C', the time lag on the recorder trace has been taken into consideration. The overall results are not much different from previous run. Figure 54 to 56 are the results for Run 6076, in which the mass flux is 136 kg/m^2sec and ΔT_{sub} is 0°C. The probe temperature, which is the temperature of fluid, drops much less during quenching than those of previous runs.

5.2.2 3-Rod Bundle Results

A series of experimental runs was conducted for G varied from 34 - 68 kg/m^2sec and ΔT_{sub} from 7°C to 13.9°C. A typical result of G = 68 kg/m^2sec and ΔT_{sub} = 13.9°C

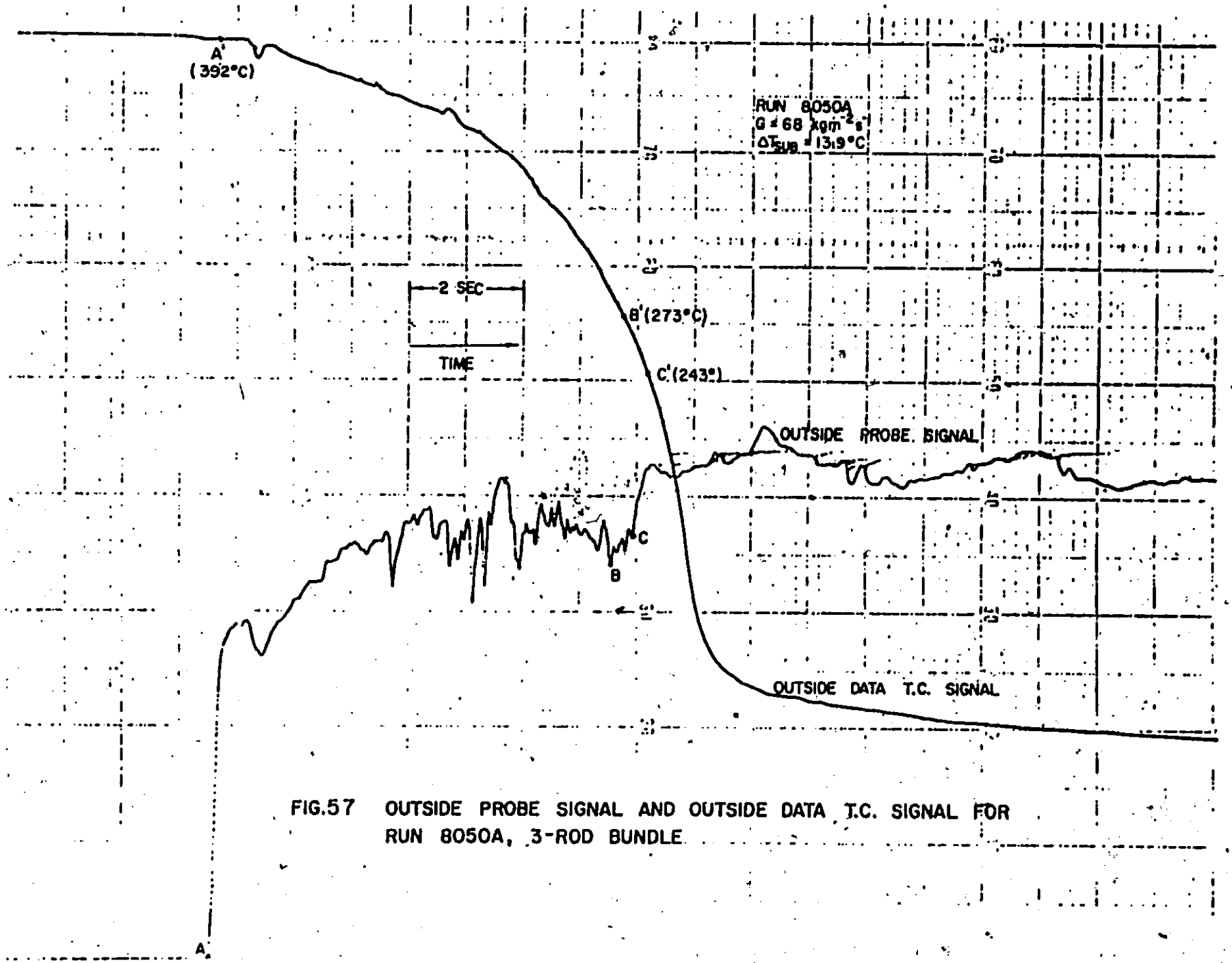

FIG.57 OUTSIDE PROBE SIGNAL AND OUTSIDE DATA T.C. SIGNAL FOR RUN 8050A, 3-ROD BUNDLE

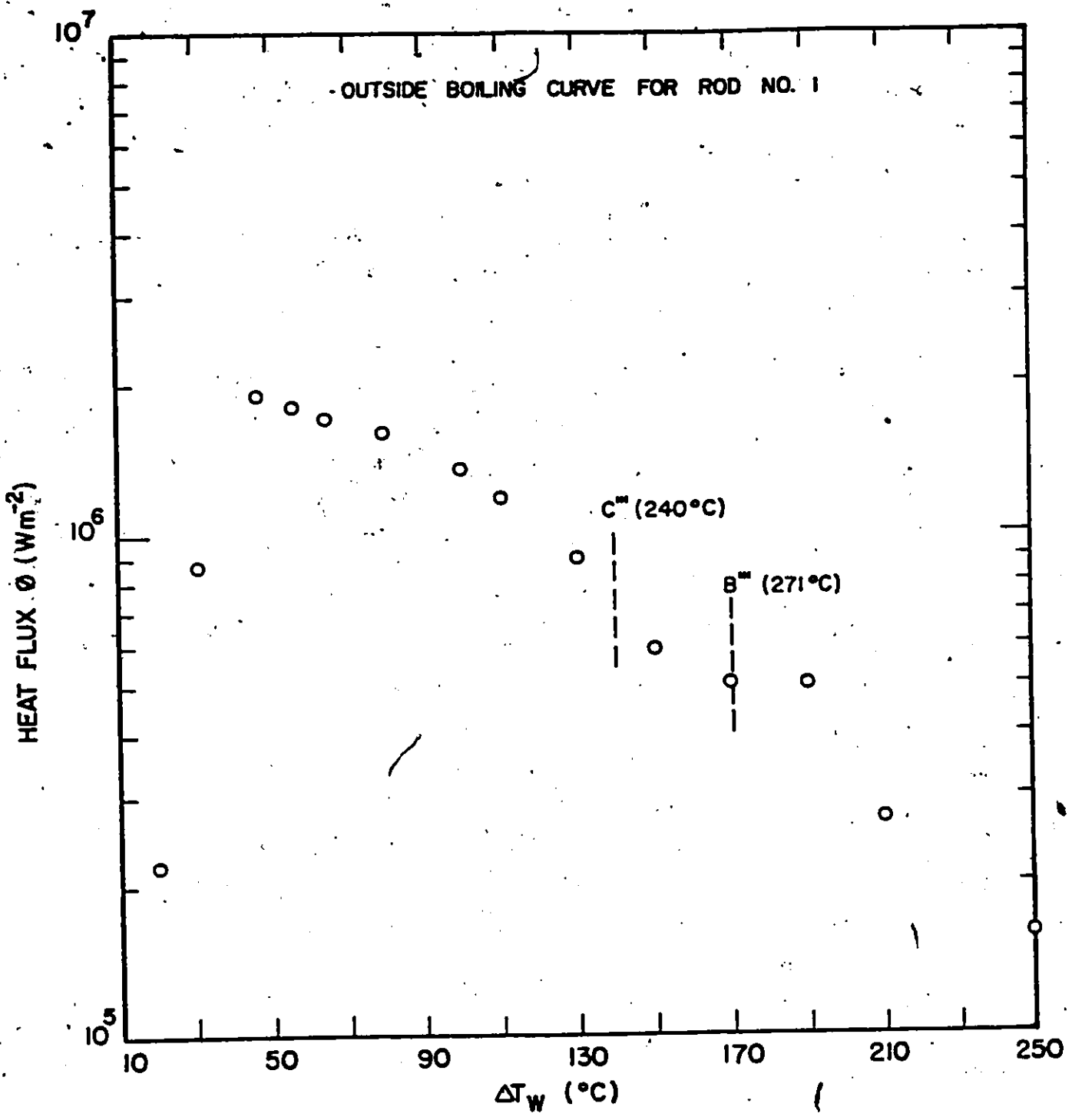

FIG.58 BOILING CURVE OF DISTILLED WATER FOR RUN 8050A, 3-ROD BUNDLE, AT $G = 68\ kgm^{-2}s^{-1}$ AND $\Delta T_{SUB} = 13.9°C$

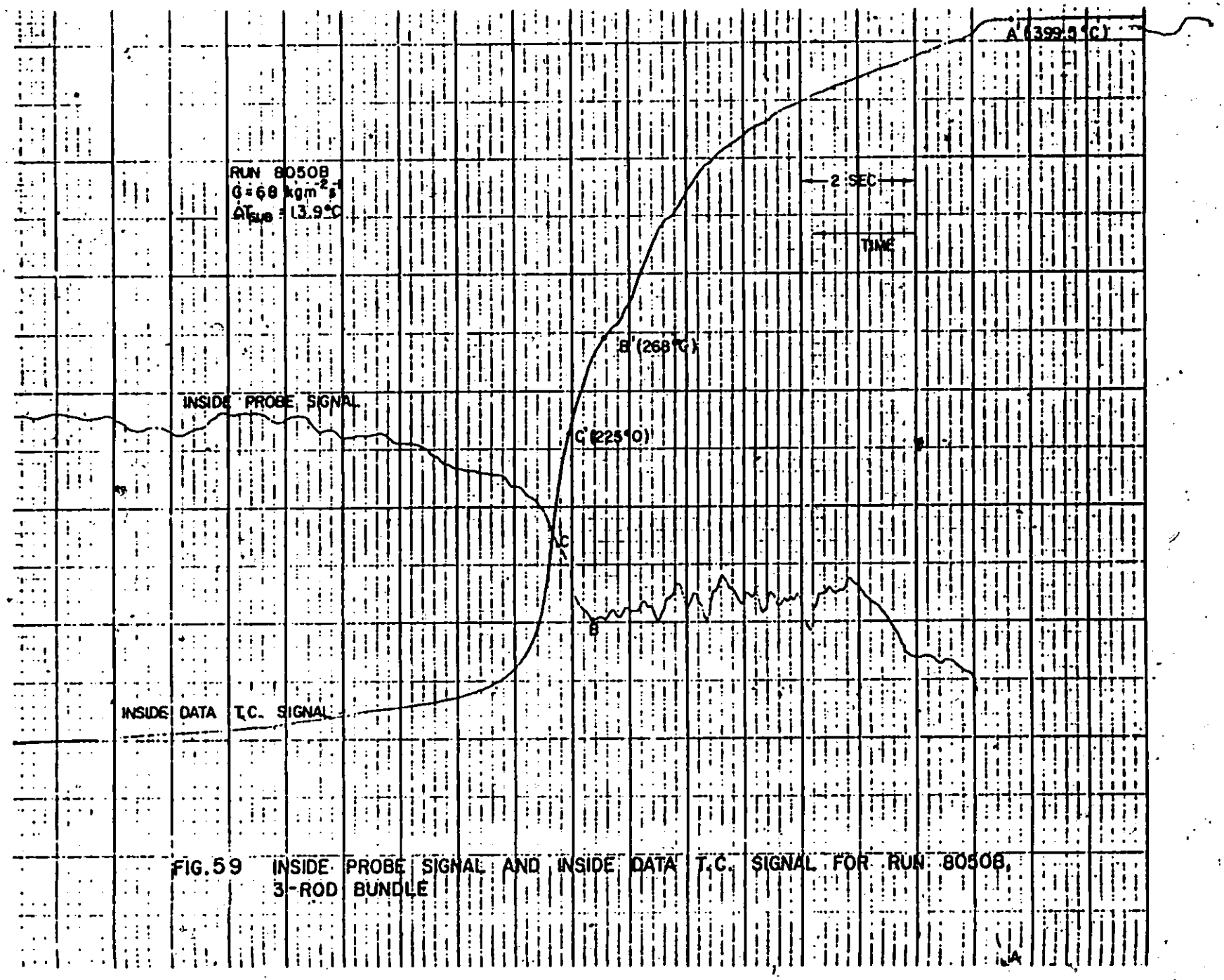

FIG. 59 INSIDE PROBE SIGNAL AND INSIDE DATA T.C. SIGNAL FOR RUN 80508, 3-ROD BUNDLE

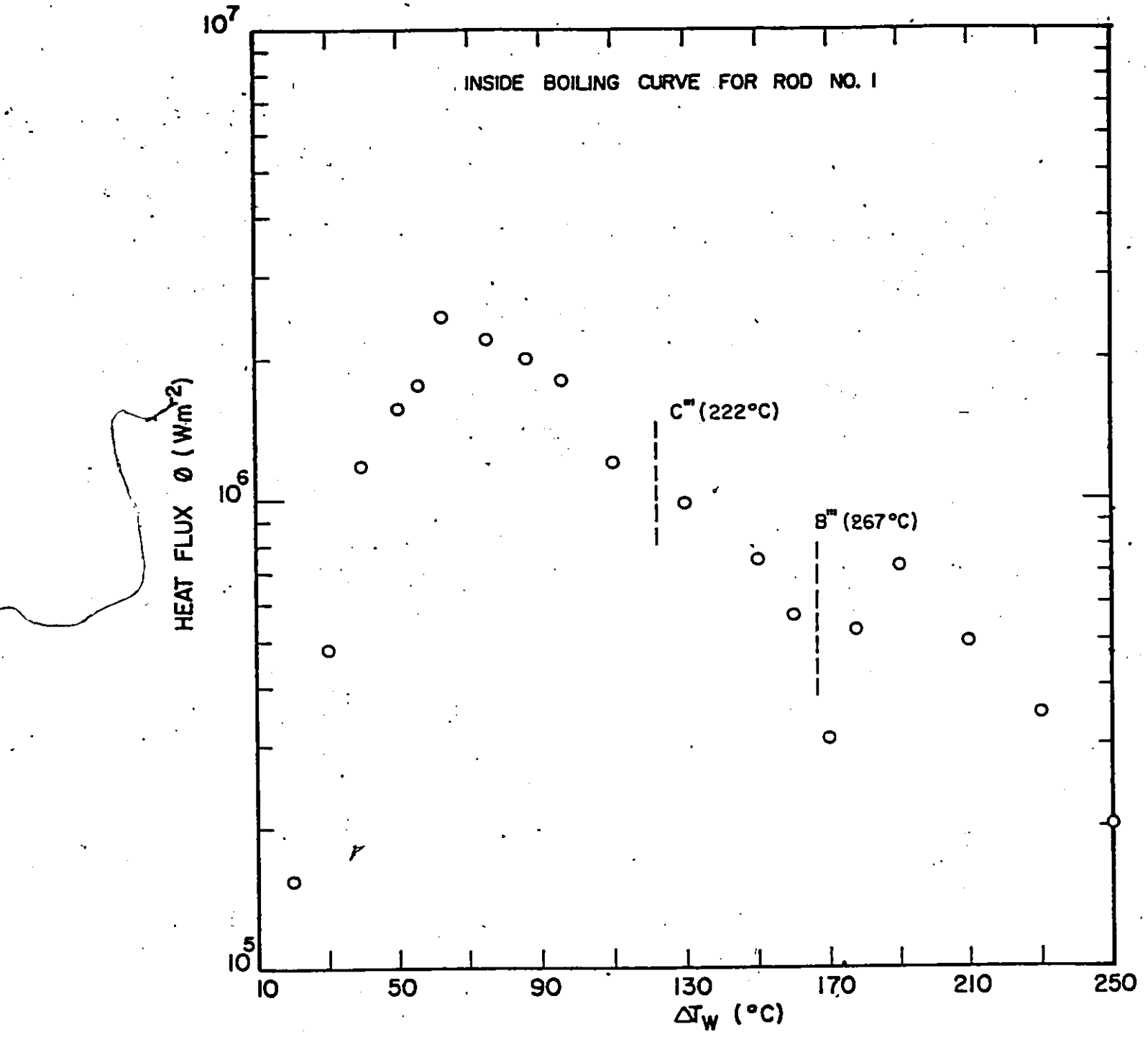

FIG. 6 0 . BOILING CURVE OF DISTILLED WATER FOR RUN 80508, 3-ROD BUNDLE , AT $G = 68\ kgm^{-2}s^{-1}$ AND $\Delta T_{SUB} = 13.9\ °C$

is shown in Figure 57 to 60. There are two thermocouples in each rod and two probes inserting into the test section, namely, the outside probe and inside probe, as shown in Figure 23. Figure 57 shows the outside probe signal generated for rod #1 (see Figure 23) with the probe located close to the outside data T.C., and the outside data T.C. signal. Similarly, the inside probe signal and the inside data T.C. signal are shown in Figure 59. Comparing Figure 57 (3-rod bundle) with Figure 46 (single rod), the trend of temperature history of both tests is very close.

The time for film boiling is shorter in the 3-rod test than single rod. This is because the percentage of rod area in the flow channel is smaller for the 3-rod case. However, the signal of probe also indicates the fluctuation due to droplet collision which is similar to single rod. The probe signal for nucleate boiling for 3-rod bundle is also similar to single rod. The same method as was used for the single rod is applied to determine points A, B, C, A', B', and C'. These are shown on Figure 57 and 59. The corresponding points B''' and C''' are plotted on outside and inside Boiling curves (Figure 58 and 60). The two boiling curves look quite the same, except the inside boiling curve has slightly higher values of heat flux around the CHF region. For the outside probe and thermocouple (Figure 57), point B is the rewetting point from the probe signal. Its

corresponding B' of thermocouple indicates the temperature is 273°C. Point C is the CHF point from probe signal and its corresponding point C' temperature is 243°C. After the correction for the distance between the thermocouple and test section wall, point B''' and C''' are 271°C and 240°C, respectively, as plotted in Figure 58. Similarly, points A, B, C, A',B' ,C' ,A''', B''', and C''' are determined based on inside probe and inside data thermocouple signals. It is obvious that the minimum points are in good agreement for both the probe result and the boiling curve. However, the CHF temperature from probe signal is much higher than that from the boiling curve. The reason may be due to subchannel effects, thus the flow is much more violent. Based on the experimental studies, it seems to indicate that the probe cannot respond to this violent physical phenomenon.

5.2.3 Comparison for Minimum Point

The present experiment measures the CHF and minimum film boiling points on the copper surface only for a small range of mass flux and subcooling. Outside this range, stable film boiling is very hard to establish in this experiment. In addition, the flow is so violent that the probe cannot respond properly under this physical situation. The rewetting temperature for single rod tests is 251°C for G = 68 kg/m^{2}sec, and ΔT_{sub} = 13.9°C; 211°C for G = 136 kg/m^{2}sec,

and ΔT_{sub} = 0°C. In the three rod test, the minimum temperature is between 267 to 271°C for G = 68 kg/m^2sec and ΔT_{sub}= 13.9°C.

The empirical correlation suggested by Stewart [3] is:

$$T_{min} = 284.7 + 44.11P - 3.72P^2 - \frac{x \cdot 10^4}{2.819 + 1.22P}$$

$x \leq 0$, $P \prec 9$ MPa

P = pressure in MPa

T_{min} = minimum temperature in °C

For run 6022 (P = .101 MPa, G = 68 kg/m^2sec), the local quality x obtained by a heat balance in the flow channel is -0.0027. Using the above correlation, the calculated T_{min} is 295°C, which is higher than the present experimental value (251°C). It should be noted that Stewart's correlation is based mostly on his high pressure experimental data, and the mass flux term is not included because the effect of mass flux is negligibly small. While the mass flux effect is an important factor in this experiment, one of the reasons for this large discrepancy could be due to the different configurations of test sections.

Chapter VI

CONCLUSION AND RECOMMENDATION

6.1 PRESSURIZED LOOP FOR TRANSITION BOILING

In the present quenching experiment, the system approaches a temperature controlled system. The test covers a small range of system pressure(101 to 686 kPa), mass flux(68 to 203 kg/m^2sec) and inlet subcooling(13.9 to 27.8°C). These test results which show the pressure effect on transition boiling, extend Cheng's previous study. The results from this experiment indicate that under the pressurized condition, the subcooling effect has no significant influence on transition boiling, which is contradictory to the results at atmospheric condition. The transition boiling data increase with pressure and mass flux within the above mentioned flow parameters range. A correlation including pressure, mass flux, subcooling and surface properties(thermal conductiviy, density and specific heat) effects has been established for the present testing conditions.

6.2 STUDIES OF ELECTRIC RESISTANCE PROBE

The probe method in measuring the CHF is in good agreement with the CHF point from the boiling curve for the single rod experiment. This method is not so successful for three rod bundle. The reason for this seems to be due to the subchannel effect during quenching. The rewetting temperature measured by probe method is close to the minimum film boiling temperature from the boiling curve for both single and three rod test sections.

6.3 RECOMMENDATION FOR FUTURE WORK

In the present project the transition boiling data at slightly elevated pressure, CHF and minimum film boiling points at the atmospheric condition have been measured. The transition boiling data and probe study results from this project cover only a small range of flow parameters. It is advisable to

1. extend to higher pressures for transition boiling data.
2. use the probe approach to confirm the minimum and CHF points for the transition boiling results at elevated pressure.
3. conduct experiment with different surface properties $k\rho C_p$.

BIBLIOGRAPHY

1. Berenson,P.J., "Experiments on Pool-Boiling Heat Transfer.", Int. J. Heat And Mass Transfer. vol. 5, pp. 985-999, 1962.

2. Bradfield, W.S., "Liquid-Solid Contact in Stable Film Boiling ", I & EC Fundamentals, Vol.5 No.2, May 1966.

3. Fung, K.K., "Subcooled and Low Quality Film Boiling of Water in Vertical Flow at Atmospheric Pressure", Ph.D. Thesis, U. of Ottawa, 1981.

4. Stewart, J.C., "Low Quality Film Boiling at Intermediate and Elevated Pressures" M.A.Sc. Thesis U. of Ottawa,1981

5. Collier, J.G., Convective Boiling And Condensation, McGraw-Hill Book Company (U.K) Ltd., 1981

6. McDonough, J.B., Milich, W. and King, E.C., "An Experimental Study of Partial Film Boiling Region with water at elevated Pressures in a round Vertical Tube", Chem. Eng. Prog. Symposium Series, Vol. 57 No. 32, pp. 197-208, 1961.

7. Jens, W.H. and Lottes, P.A., "Analysis of Heat Transfer, Burnout, Pressure Drop, and Density Data for High Pressure water", ANL-4627,1951.

8. Weisman, J., Kao, Y.K. and Rahrooh, G., "Transition Boiling Heat Transfer in a Vertical Round Tube", ASME 79 HT-47 1979.

9. Rama, K. and Weisman, J., Nuclear Eng. and Design, vol. 40, pp.285, 1977.

10. Ellion, M. E., "A Study of the Mechanism of Boiling Heat Transfer", California Inst. of Technology report JPL-MEMO-20-88, 1954.

11. Cheng, S.C. and Ng, W., "Transition Boiling Heat transfer in Forced Vertical Flow via a High Thermal Capacity Heating Process", Letters in Heat Transfer Vol 3, pp.333-342, 1976.

12. Yao, S.C. and Henry, R.E., "An Investigation of the Minimum Film boiling Temperature on Horizontal Surface", J. of Heat Transfer, Vol 100, pp. 260-266, May 1978.

13. Dua, S.S. and Tien, C.L., "An Experimental Investigation of Fall Film Rewetting", Int. J. Heat and Mass Transfer, Vol 21, pp.955-964, 1978.

14. Kim, A.K. and Lee, Y., "A Correlation of Rewetting Temperature", Letters in Heat and Mass Transfer, Vol. 6, pp. 117-123, 1979.

15. Hewitt, G.F., King, R.D. and Lovegrove, P.C., "Techniques for Liquid Film and Pressure Drop Studies in annual Two Phase Flow", A.E.R.E.-R3921, 1962.

16. Griffith, P., "The Slug Annular Flow Regime Transition at Elevated Pressure", A.N.L.-6796, Nov. 1963.

17. Ragheb, H.S., "Development of Electric Probes to Detect Phase Change at a Heated Surface", M.A.Sc. Thesis, U. of Ottawa, 1977.

18. Bencze, I. and Orbeck, I., "Development and Application of an Instrument for Digital Measurement and Analysis of Void Using an Impedance Probe", K R (Kjeller Norway), 1973.

19. Dukler, A.E. and Bergelin, O.P., "Characteristics of Flow in Falling Liquid Films", Chem. Eng. Prog. 48(11), pp.557-563,1952.

20. Tailby, S.R. and Portalski, S., "The Hydrodynamics of Liquid Films Flow on a Vertical Surface", Trans. Inst. Chem. Eng., 38(6), pp. 324-330, 1960.

21. Cheng, S.C., Poon, K.T. and Ng, W., "Transition Boiling Heat Transfer in Forced Vertical Flow", Final Report (1979-81), Argonne Contract Nos. 31-109-38-3564 and 31-109-38-5503, June 1981.

22. IBM System 1360 Continuous System Modeling Program User's Manual, Program No.360 A-CX-16X, 1972.

23. Cheng, S.C., Kulkarni, K. and Birta, L.G., "Insurge Transients from a Surge Tank using CSMP", Similations Vol. 23, No.4 pp.109-114, 1974.

24. Cheng, S.C., Ragheb, H.S. and Groeneveld, D. C., "Measurements of Boiling Boundaries under Forced Convective Flow", Int. J. Heat and Mass Transfer, vol. 21, pp. 1621-1642,April 1978.

25. Tong, L.S. and Young, J.D., "A Phenomenological Transition and Film Boiling Heat Transfer Correlation", Proceedings of 5th Int. Heat Transfer Conference, Tokyo, Vol. IV, 1974.

26. Hsu, Y.Y., "Tentative Correlation of Reflood Heat Transfer", presented at the Third Water Reactor Safety Information Meeting, Germantown, Maryland, 1975.

27. Kutateladze, S.S., Problems of Heat Transfer Hydraulics of Two Phase Media, Pergamon Press, 1969.

28. Cheng, S.C. et al, "Transition Boiling Heat Transfer in Forced Vertical Flow", Final Report (1977-1978), Argonne Contract No. 31-109-38-3564, June 1978.

29. Groeneveld, D.C. and Fung, K.K. "Forced Convective Transition Boiling Review of Literature and Comparison of Prediction Methods", AECL-5543, June 1976.

30. Jackson, T.W. and Jen, H.H., "A Simplified Solution for Transient Film Boiling with Constant Heat Flux", 4th Int. Heat Transfer Conference, 1970.

31. Petukhov, B.S., Kovalev, S.A., Zhukov, V.M. and Kuzma-Kichta, Y.A., "Investigation of the Mechanism of Heat Transfer Upon Film Boiling of Liquid", Proceedings 5th Int. Heat Transfer Conference, 1974.

32. Van Stralen, S.V. and Cole, R., Boiling Phenomena. Hemisphere Publishing Corp., 1979.

33. Iida, Y. and Kobayasi, K., "An experimental Investigation on the Mechanism of Pool Boiling Phenomena by a Probe Method", Proceeding 4th Int. Heat Transfer Conference, Vol. 5, Paper B1.3, 1970.

APPENDIX I CSMP Program for Composite Test Section

```
     *****  CONTINUOUS SYSTEM MODELING PROGRAM  *****

*************************************************************
*                      RUN NO. 5450                         *
*   MASS FLUX = 136 KG/SQ.M.-SEC.      PRESSURE = 344 KPA    *
*   SUBCOOLING = 13.9 DEGREE C                               *
*                                                            *
*************************************************************

          ***PROBLEM INPUT STATEMENTS***

        /     DIMENSION R(30)
         FIXED NPOINT
         FIXED IK
         FIXED IT
         PARAM CK=375.089,CSP=385.186,CRHO=8938.323
         PARAM SK=17.31,SSP=460.570,SRHO=7816.784
         INITIAL
         IK=10
         DELZ=(21.0/(64.0*12.0))*0.3048
         X=1.0
         Z=1.0
         CALPHA=(1.0/0.23)*2.581E-05
         TIN1=483
         TIN2=481.0
         DT=2.0
         T23=TIN1
         DT3 =DT
         RIN=(0.43/(2.0*12.0))*0.3048
         DELRO=(0.015/12.0)*0.3048
         RO=RIN+DELRO
         L=(2.0/12.0)*0.3048
         DELR=(ROUT-RIN-DELRO)/NPOINT
         DRSQ=DELR**2
         CKDR=DELR*CK
         SKDRO=SK*DELRO
         CRHOSP=CRHO*CSP
         SRHOSP=SRHO*SSP
         ROUT=(3.75/(2.0*12.0))*0.3048
         NPOINT=8
         DL=(RO+DELR/2.0)**2-(RO-DELRO/2.0)**2
         C1=((RO**2-(RO-DELRO/2.0)**2)*SRHOSP+((RO+DELR /2.0)**2-RO**2)      ...
            *CPCSP)/DL
         C2=2.0/((DELR+DELRO)*DELR)+1.0/(2.0*RO*DELR)
         C3=1.0/(2.0*RO*DELRO)-2.0/((DELR+DELRO)*DELRO)
         IC53=123
         IC43=123
         IC53=123
         IC63=123
         IC73=123
```

```
IC63=123
IC93=123
ICA3=123
CCEFFA=1.0/(2.0*3.14159*RIN)
NOSORT
DO 1 N=1,NECIAT
R(N)=RC+N*DELR
1 CONTINUE
*************************************************************
*************************************************************
**********************    5450    ***************************
FUNCTION THISC=0.483.2,481.4,480.6,478.5,10,477.2,20,471,...
30,463.3,40,455.5C,448.2,60,440.3,70,433,80,425.5,90,418,...
100,410.5,11C,403.12C,395.2,130,388.140,379.3,150,370.7,...
160,362.C,17C,353.180,344.7,190,337.2,200,326.2,210,317.5,...
220,304.225,301.227,298.7,229,296.7,231,258.5,233,241.2,...
235,235.5,240,226,250,211,260,197.5,270,187.5,280,179.2,...
290,172.7
DYNAMIC
*
*
*   T23=ALFGEN(THISC,TIME)
*
*************************************************************
T33=INTGRL(IC33,DT33)
T43=INTGRL(IC43,DT43)
T53=INTGRL(IC53,DT53)
T63=INTGRL(IC63,DT63)
T73=INTGRL(IC73,DT73)
T83=INTGRL(IC83,DT83)
T93=INTGRL(IC93,DT93)
TA3=T93
*************************************************************
*
*       FINITE DIFF. EQ'S FOR PLANE C
*
*************************************************************
DT33 = CALPHA*(((T43-T33)-2*(T33-T23))/DRSC                    ...
      +((T43-T33)+2*(T33-T23))/(2.0*DELR*R(1)))
DT43 = CALPHA*((T33-2.0*T43+T53)/DRSC +(T53-T33)/(2.0*DELR*R(2)))
DT53 = CALPHA*((T43-2.0*T53+T63)/DRSC +(T63-T43)/(2.0*DELR*R(3)))
DT63 = CALPHA*((T53-2.0*T63+T73)/DRSC +(T73-T53)/(2.0*DELR*R(4)))
DT73 = CALPHA*((T63-2.0*T73+T83)/DRSC +(T83-T63)/(2.0*DELR*R(5)))
DT83 = CALPHA*((T73-2.0*T83+T93)/DRSC +(T93-T73)/(2.0*DELR*R(6)))
DT93 = CALPHA*((T83-2.0*T93+TA3)/DRSC +(TA3-T83)/(2.0*DELR*R(7)))
*************************************************************
*       TO CALCULATE T13
*************************************************************
```

```
D123=DERIV(DTDT23,T23)
T13 = T23 - (C1*D123-C2*CK*Z*(T33-T23))/(C3*SK)
*****************************************************************
*       TO CALCULATE HEAT FLUX -- PLANE C                       *
*****************************************************************
HCONTC = 2.0*3.14159*DEL2*((T13*RIN+T23*(RIN+DELRC))*DELRO*SROSE/2.0...
        +(0.5*T23*(RIN+DELRC)+T33*R(1)+T43*R(2)+T53*R(3)+T63*R(4)   ...
        +T73*R(5)+T83*R(6)+T93*R(7)+TA3*R(8)+0.5)*DELR*CROSP)
HTCS=DERIV(0.0,HCONTC)
HT = -HTCS*COEFFR/DEL2
CPLOT=HT    /150000.
HT3=SK*(T23-T13)/DELRO
PLOT3=HT3/150000.
IT =TIME
METHOD RKSFX
NOSORT
      IF(IT.NE.IK) GO TO 98
      WRITE(6,96)TIME
      WRITE(6,93) T13,T23,T33,T43,T53,T63,T73,T83,T93,TA3
      WRITE(6,80) TZ
IK=IK+7
80    FORMAT(20X,F5.1)
93    FORMAT(1X,'PLANE C ',10(F 5.1,5X),/)
99    FORMAT(2F5.1)
96    FORMAT(30X,'TEMPERATURE DISTRIBUTION AT TIME =  ',F5.1,//)
98    CONTINUE
SORT
TWALL=T13
TMSURF=T23
TIMER FINTIM=350.00,DELT=0.1,PRDEL= 7.0,OUTDEL=0.5
LABEL  PLANE   C
PRPLT HT (TWALL,TMSURF,HT3)
CRSPLT TWALL(HT)
END
STOP
```

MAXIMUM
3.22712 06
HT VERSUS TIME
MINIMUM
0.0
HT
TIME

TENSURE
TAILL
MAXIMUM
3.2271E 06
HT VERSUS TIME
MINIMUM
0.0
HT
TIME

MAXIMUM
3.2271E 06
HT VERSUS TIME
MINIMUM
0.0
HT
TIME

MINIMUM 0.0 HT VERSUS TIME MAXIMUM 3.2271E 06

TIME	FT	I	TWALL	TPSURF
6.6000E 01	5.2584E 05	---------+	4.2515E 02	4.3545E 02
6.6500E 01	5.3065E 05	---------+	4.2401E 02	4.3549E 02
6.7000E 01	5.2234E 05	---------+	4.2447E 02	4.3513E 02
6.7500E 01	5.2431E 05	---------+	4.2412E 02	4.3477E 02
6.8000E 01	5.2015E 05	---------+	4.2379E 02	4.3441E 02
6.8500E 01	5.2343E 05	---------+	4.2345E 02	4.3406E 02
6.9000E 01	5.2037E 05	---------+	4.2312E 02	4.3370E 02
6.9500E 01	5.2453E 05	---------+	4.2280E 02	4.3335E 02
7.0000E 01	5.1556E 05	--------+	4.2247E 02	4.3300E 02
7.0500E 01	5.1606E 05	---------+	4.2215E 02	4.3263E 02
7.1000E 01	5.1447E 05	--------+	4.2182E 02	4.3226E 02
7.1500E 01	5.1804E 05	---------+	4.2150E 02	4.3189E 02
7.2000E 01	5.1994E 05	---------+	4.2118E 02	4.3152E 02
7.2500E 01	5.1404E 05	--------+	4.2085E 02	4.3114E 02
7.3000E 01	5.2212E 05	---------+	4.2053E 02	4.3077E 02
7.3500E 01	5.2278E 05	---------+	4.2021E 02	4.3040E 02
7.4000E 01	5.1666E 05	---------+	4.1989E 02	4.3002E 02
7.4500E 01	5.2759E 05	---------+	4.1956E 02	4.2965E 02
7.5000E 01	5.2147E 05	---------+	4.1924E 02	4.2927E 02
7.5500E 01	5.2147E 05	---------+	4.1893E 02	4.2889E 02
7.6000E 01	5.1797E 05	---------+	4.1861E 02	4.2852E 02
7.6500E 01	5.2125E 05	---------+	4.1829E 02	4.2815E 02
7.7000E 01	5.2103E 05	---------+	4.1797E 02	4.2777E 02
7.7500E 01	5.1906E 05	---------+	4.1766E 02	4.2739E 02
7.8000E 01	5.2212E 05	---------+	4.1734E 02	4.2702E 02
7.8500E 01	5.2496E 05	---------+	4.1702E 02	4.2664E 02
7.9000E 01	5.2037E 05	---------+	4.1671E 02	4.2626E 02
7.9500E 01	5.2606E 05	---------+	4.1639E 02	4.2588E 02
8.0000E 01	5.3130E 05	---------+	4.1608E 02	4.2550E 02
8.0500E 01	5.2693E 05	---------+	4.1576E 02	4.2512E 02
8.1000E 01	5.2594E 05	---------+	4.1545E 02	4.2475E 02
8.1500E 01	5.2737E 05	---------+	4.1513E 02	4.2437E 02
8.2000E 01	5.2606E 05	---------+	4.1482E 02	4.2400E 02
8.2500E 01	5.2780E 05	---------+	4.1451E 02	4.2362E 02
8.3000E 01	5.2606E 05	---------+	4.1420E 02	4.2325E 02
8.3500E 01	5.2453E 05	---------+	4.1389E 02	4.2287E 02
8.4000E 01	5.2999E 05	---------+	4.1358E 02	4.2250E 02
8.4500E 01	5.2125E 05	---------+	4.1327E 02	4.2212E 02
8.5000E 01	5.2627E 05	---------+	4.1296E 02	4.2175E 02
8.5500E 01	5.2955E 05	---------+	4.1265E 02	4.2137E 02
8.6000E 01	5.2846E 05	---------+	4.1234E 02	4.2100E 02
8.6500E 01	5.2715E 05	---------+	4.1203E 02	4.2062E 02
8.7000E 01	5.3283E 05	---------+	4.1172E 02	4.2025E 02
8.7500E 01	5.2474E 05	---------+	4.1141E 02	4.1987E 02

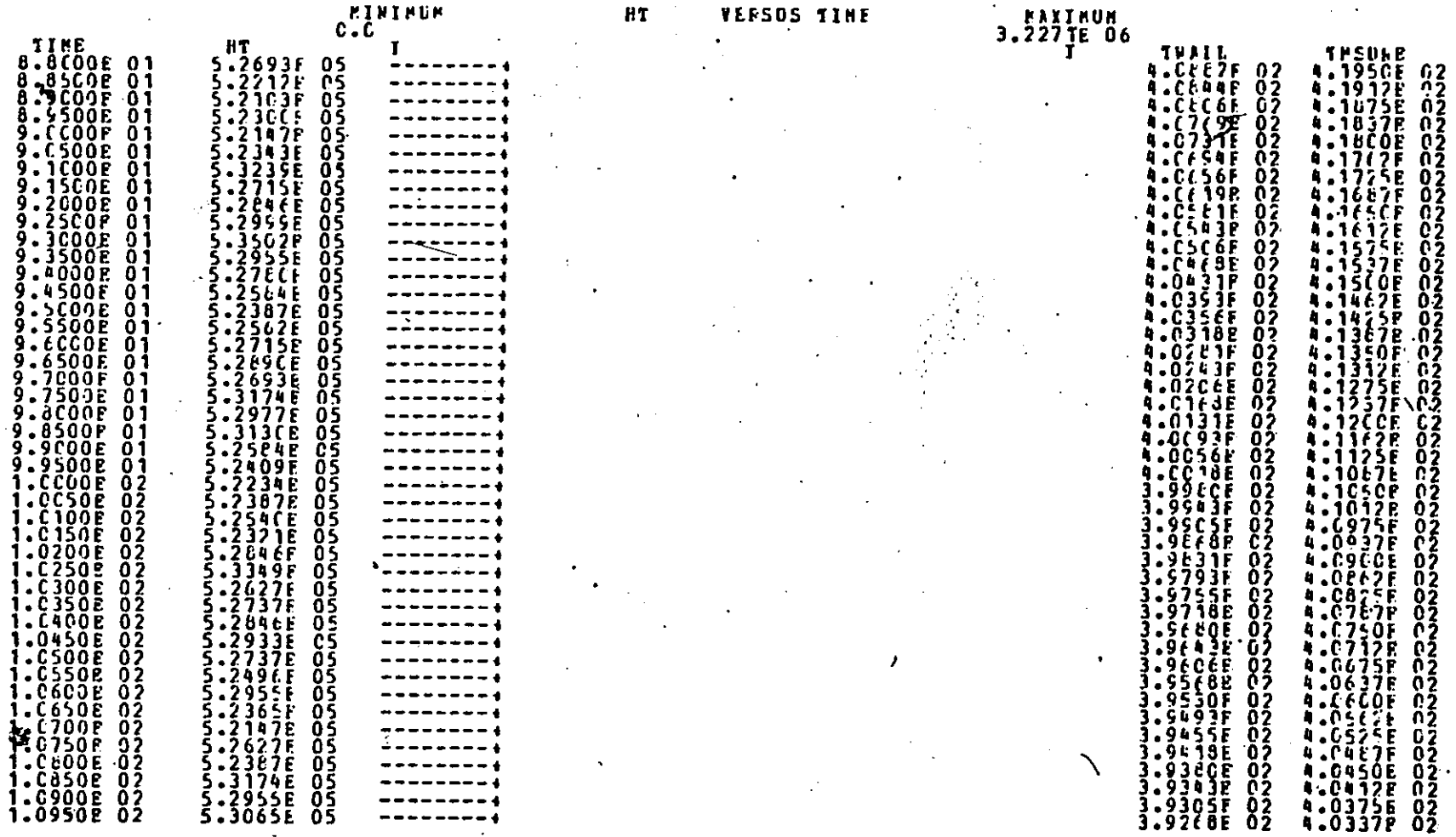
MINIMUM
C.C
I
HT
VERSUS TIME
MAXIMUM
3.227TE 06
I
TIME
HT
TRAIL
TMSUBE
5.2693E 05
5.2717E 05
5.2103E 05
5.2300E 05
5.2197E 05
5.2343E 05
5.3239E 05
5.2715E 05
5.2846E 05
5.2959E 05
5.3502E 05
5.2955E 05
5.2778E 05
5.2564E 05
5.2387E 05
5.2562E 05
5.2715E 05
5.2896E 05
5.2693E 05
5.3174E 05
5.2977E 05
5.3130E 05
5.2584E 05
5.2409E 05
5.2234E 05
5.2387E 05
5.2540E 05
5.2321E 05
5.2846E 05
5.3349E 05
5.2627E 05
5.2737E 05
5.2846E 05
5.2933E 05
5.2737E 05
5.2496E 05
5.2955E 05
5.2365E 05
5.2197E 05
5.2627E 05
5.2387E 05
5.3174E 05
5.2955E 05
5.3065E 05

MINIMUM 0.0 HT VERSUS TIME MAXIMUM 3.2271E 06

TIME	HT	I	TRAIL	TRSURE
1.1000E 02	5.2824E 05	--------+	3.9230E 02	4.0300E 02
1.1050E 02	5.2897E 05	--------+	3.9195E 02	4.0262E 02
1.1100E 02	5.3305E 05	--------+	3.9150E 02	4.0223E 02
1.1150E 02	5.3349E 05	--------+	3.9111E 02	4.0185E 02
1.1200E 02	5.2671E 05	--------+	3.9071E 02	4.0146E 02
1.1250E 02	5.2693E 05	--------+	3.9032E 02	4.0108E 02
1.1300E 02	5.2999E 05	--------+	3.8991E 02	4.0069E 02
1.1350E 02	5.3263E 05	--------+	3.8952E 02	4.0030E 02
1.1400E 02	5.3523E 05	--------+	3.8911E 02	3.9992E 02
1.1450E 02	5.3392E 05	--------+	3.8871E 02	3.9953E 02
1.1500E 02	5.3239E 05	--------+	3.8831E 02	3.9914E 02
1.1550E 02	5.3720E 05	--------+	3.8790E 02	3.9875E 02
1.1600E 02	5.2602E 05	--------+	3.8750E 02	3.9836E 02
1.1650E 02	5.3235E 05	--------+	3.8709E 02	3.9797E 02
1.1700E 02	5.2955E 05	--------+	3.8669E 02	3.9757E 02
1.1750E 02	5.3655E 05	--------+	3.8628E 02	3.9718E 02
1.1800E 02	5.3982E 05	--------+	3.8587E 02	3.9678E 02
1.1850E 02	5.3567E 05	--------+	3.8546E 02	3.9639E 02
1.1900E 02	5.4157E 05	--------+	3.8505E 02	3.9599E 02
1.1950E 02	5.4376E 05	--------+	3.8464E 02	3.9560E 02
1.2000E 02	5.4245E 05	--------+	3.8422E 02	3.9520E 02
1.2050E 02	5.3414E 05	--------+	3.8381E 02	3.9481E 02
1.2100E 02	5.3961E 05	--------+	3.8339E 02	3.9440E 02
1.2150E 02	5.3217E 05	--------+	3.8298E 02	3.9400E 02
1.2200E 02	5.3829E 05	--------+	3.8256E 02	3.9361E 02
1.2250E 02	5.3073E 05	--------+	3.8214E 02	3.9320E 02
1.2300E 02	5.3567E 05	--------+	3.8172E 02	3.9280E 02
1.2350E 02	5.3962E 05	--------+	3.8130E 02	3.9241E 02
1.2400E 02	5.2759E 05	--------+	3.8088E 02	3.9201E 02
1.2450E 02	5.2977E 05	--------+	3.8046E 02	3.9161E 02
1.2500E 02	5.3196E 05	--------+	3.8003E 02	3.9121E 02
1.2550E 02	5.2802E 05	--------+	3.7961E 02	3.9081E 02
1.2600E 02	5.2760E 05	--------+	3.7918E 02	3.9041E 02
1.2650E 02	5.2516E 05	--------+	3.7875E 02	3.9001E 02
1.2700E 02	5.2306E 05	--------+	3.7832E 02	3.8961E 02
1.2750E 02	5.2453E 05	--------+	3.7789E 02	3.8921E 02
1.2800E 02	5.2343E 05	--------+	3.7746E 02	3.8881E 02
1.2850E 02	5.1556E 05	--------+	3.7703E 02	3.8841E 02
1.2900E 02	5.1994E 05	--------+	3.7660E 02	3.8801E 02
1.2950E 02	5.2125E 05	--------+	3.7617E 02	3.8761E 02
1.3000E 02	5.1644E 05	--------+	3.7574E 02	3.8720E 02
1.3050E 02	5.2103E 05	--------+	3.7530E 02	3.8680E 02
1.3100E 02	5.2081E 05	--------+	3.7487E 02	3.8640E 02
1.3150E 02	5.2300E 05	--------+	3.7443E 02	3.8599E 02

HT VERSUS TIME

MINIMUM 0.0

MAXIMUM 3.2271E 06

TIME	HT	I
1.3200E 02	5.2755E 05	
1.3250E 02	5.3086E 05	
1.3300E 02	5.3327E 05	
1.3350E 02	5.3436E 05	
1.3400E 02	5.3742E 05	
1.3450E 02	5.4261E 05	
1.3500E 02	5.4026E 05	
1.3550E 02	5.5316E 05	
1.3600E 02	5.5075E 05	
1.3650E 02	5.5359E 05	
1.3700E 02	5.5462E 05	
1.3750E 02	5.6116E 05	
1.3800E 02	5.6015E 05	
1.3850E 02	5.6343E 05	
1.3900E 02	5.6867E 05	
1.3950E 02	5.6307E 05	
1.4000E 02	5.7696E 05	
1.4050E 02	5.7207E 05	
1.4100E 02	5.7673E 05	
1.4150E 02	5.7545E 05	
1.4200E 02	5.7475E 05	
1.4250E 02	5.7720E 05	
1.4300E 02	5.8266E 05	
1.4350E 02	5.8747E 05	
1.4400E 02	5.8520E 05	
1.4450E 02	5.8266E 05	
1.4500E 02	5.8311E 05	
1.4550E 02	5.9097E 05	
1.4600E 02	5.9009E 05	
1.4650E 02	5.8956E 05	
1.4700E 02	5.9075E 05	
1.4750E 02	5.8550E 05	
1.4800E 02	5.8661E 05	
1.4850E 02	5.9114E 05	
1.4900E 02	5.9228E 05	
1.4950E 02	5.9293E 05	
1.5000E 02	5.9337E 05	
1.5050E 02	5.9337E 05	
1.5100E 02	5.9643E 05	
1.5150E 02	5.8900E 05	
1.5200E 02	5.9460E 05	
1.5250E 02	5.9301E 05	
1.5300E 02	5.9577E 05	
1.5350E 02	5.9736E 05	

TRAIL	TRSUBR
3.7562E 02	3.8638E 02
3.7515E 02	3.8559E 02
3.7469E 02	3.8555E 02
3.7421E 02	3.8513E 02
3.7373E 02	3.8470E 02
3.7325E 02	3.8427E 02
3.7275E 02	3.8384E 02
3.7225E 02	3.8340E 02
3.7175E 02	3.8296E 02
3.7124E 02	3.8252E 02
3.7073E 02	3.8207E 02
3.7021E 02	3.8162E 02
3.6968E 02	3.8116E 02
3.6915E 02	3.8070E 02
3.6862E 02	3.8024E 02
3.6808E 02	3.7977E 02
3.6754E 02	3.7930E 02
3.6712E 02	3.7882E 02
3.6667E 02	3.7834E 02
3.6622E 02	3.7785E 02
3.6577E 02	3.7757E 02
3.6532E 02	3.7714E 02
3.6487E 02	3.7671E 02
3.6442E 02	3.7628E 02
3.6397E 02	3.7585E 02
3.6352E 02	3.7542E 02
3.6307E 02	3.7499E 02
3.6264E 02	3.7456E 02
3.6219E 02	3.7413E 02
3.6175E 02	3.7370E 02
3.6131E 02	3.7327E 02
3.6087E 02	3.7284E 02
3.6043E 02	3.7241E 02
3.6000E 02	3.7198E 02
3.5956E 02	3.7156E 02
3.5912E 02	3.7113E 02
3.5868E 02	3.7070E 02
3.5823E 02	3.7027E 02
3.5778E 02	3.6983E 02
3.5734E 02	3.6940E 02
3.5689E 02	3.6897E 02
3.5645E 02	3.6853E 02
3.5600E 02	3.6810E 02
3.5556E 02	3.6767E 02

MINIMUM HT VERSUS TIME MAXIMUM

0.0 3.2271E 06

TIME	HT	I	TWAIL	TMSUWE
1.5400E 02	5.9883E 05	----------+	3.5511E 02	3.6723E 02
1.5450E 02	5.9971E 05	----------+	3.5466E 02	3.6600E 02
1.5500E 02	6.0056E 05	----------+	3.5422E 02	3.6636E 02
1.5550E 02	5.9774E 05	----------+	3.5377E 02	3.6593E 02
1.5600E 02	5.9774E 05	----------+	3.5332E 02	3.6549E 02
1.5650E 02	5.9424E 05	----------+	3.5288E 02	3.6505E 02
1.5700E 02	6.0056E 05	----------+	3.5243E 02	3.6462E 02
1.5750E 02	5.9993E 05	----------+	3.5198E 02	3.6418E 02
1.5800E 02	5.9556E 05	----------+	3.5153E 02	3.6375E 02
1.5850E 02	6.0124E 05	----------+	3.5109E 02	3.6331E 02
1.5900E 02	6.0036E 05	----------+	3.5064E 02	3.6287E 02
1.5950E 02	5.9864E 05	----------+	3.5019E 02	3.6244E 02
1.6000E 02	5.9665E 05	----------+	3.4974E 02	3.6200E 02
1.6050E 02	6.0102E 05	----------+	3.4929E 02	3.6156E 02
1.6100E 02	6.0167E 05	----------+	3.4885E 02	3.6113E 02
1.6150E 02	6.0167E 05	----------+	3.4840E 02	3.6069E 02
1.6200E 02	6.0169E 05	----------+	3.4795E 02	3.6026E 02
1.6250E 02	6.0648E 05	----------+	3.4750E 02	3.5982E 02
1.6300E 02	6.0169E 05	----------+	3.4705E 02	3.5938E 02
1.6350E 02	6.0714E 05	----------+	3.4661E 02	3.5895E 02
1.6400E 02	6.0517E 05	----------+	3.4616E 02	3.5851E 02
1.6450E 02	6.0954E 05	----------+	3.4571E 02	3.5807E 02
1.6500E 02	6.1027E 05	----------+	3.4526E 02	3.5764E 02
1.6550E 02	6.1413E 05	----------+	3.4481E 02	3.5720E 02
1.6600E 02	6.1370E 05	----------+	3.4437E 02	3.5676E 02
1.6650E 02	6.1326E 05	----------+	3.4392E 02	3.5633E 02
1.6700E 02	6.1195E 05	----------+	3.4347E 02	3.5589E 02
1.6750E 02	6.1781E 05	----------+	3.4302E 02	3.5545E 02
1.6800E 02	6.1872E 05	----------+	3.4257E 02	3.5502E 02
1.6850E 02	6.1610E 05	----------+	3.4212E 02	3.5458E 02
1.6900E 02	6.2047E 05	----------+	3.4168E 02	3.5414E 02
1.6950E 02	6.2025E 05	----------+	3.4123E 02	3.5371E 02
1.7000E 02	6.1654E 05	----------+	3.4078E 02	3.5327E 02
1.7050E 02	6.1960E 05	----------+	3.4033E 02	3.5283E 02
1.7100E 02	6.1765E 05	----------+	3.3988E 02	3.5240E 02
1.7150E 02	6.1931E 05	----------+	3.3944E 02	3.5196E 02
1.7200E 02	6.1763E 05	----------+	3.3899E 02	3.5152E 02
1.7250E 02	6.1632E 05	----------+	3.3854E 02	3.5109E 02
1.7300E 02	6.1581E 05	----------+	3.3809E 02	3.5065E 02
1.7350E 02	6.1094E 05	----------+	3.3764E 02	3.5021E 02
1.7400E 02	6.0867E 05	----------+	3.3720E 02	3.4978E 02
1.7450E 02	6.1282E 05	----------+	3.3675E 02	3.4934E 02
1.7500E 02	6.1085E 05	----------+	3.3630E 02	3.4890E 02
1.7550E 02	6.1260E 05	----------+	3.3585E 02	3.4847E 02

INSULFR
TAILE
MAXIMUM
3.2271E 06
HT
VERSUS TIME
MINIMUM
0.0
HT
TIME

MAXIMUM
3.2271E 06
HT VERSUS TIME
MINIMUM
0.0
HT
TIME

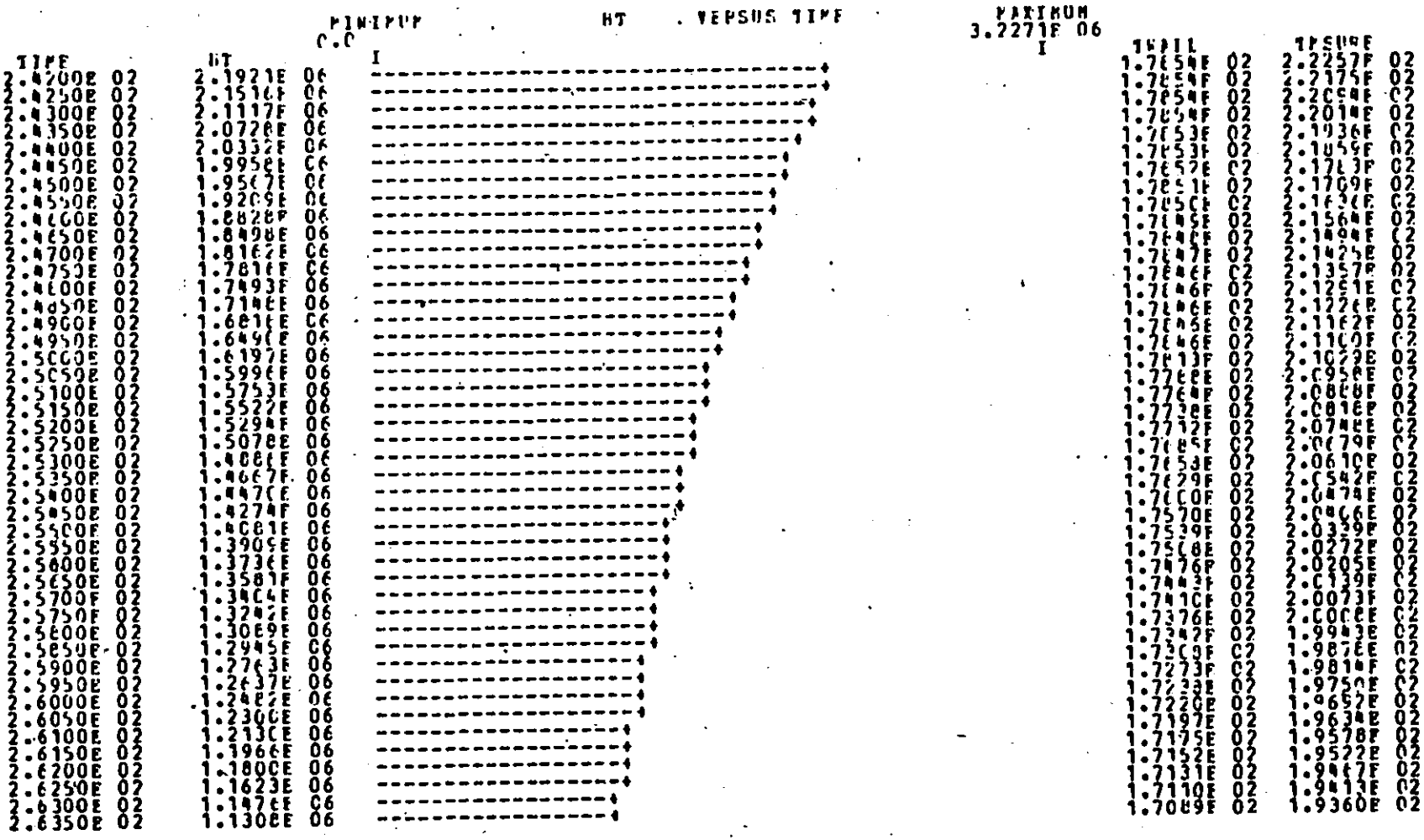
MINIMUM
0.0
HT
VERSUS TIME
MAXIMUM
3.2271E 06
TIME
HT
TAIL
TSURF
2.42000E 02
2.19221E 06
1.76594E 02
2.22557E 02
2.42500E 02
2.15161E 06
1.76594E 02
2.21756E 02
2.43000E 02
2.11177E 06
1.76594E 02
2.20958E 02
2.43500E 02
2.07226E 06
1.76594E 02
2.20161E 02
2.44000E 02
2.03322E 06
1.76538E 02
2.19366E 02
2.44500E 02
1.99502E 06
1.76538E 02
2.18573E 02
2.45000E 02
1.95777E 06
1.76522E 02
2.17783E 02
2.45500E 02
1.92099E 06
1.76511E 02
2.17009E 02
2.46000E 02
1.88428E 06
1.76505E 02
2.16236E 02
2.46500E 02
1.84988E 06
1.76485E 02
2.15464E 02
2.47000E 02
1.81622E 06
1.76467E 02
2.14695E 02
2.47500E 02
1.78316E 06
1.76467E 02
2.13929E 02
2.48000E 02
1.74993E 06
1.76446F 02
2.13165E 02
2.48500E 02
1.71788E 06
1.76446E 02
2.12404E 02
2.49000E 02
1.68611E 06
1.76446E 02
2.11645E 02
2.49500E 02
1.64961E 06
1.76446E 02
2.10888E 02
2.50000E 02
1.61977E 06
1.76413F 02
2.10133E 02
2.50500E 02
1.59996E 06
1.77688E 02
2.09380E 02
2.51000E 02
1.57539E 06
1.77688E 02
2.08630E 02
2.51500E 02
1.55227E 06
1.77688E 02
2.07881E 02
2.52000E 02
1.52944E 06
1.77732E 02
2.07135E 02
2.52500E 02
1.50708E 06
1.76853E 02
2.06390E 02
2.53000E 02
1.48516E 06
1.76853E 02
2.05647E 02
2.53500E 02
1.46667E 06
1.76299E 02
2.04906E 02
2.54000E 02
1.44470E 06
1.76299E 02
2.04166E 02
2.54500E 02
1.42274E 06
1.76299E 02
2.03429E 02
2.55000E 02
1.40081E 06
1.75570E 02
2.02693E 02
2.55500E 02
1.39095E 06
1.75399E 02
2.02272E 02
2.56000E 02
1.37336E 06
1.75408E 02
2.02055E 02
2.56500E 02
1.35581E 06
1.74763E 02
2.01339E 02
2.57000E 02
1.33804E 06
1.74763E 02
2.00733E 02
2.57500E 02
1.32042E 06
1.74101E 02
2.00128E 02
2.58000E 02
1.30289E 06
1.73766E 02
1.99523E 02
2.58500E 02
1.29455E 06
1.73766E 02
1.99220E 02
2.59000E 02
1.27638E 06
1.73273E 02
1.98617E 02
2.59500E 02
1.26378E 06
1.73273E 02
1.98316E 02
2.60000E 02
1.24822E 06
1.72720E 02
1.97715E 02
2.60500E 02
1.23066E 06
1.72720E 02
1.97415E 02
2.61000E 02
1.21336E 06
1.71977E 02
1.96815E 02
2.61500E 02
1.19666E 06
1.71755E 02
1.96516E 02
2.62000E 02
1.18006E 06
1.71526E 02
1.95917E 02
2.62500E 02
1.16236E 06
1.71311E 02
1.95618E 02
2.63000E 02
1.14766E 06
1.71109E 02
1.95020E 02
2.63500E 02
1.13088E 06
1.70889E 02
1.93600E 02

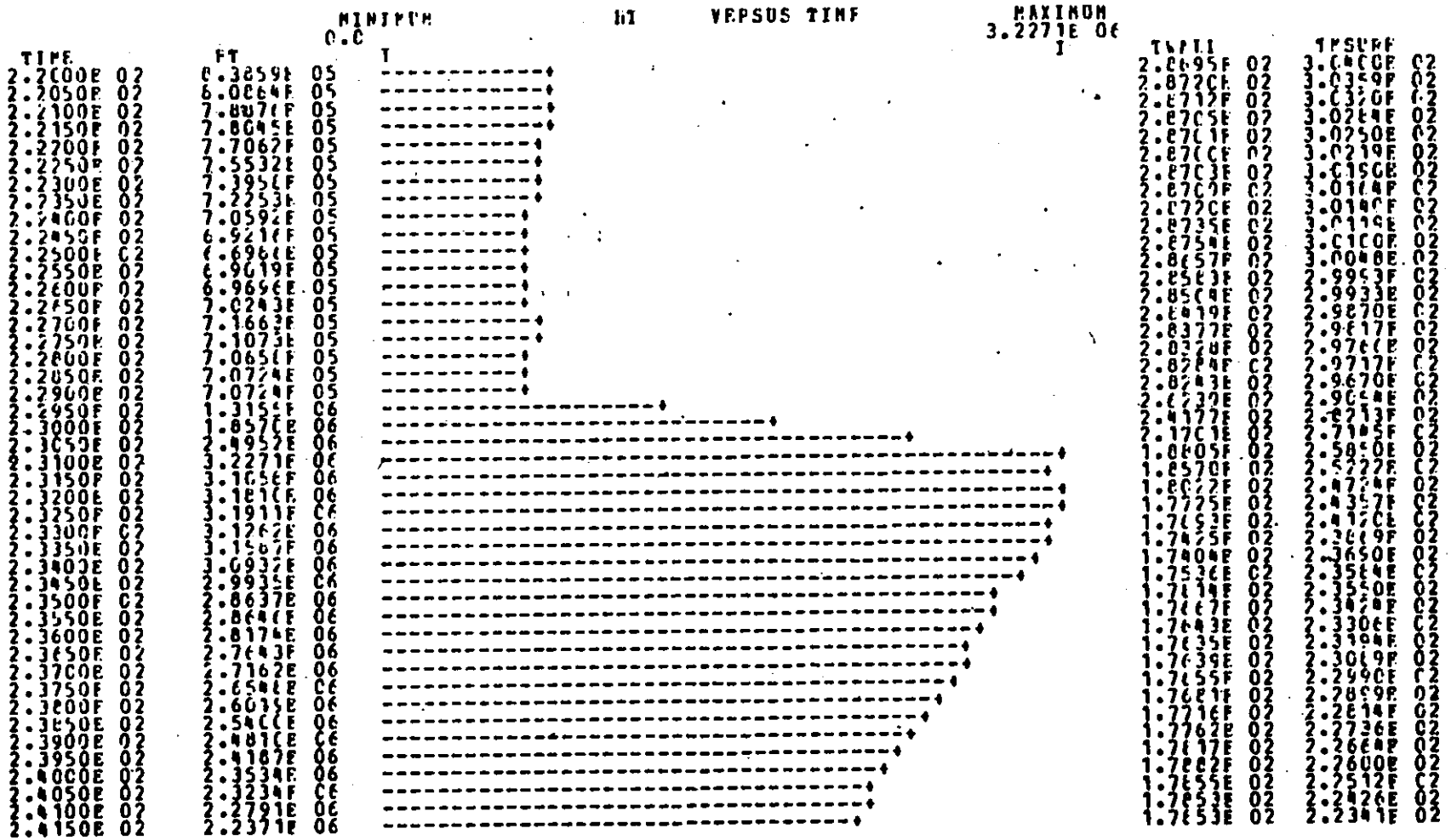
MINIMUM
0.0
MI VERSUS TIME
MAXIMUM
3.2271E 06
TIME
FT
I

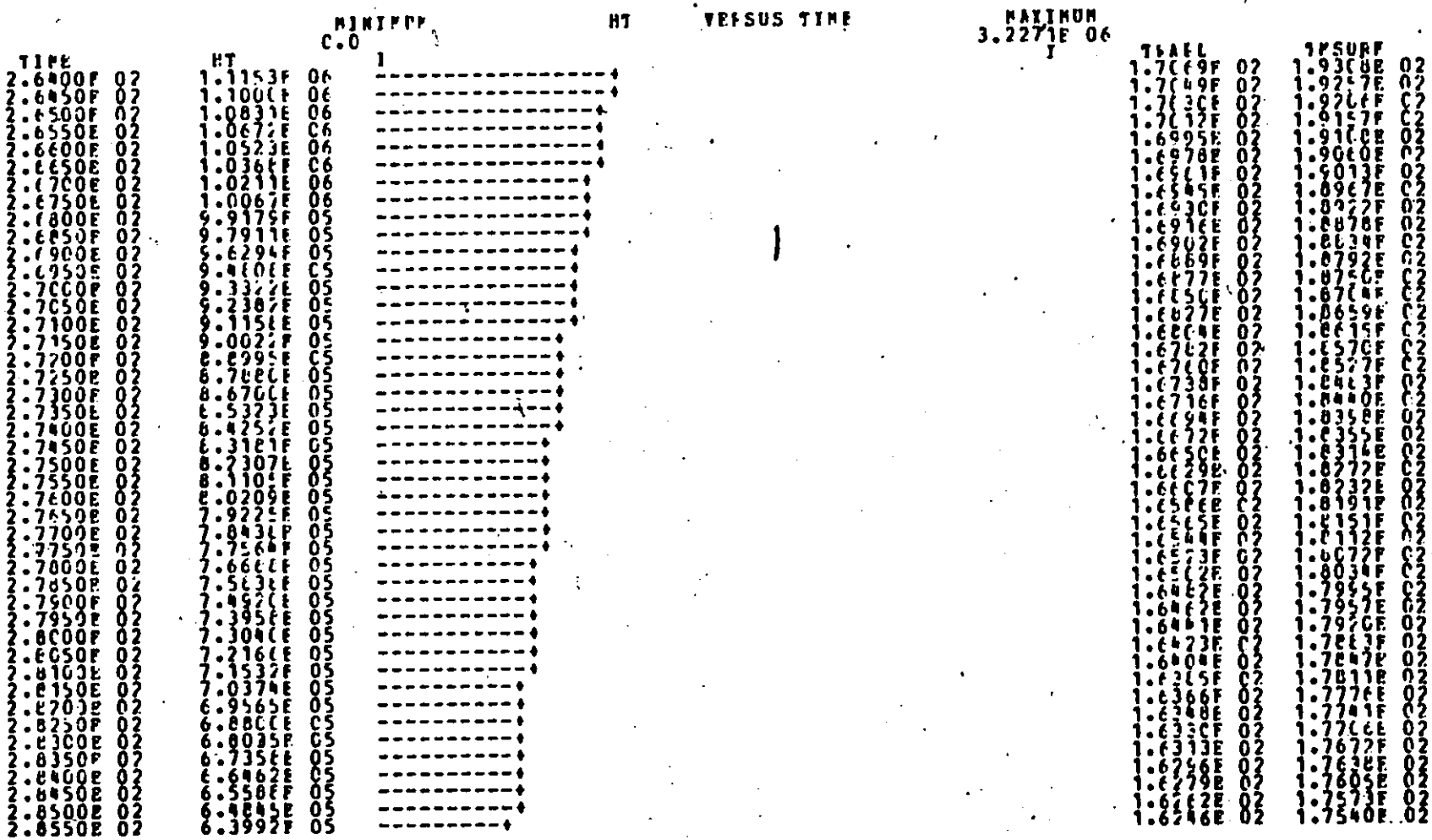
MINIMUM
0.0
HT
VERSUS TIME
MAXIMUM
3.2271E 06
TIME
HT
1

MAXIMUM
3.2271E 06
HT VERSUS TIME
MINIMUM
0.0

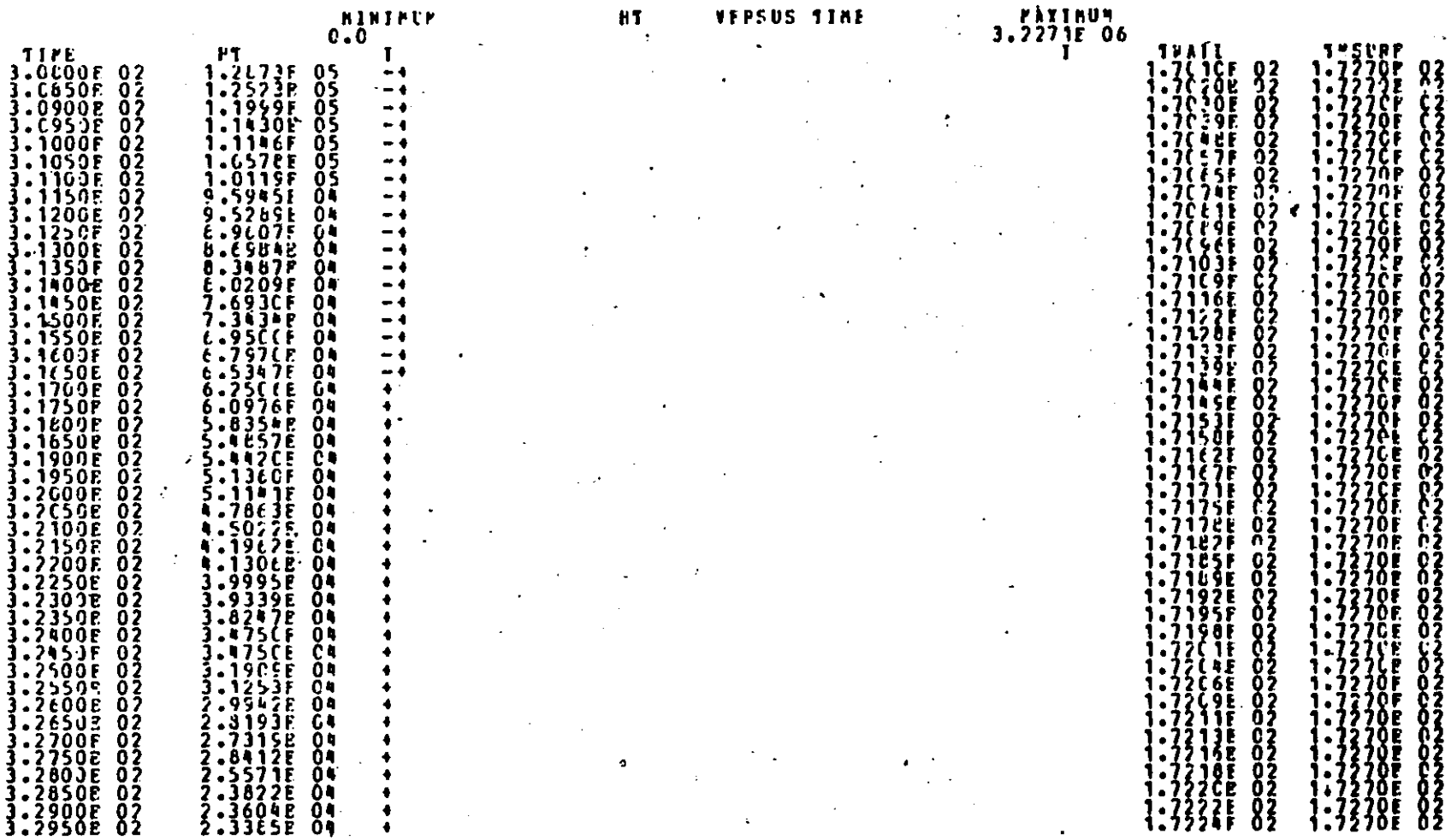
MINIMUM
0.0
HT
VERSUS TIME
MAXIMUM
3.2271E 06
TIME
HT
I
TRAIL
TRUE

MINIMUM PT VERSUS TIME MAXIMUM
0.0 3.2271E 06

TIME	PT	I	TWALL	TWSURF
3.3000E 02	2.1637E 04	*	1.7225E 02	1.7270E 02
3.3050E 02	2.1418E 04	*	1.7227E 02	1.7270E 02
3.3100E 02	1.8796E 04	*	1.7229E 02	1.7270E 02
3.3150E 02	1.9670E 04	*	1.7230E 02	1.7270E 02
3.3200E 02	1.8577E 04	*	1.7232E 02	1.7270E 02
3.3250E 02	1.7921E 04	*	1.7233E 02	1.7270E 02
3.3300E 02	1.6610E 04	*	1.7235E 02	1.7270E 02
3.3350E 02	1.5517E 04	*	1.7236E 02	1.7270E 02
3.3400E 02	1.7921E 04	*	1.7238E 02	1.7270E 02
3.3450E 02	1.6173E 04	*	1.7239E 02	1.7270E 02
3.3500E 02	1.5517E 04	*	1.7240E 02	1.7270E 02
3.3550E 02	1.4206E 04	*	1.7241E 02	1.7270E 02
3.3600E 02	1.5517E 04	*	1.7242E 02	1.7270E 02
3.3650E 02	1.2457E 04	*	1.7243E 02	1.7270E 02
3.3700E 02	1.1602E 04	*	1.7244E 02	1.7270E 02
3.3750E 02	1.1385E 04	*	1.7245E 02	1.7270E 02
3.3800E 02	1.1385E 04	*	1.7246E 02	1.7270E 02
3.3850E 02	1.0928E 04	*	1.7247E 02	1.7270E 02
3.3900E 02	1.0926E 04	*	1.7248E 02	1.7270E 02
3.3950E 02	9.3978E 03	*	1.7249E 02	1.7270E 02
3.4000E 02	9.8345E 03	*	1.7250E 02	1.7270E 02
3.4050E 02	9.8345E 03	*	1.7251E 02	1.7270E 02
3.4100E 02	8.5235E 03	*	1.7251E 02	1.7270E 02
3.4150E 02	7.6493E 03	*	1.7252E 02	1.7270E 02
3.4200E 02	7.6493E 03	*	1.7253E 02	1.7270E 02
3.4250E 02	7.2122E 03	*	1.7253E 02	1.7270E 02
3.4300E 02	8.5235E 03	*	1.7254E 02	1.7270E 02
3.4350E 02	5.0267E 03	*	1.7255E 02	1.7270E 02
3.4400E 02	6.5566E 03	*	1.7255E 02	1.7270E 02
3.4450E 02	6.3386E 03	*	1.7256E 02	1.7270E 02
3.4500E 02	6.7751E 03	*	1.7256E 02	1.7270E 02
3.4550E 02	4.8022E 03	*	1.7257E 02	1.7270E 02
3.4600E 02	6.5566E 03	*	1.7257E 02	1.7270E 02
3.4650E 02	5.9006E 03	*	1.7258E 02	1.7270E 02
3.4700E 02	6.1195E 03	*	1.7258E 02	1.7270E 02
3.4750E 02	5.6624E 03	*	1.7259E 02	1.7270E 02
3.4800E 02	4.1525E 03	*	1.7259E 02	1.7270E 02
3.4850E 02	3.9339E 03	*	1.7260E 02	1.7270E 02
3.4900E 02	4.1525E 03	*	1.7260E 02	1.7270E 02
3.4950E 02	5.4630E 03	*	1.7260E 02	1.7270E 02
3.5000E 02	3.7154E 03	*	1.7261E 02	1.7270E 02

APPENDIX II CSMP Program for Rod Test Section

```
          ****CONTINUOUS SYSTEM MODELING PROGRAM****

*****************************************************************
*                                                               *
*              ROD TEST SECTION       RUN NO. 6022              *
*  MASS FLUX = 68 MG/SQ.F.-SEC.   SUBCOOLING =13.9 DEGREE C     *
*                                                               *
*****************************************************************

     ***PROBLEM INPUT STATEMENTS***

/      DIMENSION  R(7)
 FIXED  NPOINT,I
 PARAM  CK=379.089,CSP=365.196,CRHO=8938.323
 PARAM  SK=17.31,SSP=460.570,SRHO=7861.784
 INITIAL
 NPOINT = 5
 RCUT = (0.5/(2.0*12.0))*0.3048
 DELTA = (0.010/12.0)*(.3048
 DELTO = (0.02/12.0)*0.3048
 ALPHSS = SK/(SSP*SRHO)
 ALPHCU = CK/(CSP*CRHO)
 DELTP = (RCUT - DELTO -DELTA) / NPOINT
 D62D61 = (442.5 - 441.2) / ( 0.0 - 1.0)
 IC1 = 442.5
 IC2 = IC1
 IC3 = IC1
 IC4 = IC1
 IC5 = IC1
 IC6 = IC1
 NOSORT
 R(1) = DELTA
 DO 1 I = 2, 6
       R(I) = R (I-1) + DELTA
 1 CONTINUE
 R(7) = RCUT
*****************************************************************
*****************************************************************
**********************      6022     ********************************
FUNCTION THISC=0,442.5,1,441.2,2,440.0,3,435.5,4,432.5,426.5,...
6,424,7,419.8,414.9,410,10,405,11,400,12,395,13,390,14,383.5,15,374,...
16,366,17,348,17.5,339,18,325,18.5,310,19,294,19.2,287.5,...
19.4,276,19.6,266,19.8,256,20,246,20.2,233,20.4,219,20.6,202,...
20.8,182,20.9,172.0,21,157,21.2,149,21.5,130.5,22,120.5,22.5,117.5,...
23,114.5,24,110,25,108
*
*
DYNAMIC
```

```
*                                                                      *
*     T6 = NLFGEN ( THISC,TIME)                                        *
*                                                                      *
************************************************************************
 T1 = INTGRL (IC1,DT1)
 T2 = INTGRL (IC2,DT2)
 T3 = INTGRL (IC3,DT3)
 T4 = INTGRL (IC4,DT4)
 T5 = INTGRL (IC5,DT5)
*
*
*
 DT1 = 2.0*ALPHCU*(T2-T1)/DELTR**2
 DT2 = ALPHCU*((T1-2.0*T2+T3)/(DELTR**2) + (T3-T1)/2.0*DELTR*R(2))
 DT3 = ALPHCU*((T2-2.0*T3+T4)/(DELTR**2) + (T4-T2)/2.0*DELTR*R(3))
 DT4 = ALPHCU*((T3-2.0*T4+T5)/(DELTR**2) + (T5-T3)/2.0*DELTR*R(4))
 DT5 = ALPHCU*((T4-2.0*T5+T6)/(DELTR**2) + (T6-T4)/2.0*DELTR*R(5))
 DT6 = DERIV (DT5,T6)
*
*
 T7 = (DT6*(DELTR+DELTO)/ALPHCU + 2.0*(T6-T5)/DELTR + T5/R(6) + ...
       2.0*T6/DELTO) / (2.0/DELTO + 1.0/R(6))
 Q = CPHC*CSE*(0.5*T7*HOUT*DELTO+0.5*T6*R(6)*(DELTO+DELTR)+(T5*R(5) +...
       T4*R(4)+T3*R(3)+T2*R(2))*DELTR+0.5*((DELTA+0.5*DELTR)**2 - ...
       DELTA**2)*T1 + DELTA**2*T1*0.5)
 DQDT = DERIV (0.0,Q)
 HTCA = -DQDT/HOUT
 NOSORT
 20    FORMAT (1X,8(F10.3,2X))
 TERMINAL
 WRITE (6,60) (R(I) , I=1,7)
 60    FORMAT (1X,7(F10.5,2X))
 METHOD RKS
 TIMER FINTIM=25.00,DELT=0.005,PRDEL=1.0,OUTDEL=0.05
 LABEL HEAT TRANSFER / UNIT AREA(OUTER SURFACE), ANNULAR FLOW
 PRTPLT  HTOA  (T7,T6)
 END
 STOP
```

MINIMUM HTCA VERSUS TIME MAXIMUM

0.0 1.6797E 06

TIME	HTCA	I	T7	T6
0.0	0.0	*	4.4249E 02	4.4250E 02
5.0000E-02	9.6945E 03	*	4.4242E 02	4.4243E 02
1.0000E-01	1.1339E 04	*	4.4235E 02	4.4237E 02
1.5000E-01	1.2667E 04	*	4.4228E 02	4.4230E 02
2.0000E-01	1.2844E 04	*	4.4221E 02	4.4224E 02
2.5000E-01	1.3337E 04	*	4.4215E 02	4.4217E 02
3.0000E-01	1.4331E 04	*	4.4208E 02	4.4211E 02
3.5000E-01	1.4439E 04	*	4.4201E 02	4.4204E 02
4.0000E-01	1.3228E 04	*	4.4195E 02	4.4198E 02
4.5000E-01	1.3769E 04	*	4.4188E 02	4.4191E 02
5.0000E-01	1.3947E 04	*	4.4182E 02	4.4185E 02
5.5000E-01	1.4518E 04	*	4.4175E 02	4.4178E 02
6.0000E-01	1.4644E 04	*	4.4169E 02	4.4172E 02
6.5000E-01	1.4603E 04	*	4.4162E 02	4.4165E 02
7.0000E-01	1.4416E 04	*	4.4156E 02	4.4159E 02
7.5000E-01	1.4173E 04	*	4.4149E 02	4.4152E 02
8.0000E-01	1.4600E 04	*	4.4143E 02	4.4146E 02
8.5000E-01	1.4486E 04	*	4.4136E 02	4.4139E 02
9.0000E-01	1.4173E 04	*	4.4130E 02	4.4133E 02
9.5000E-01	1.3996E 04	*	4.4123E 02	4.4126E 02
1.0000E 00	1.3658E 04	*	4.4117E 02	4.4120E 02
1.0500E 00	1.3701E 04	*	4.4111E 02	4.4114E 02
1.1000E 00	1.4331E 04	*	4.4105E 02	4.4107E 02
1.1500E 00	1.4173E 04	*	4.4098E 02	4.4101E 02
1.2000E 00	1.4173E 04	*	4.4092E 02	4.4095E 02
1.2500E 00	1.4331E 04	*	4.4086E 02	4.4089E 02
1.3000E 00	1.4803E 04	*	4.4080E 02	4.4083E 02
1.3500E 00	1.3760E 04	*	4.4074E 02	4.4077E 02
1.4000E 00	1.3209E 04	*	4.4068E 02	4.4071E 02
1.4500E 00	1.3524E 04	*	4.4062E 02	4.4065E 02
1.5000E 00	1.3012E 04	*	4.4056E 02	4.4059E 02
1.5500E 00	1.3690E 04	*	4.4050E 02	4.4053E 02
1.6000E 00	1.3306E 04	*	4.4044E 02	4.4047E 02
1.6500E 00	1.3071E 04	*	4.4038E 02	4.4041E 02
1.7000E 00	1.2530E 04	*	4.4032E 02	4.4035E 02
1.7500E 00	1.3543E 04	*	4.4026E 02	4.4029E 02
1.8000E 00	1.2962E 04	*	4.4020E 02	4.4023E 02
1.8500E 00	1.3071E 04	*	4.4015E 02	4.4017E 02
1.9000E 00	1.2441E 04	*	4.4009E 02	4.4012E 02
1.9500E 00	1.3159E 04	*	4.4003E 02	4.4006E 02
2.0000E 00	1.2610E 04	*	4.3997E 02	4.4000E 02
2.0500E 00	2.7087E 04	*	4.3990E 02	4.3994E 02
2.1000E 00	3.0148E 04	*	4.3984E 02	4.3987E 02
2.1500E 00	3.3258E 04	*	4.3947E 02	4.3953E 02

MAXIMUM
1.6797E 06
HTCA VERSUS TIME
MINIMUM
0.0
TIME

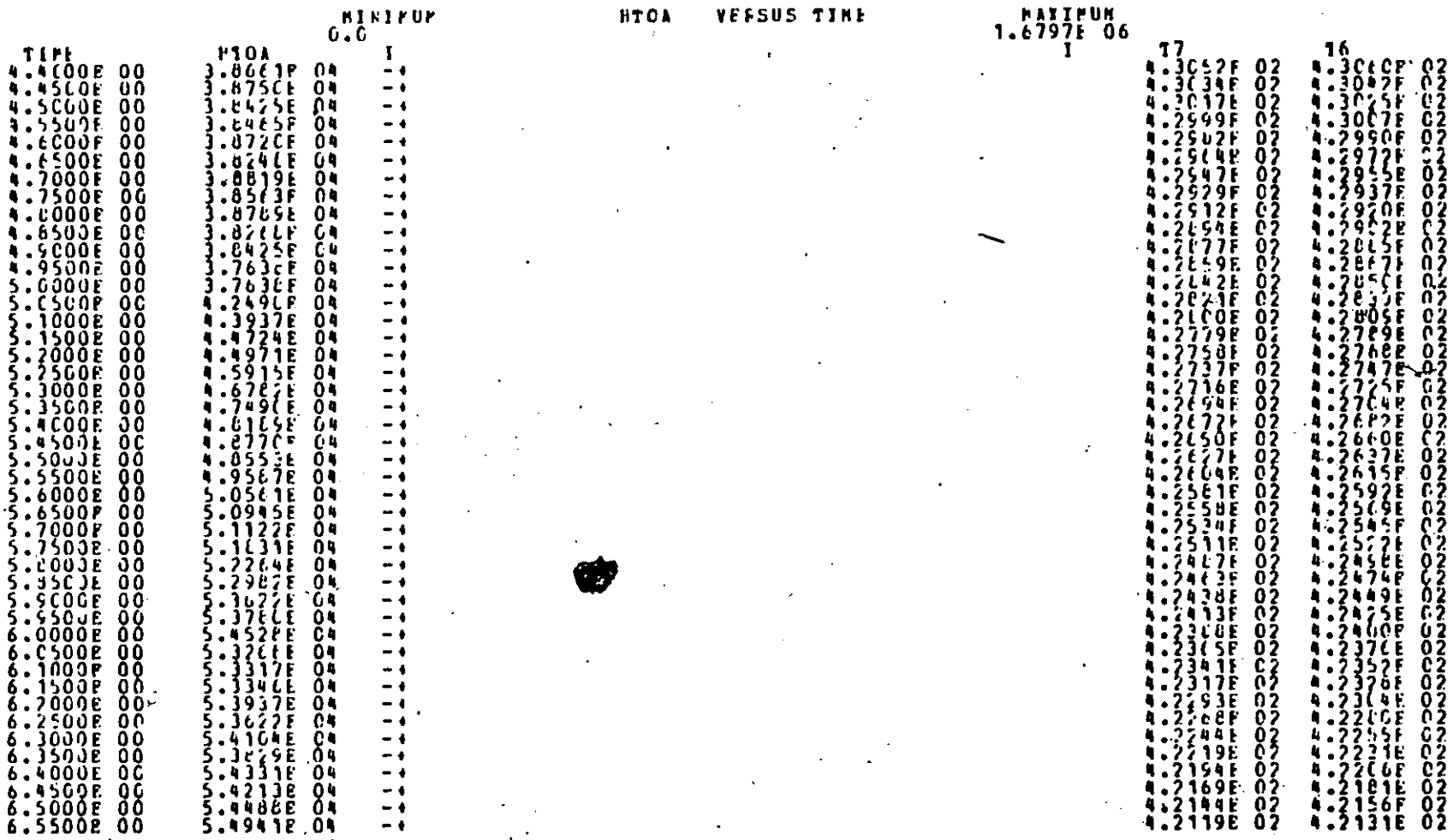
MINIMUM
0.0
HTOA VERSUS TIME
MAXIMUM
1.6797E 06
TIME
HTOA
I
T7
T6

HTOA VERSUS TIME

MINIMUM 0.0 I

MAXIMUM 1.6797E 06 I

TIME	HTOA	I	17	16
6.6000E 00	5.5141E 04	-+	4.2094E 02	4.2106E 02
6.6500E 00	5.5906E 04	-+	4.2069E 02	4.2081E 02
6.7000E 00	5.6356E 04	-+	4.2043E 02	4.2055E 02
6.7500E 00	5.6117E 04	-+	4.2018E 02	4.2030E 02
6.8000E 00	5.6305E 04	-+	4.1992E 02	4.2004E 02
6.8500E 00	5.6772E 04	-+	4.1966E 02	4.1978E 02
6.9000E 00	5.7451E 04	-+	4.1940E 02	4.1952E 02
6.9500E 00	5.7303E 04	-+	4.1914E 02	4.1926E 02
7.0000E 00	5.7953E 04	-+	4.1888E 02	4.1900E 02
7.0500E 00	5.5111E 04	-+	4.1863E 02	4.1875E 02
7.1000E 00	5.5035E 04	-+	4.1839E 02	4.1850E 02
7.1500E 00	5.6063E 04	-+	4.1813E 02	4.1825E 02
7.2000E 00	5.4872E 04	-+	4.1788E 02	4.1800E 02
7.2500E 00	5.4864E 04	-+	4.1763E 02	4.1775E 02
7.3000E 00	5.5354E 04	-+	4.1738E 02	4.1750E 02
7.3500E 00	5.4631E 04	-+	4.1713E 02	4.1725E 02
7.4000E 00	5.5207E 04	-+	4.1688E 02	4.1700E 02
7.4500E 00	5.5045E 04	-+	4.1663E 02	4.1675E 02
7.5000E 00	5.5472E 04	-+	4.1638E 02	4.1650E 02
7.5500E 00	5.5591E 04	-+	4.1613E 02	4.1625E 02
7.6000E 00	5.5305E 04	-+	4.1588E 02	4.1600E 02
7.6500E 00	5.5177E 04	-+	4.1563E 02	4.1575E 02
7.7000E 00	5.5315E 04	-+	4.1538E 02	4.1550E 02
7.7500E 00	5.5177E 04	-+	4.1513E 02	4.1525E 02
7.8000E 00	5.5131E 04	-+	4.1488E 02	4.1500E 02
7.8500E 00	5.4961E 04	-+	4.1463E 02	4.1475E 02
7.9000E 00	5.4784E 04	-+	4.1438E 02	4.1450E 02
7.9500E 00	5.5271E 04	-+	4.1413E 02	4.1425E 02
8.0000E 00	5.5443E 04	-+	4.1388E 02	4.1400E 02
8.0500E 00	5.1142E 04	-+	4.1366E 02	4.1378E 02
8.1000E 00	5.0610E 04	-+	4.1345E 02	4.1355E 02
8.1500E 00	4.9134E 04	-+	4.1323E 02	4.1334E 02
8.2000E 00	4.8593E 04	-+	4.1301E 02	4.1312E 02
8.2500E 00	4.8276E 04	-+	4.1280E 02	4.1291E 02
8.3000E 00	4.7264E 04	-+	4.1259E 02	4.1269E 02
8.3500E 00	4.6614E 04	-+	4.1239E 02	4.1249E 02
8.4000E 00	4.5669E 04	-+	4.1218E 02	4.1228E 02
8.4500E 00	4.5285E 04	-+	4.1198E 02	4.1208E 02
8.5000E 00	4.4774E 04	-+	4.1178E 02	4.1187E 02
8.5500E 00	4.4516E 04	-+	4.1158E 02	4.1168E 02
8.6000E 00	4.3691E 04	-+	4.1139E 02	4.1148E 02
8.6500E 00	4.3256E 04	-+	4.1119E 02	4.1129E 02
8.7000E 00	4.2646E 04	-+	4.1100E 02	4.1109E 02
8.7500E 00	4.2431E 04	-+	4.1082E 02	4.1091E 02

TAXIPUM
1.E797P 06
PTCA VERSUS TIME

MAXIMUM
1.6797E 06
1
HTCB VERSUS TIME
MINIMUM
0.0
1
TIME

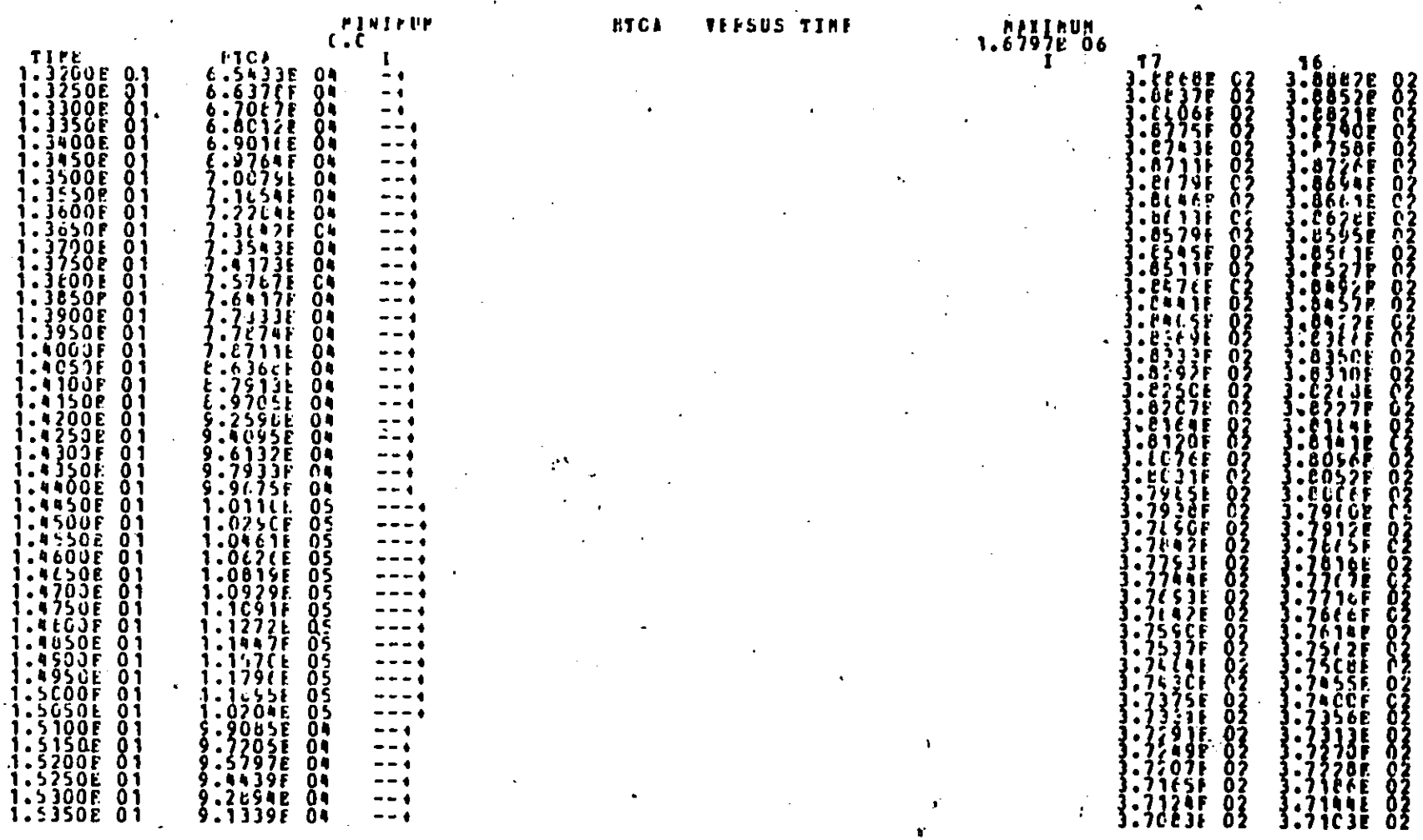
MINIMUM
0.0
HTCA VERSUS TIME
MAXIMUM
1.6797E 06
TIME
HTCA
I
T7
T6

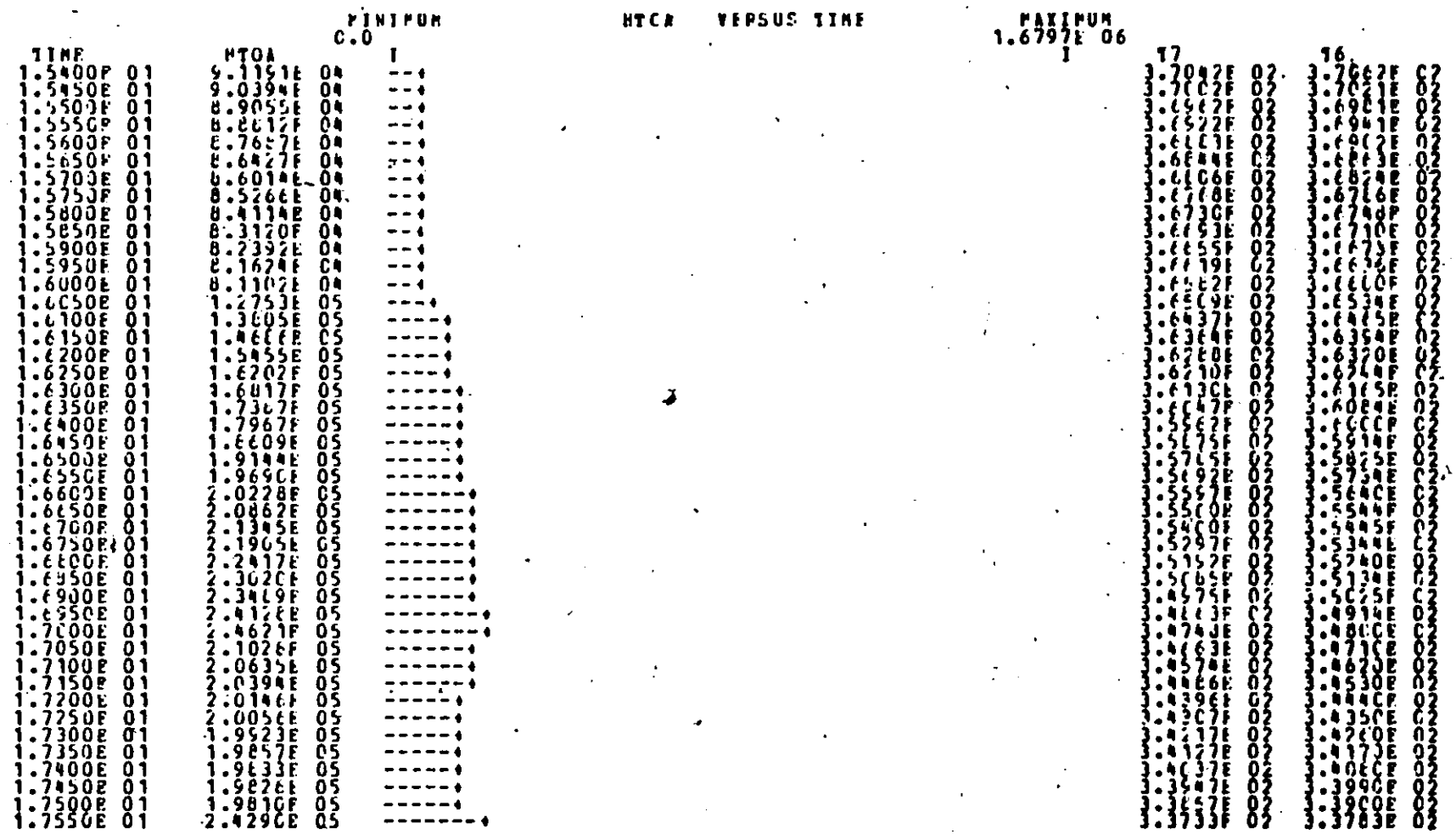
MINIMUM
0.0
HTCR VERSUS TIME
MAXIMUM
1.6797E 06
TIME
MTOA
I
T7
T6

MAXIMUM
1.679E 06
VERSUS TIME
0.0
TIME

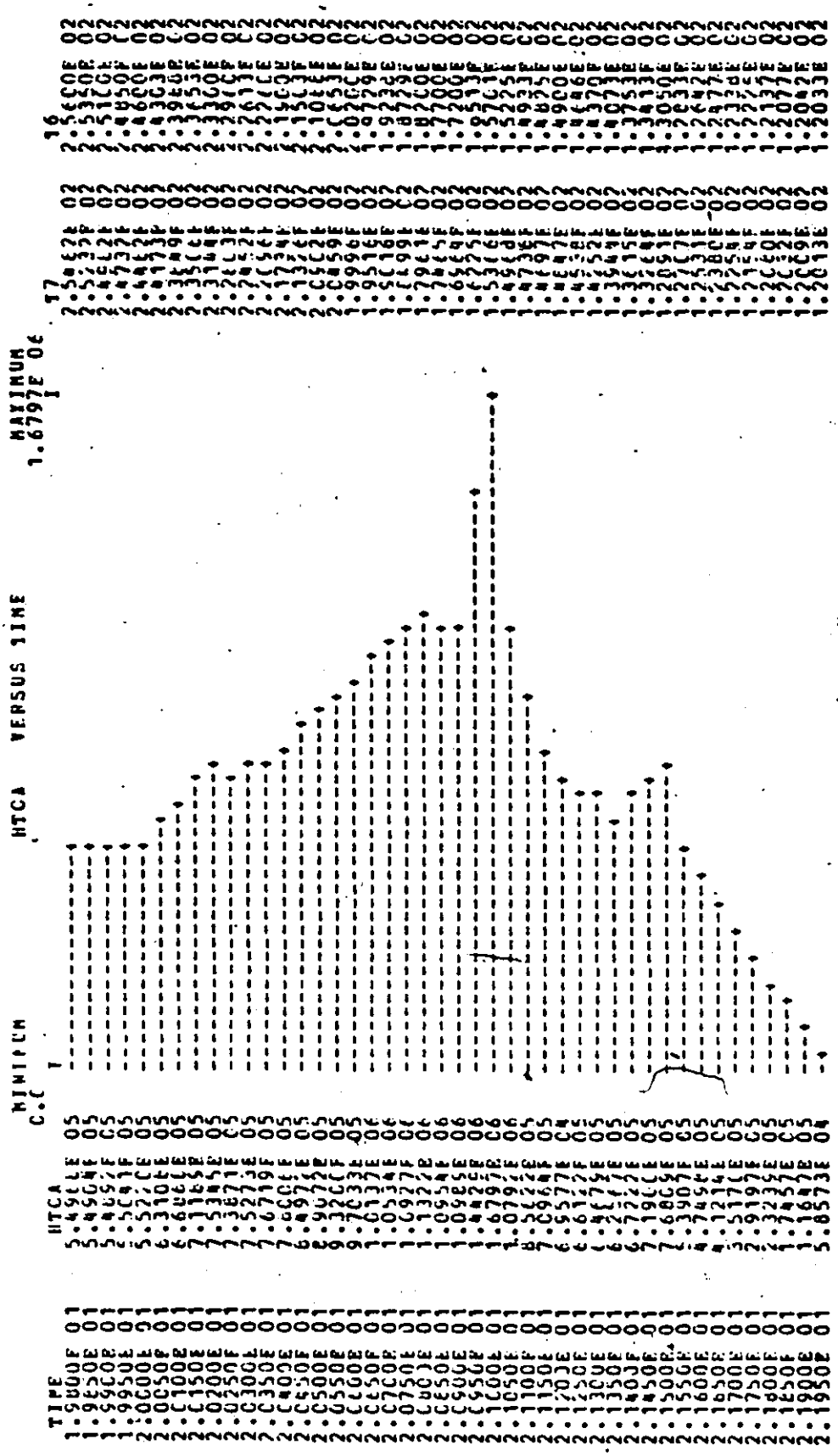
MAXIMUM
1.6797E 0
HTCA VERSUS TIME
MINIMUM
HTCA
TIME

MAXIMUM
1.279E 06
HTCA VERSUS TIME

MTCA VERSUS TIME

MINIMUM 0.0 MAXIMUM 1.6797E 06

TIME	MTOA	I	T7	T6
2.4200E 01	3.1929E 04	+	1.0933E 02	1.0940E 02
2.4250E 01	3.0571E 04	+	1.0940E 02	1.0927E 02
2.4300E 01	2.9134E 04	+	1.0967E 02	1.0913E 02
2.4350E 01	2.7766E 04	+	1.0995E 02	1.0900E 02
2.4400E 01	2.6356E 04	+	1.1023E 02	1.0887E 02
2.4450E 01	2.4872E 04	+	1.1052E 02	1.0873E 02
2.4500E 01	2.3454E 04	+	1.1080E 02	1.0859E 02
2.4550E 01	2.2156E 04	+	1.1108E 02	1.0845E 02
2.4600E 01	2.0827E 04	+	1.1137E 02	1.0832E 02
2.4650E 01	1.9466E 04	+	1.1165E 02	1.0818E 02
2.4700E 01	1.8159E 04	+	1.1193E 02	1.0804E 02
2.4750E 01	1.6742E 04	+	1.1222E 02	1.0791E 02
2.4800E 01	1.5266E 04	+	1.1250E 02	1.0777E 02
2.4850E 01	1.3917E 04	+	1.1278E 02	1.0763E 02
2.4900E 01	1.2526E 04	+	1.1307E 02	1.0750E 02
2.4950E 01	1.1093E 04	+	1.1335E 02	1.0736E 02
2.5000E 01	9.6949E 03	+	1.0798E 02	1.0800E 02

APPENDIX III Tables of Transition Boiling Data

TABLE I. Boiling Curve Data for 5800 Run Series

(Inconel-Copper Test Section at G=66 kg $m^{-2} s^{-1}$ and Tsub=13.9°C)

Run No. 5835		Run No. 5855		Run No. 5885		Run No. 5895	
P=206 Kpa		P = 344 Kpa		P = 550 Kpa		P = 686 Kpa	
ΔT_s(°C)	$\phi(10^5 W/m^2)$	ΔT_s(°C)	$\phi(10^5 W/m^2)$	ΔT_s(°C)	$\phi(10^5 W/m^2)$	ΔT_s(°C)	$\phi(10^5 W/m^2)$
						33.0	4.40
						41.0	7.30
		34.0	4.40			44.0	11.00
36.0	3.30	42.0	6.10	36.0	3.70	49.0	16.00
46.0	5.50	50.0	8.60	41.0	7.00	58.0	30.00
56.0	8.85	56.0	13.00	48.0	10.00	68.0	28.50
66.0	15.50	61.0	22.60	53.0	15.00	86.0	26.30
76.0	18.50	78.0	21.00	62.0	26.00	96.0	23.80
86.0	17.30	91.0	16.60	74.0	24.00	106.0	21.80
96.0	15.50	106.0	15.90	86.0	22.50	126.0	17.90
106.0	14.00	120.0	13.00	106.0	19.00	146.0	13.00
126.0	9.10	131.0	10.50	126.0	15.50	158.0	10.40
146.0	6.00	146.0	7.50	146.0	11.30	166.0	8.70
166.0	5.30	166.0	5.95	166.0	7.50	186.0	6.70
186.0	4.80	186.0	5.20	186.0	6.00	206.0	5.55
206.0	4.30	206.0	4.40	206.0	5.05	226.0	4.75
226.0	4.10	226.0	4.35	226.0	4.50	246.0	4.45
246.0	3.66	246.0	4.00	246.0	4.40	266.0	4.34
266.0	3.90	266.0	3.95	266.0	4.25	286.0	4.12
286.0	3.75	286.0	4.02	286.0	4.10	306.0	3.89
306.0	3.80	306.0	3.90	306.0	4.00		

TABLE II. Boiling Curve Data for 5700 Run Series

(Inconel-Copper Test Section at G=136 kg $m^{-2}s^{-1}$ and Tsub=13.9°C)

Run No. 5700 P=101 Kpa		Run No. 5730 P=206 Kpa		Run No. 5750 P = 344 Kpa		Run No. 5780 P = 550 Kpa		Run No. 5790 P = 686 Kpa	
ΔT_v(°C)	$\phi(10^5 W/m^2)$	ΔT_v(°C)	$\phi(10^5 W/m^2)$	ΔT_v(°C)	$\phi(10^5 W/m^2)$	ΔT_v(°C)	$\phi(10^5 W/m^2)$	ΔT_v(°C)	$\phi(10^5 W/m^2)$
		36.0	5.50	36.0	7.20			36.0	7.20
36.0	3.90	41.0	8.40	41.0	10.20	36.0	7.50	41.0	9.40
41.0	5.50	46.0	11.30	46.0	13.90	41.0	10.20	46.0	14.80
46.0	7.00	51.0	13.80	50.0	21.10	46.0	13.20	49.0	32.20
51.0	10.50	52.0	29.60	51.0	31.80	51.0	20.80	52.0	35.90
56.0	21.50	56.0	28.00	56.0	31.00	56.0	35.00	56.0	35.60
66.0	20.00	66.0	26.20	66.0	29.00	66.0	32.60	66.0	33.70
76.0	19.00	76.0	24.30	76.0	27.00	76.0	30.00	76.0	31.50
86.0	18.00	86.0	23.00	86.0	25.00	86.0	27.00	86.0	29.00
106.0	13.40	106.0	18.00	106.0	20.00	106.0	23.40	106.0	26.50
126.0	9.00	126.0	13.30	126.0	14.50	126.0	18.60	126.0	20.00
146.0	6.00	146.0	8.10	146.0	10.00	146.0	12.60	146.0	14.50
166.0	5.00	166.0	7.00	166.0	6.40	166.0	8.70	166.0	9.80
186.0	4.70	186.0	6.50	186.0	5.60	186.0	6.10	186.0	6.90
206.0	4.70	206.0	6.20	206.0	4.30	206.0	5.00	206.0	5.70
226.0	4.50	226.0	4.80	226.0	3.90	226.0	4.40	226.0	4.90
246.0	4.00	246.0	3.90	246.0	3.70	246.0	4.20	246.0	4.44
266.0	3.90	266.0	3.80	266.0	3.60	266.0	4.05	266.0	4.40
286.0	4.00	286.0	3.60	286.0	3.60	286.0	4.00	286.0	4.30
306.0	3.10	306.0	3.60	306.0	3.60	306.0	4.02	306.0	4.40

TABLE III. Boiling Curve Data for 5800 Run Series

(Inconel-Copper Test Section at G=203 kg $s^{-2}s^{-1}$ and Tsub=13.9°C)

Run No. 5802		Run No. 5832		Run No. 5852		Run No. 5882		Run No. 5892	
P=101 Kpa		P=206 Kpa		P = 344 Kpa		P = 550 Kpa		P = 688 Kpa	
ΔTw(°C)	$\phi(10^5$ W/$m^2)$	ΔTw(°C)	$\phi(10^5$ W/$m^2)$	ΔTw(°C)	$\phi(10^5$ W/$m^2)$	ΔTw(°C)	$\phi(10^5$ W/$m^2)$	ΔTw(°C)	$\phi(10^5$ W/$m^2)$
36.0	5.00					28.0	5.10	36.0	7.50
41.0	6.00			36.0	7.00	40.0	8.90	46.0	10.35
46.0	8.70			46.0	10.60	49.0	22.00	49.0	14.00
50.0	10.00	26.0	5.00	54.0	20.00	53.0	37.80	50.0	29.00
58.0	16.00	36.0	7.20	55.0	34.10	60.0	35.50	51.0	41.00
62.0	22.50	46.0	11.80	68.0	32.00	80.0	31.20	62.0	40.00
68.0	21.00	58.0	31.50	81.0	28.30	100.0	28.00	80.0	36.00
76.0	20.00	70.0	29.00	91.0	26.20	118.0	24.50	100.0	31.30
86.0	17.50	86.0	25.00	106.0	22.50	126.0	20.30	110.0	28.20
106.0	14.50	106.0	19.50	126.0	17.00	138.0	17.00	133.0	25.00
126.0	11.30	126.0	15.00	136.0	14.20	146.0	14.50	146.0	20.00
146.0	8.20	146.0	9.60	146.0	12.00	156.0	12.00	158.0	16.00
166.0	6.20	166.0	6.85	166.0	80.00	166.0	9.45	170.0	12.00
186.0	5.00	186.0	6.00	186.0	6.50	186.0	7.20	186.0	9.25
206.0	4.60	206.0	5.40	206.0	5.38	206.0	5.85	206.0	7.00
226.0	4.65	226.0	5.30	226.0	5.53	226.0	5.25	226.0	6.00
246.0	4.50	246.0	5.00	246.0	5.50	246.0	5.35	246.0	6.20
266.0	4.15	266.0	5.20	266.0	5.55	266.0	4.95	266.0	5.85
286.0	4.20	286.0	5.10	286.0	5.40	286.0	5.00	286.0	5.56
306.0	4.10	306.0	4.85	306.0	5.30	306.0	4.94	306.0	5.80

TABLE IV. Boiling Curve Data for 5400 Run Series

(Stainless Steel-Copper Test Section at G=136 kg $m^{-2} s^{-1}$ and Tsub=13.9°C)

Run No. 5400 P=101 Kpa		Run No. 5430 P=206 Kpa		Run No. 5450 P = 344 Kpa		Run No. 5480 P = 550 Kpa		Run No. 5490 P = 686 Kpa	
ΔTv(C)	$\phi(10^5$ W/$m^2)$	ΔTv(°C)	$\phi(10^5$ W/$m^2)$	ΔTv(°C)	$\phi(10^5$ W/$m^2)$	ΔTv(°C)	$\phi(10^5$ W/$m^2)$	ΔTv(°C)	$\phi(10^5$ W/$m^2)$
36.0	12.70					36.0	16.80		
46.0	21.10	36.0	10.90	36.0	13.40	40.0	36.30	36.0	15.50
56.0	22.00	41.0	18.30	41.0	20.50	49.0	35.50	40.0	27.60
66.0	15.50	45.0	30.90	49.0	32.30	63.0	33.00	44.0	40.00
76.0	17.70	68.0	25.30	65.0	28.50	70.0	32.60	70.0	33.50
86.0	15.00	89.0	20.00	78.0	25.00	93.0	26.50	95.0	27.60
106.0	11.00	108.0	15.30	104.0	18.60	114.0	21.70	117.0	22.00
126.0	7.20	130.0	8.50	126.0	13.10	133.0	16.80	143.0	18.40
146.0	5.70	146.0	6.90	146.0	7.20	156.0	10.00	146.0	13.80
166.0	6.20	166.0	6.60	166.0	6.40	166.0	9.60	166.0	10.30
186.0	5.40	186.0	6.50	186.0	5.80	186.0	8.10	186.0	8.70
206.0	5.60	206.0	5.60	206.0	6.10	206.0	7.60	206.0	8.20
226.0	5.00	226.0	5.20	226.0	5.90	226.0	7.60	226.0	8.00
246.0	4.60	246.0	6.20	246.0	5.30	246.0	6.90	246.0	7.40
266.0	5.40	266.0	5.60	266.0	5.30	266.0	6.50	266.0	6.80
286.0	5.30	286.0	5.50	286.0	5.20	286.0	5.30	286.0	5.60
306.0	5.60	306.0	5.10	306.0	5.30	306.0	5.20	306.0	5.50

APPENDIX IV Program for Correlation of Transition Boiling

```
*************************************************************
*                                                           *
*        STATISTICAL PACKAGE FOR SOCIAL SCIENCES            *
*                                                           *
*************************************************************
```

```
RUN NAME          GEN CORR OF TRANSITION BOILING UNDER PRESSURE
VARIABLE LIST     HFLUX,DTSAT,P/
INPUT MEDIUM      CARD
N OF CASES        41
INPUT FORMAT      FIXED(F12.0,3X,F5.1,3X,F5.1)

COMPUTE           HFIUX=HFLUX/10000
COMPUTE           G=136
COMPUTE           PROP=(17*8169*435)**.5/10000
COMPUTE           P=.3126
COMPUTE           DTSUB=13.9
COMPUTE           FI=9267*(DTSAT**(-1.1891-.22599*PROP))*
                  EXP(.02012*DTSUB+.00393*G+5770/PROP)

COMPUTE           VARA=LN(HFIUX/FI)
COMPUTE           VARB=LN(P/14.7)
COMPUTE           PFI=FI*(P/14.7)**B
COMPUTE           ERROR=((PFI-HFIUX)/HFLUX)**2
PRINT FORMATS     HFIUX,DTSAT,P,FI,PFI(2)
VAR LABELS        HFIUX,HEAT FLUX/DTSAT,DIFF TW &TSAT/P,PRESSURE
LIST CASES        CASES=41/VARIABLES=HFLUX,DTSAT,P,FI,PFI/
TRANSFORM
```

ITEM	ACTUAL	MAXIMUM
VARS RECODED	0	100
VALUES RECODED	0	952
TRANSFORMATIONS	11	238
MATH OPERATORS	30	1904
LITERAL VALUES	18	192

READ INPUT DATA

CASE-N	HFIUX	DTSAT	P	FI	PFI
1	296.00	50.00	30.00	391.60	465.16
2	280.00	58.00	30.00	327.39	388.88
3	262.00	66.00	30.00	280.12	332.74
4	243.00	76.00	30.00	236.28	280.66
5	190.00	102.00	30.00	165.66	196.78
6	150.00	118.00	30.00	138.95	165.05
7	116.00	131.00	30.00	122.49	145.50
8	81.00	146.00	30.00	107.47	127.66
9	70.00	166.00	30.00	92.05	109.34
10	45.00	186.00	30.00	80.24	95.31
11	315.00	52.00	50.00	373.50	501.85
12	293.00	63.00	50.00	296.30	398.12
13	270.00	74.00	50.00	244.00	327.86
14	258.00	83.00	50.00	212.45	285.45
15	208.00	103.00	50.00	163.72	219.99
16	164.00	120.00	50.00	136.16	182.96
17	127.00	135.00	50.00	118.12	158.72
18	85.10	149.50	50.00	104.44	140.33
19	63.70	166.00	50.00	92.05	123.68
20	54.00	186.00	50.00	80.24	107.81
21	361.00	49.00	80.00	401.26	603.91
22	326.00	65.00	80.00	285.33	429.43
23	292.00	80.00	80.00	222.10	334.26
24	259.00	94.00	80.00	182.82	275.15
25	234.00	106.50	80.00	157.25	236.67
26	193.00	123.00	80.00	132.17	198.91
27	157.00	138.00	80.00	115.03	173.12
28	126.00	150.00	80.00	104.02	156.55
29	91.00	162.00	80.00	94.80	142.67
30	66.90	180.00	80.00	83.48	125.64
31	391.00	40.00	100.00	512.60	814.16
32	357.00	55.60	100.00	344.52	547.19
33	323.00	71.00	100.00	256.50	407.39
34	290.00	85.00	100.00	206.43	327.87
35	266.00	98.00	100.00	173.86	276.13
36	221.00	117.00	100.00	140.39	222.97
37	180.00	133.00	100.00	120.27	191.02
38	145.00	147.00	100.00	106.59	169.29
39	97.50	166.00	100.00	92.05	146.19
40	68.60	186.00	100.00	80.24	127.44
41	57.40	206.00	100.00	70.94	112.67

```
                REGRESSION      VARIABLES=VARA,VARB/
                                REGRESSION=VARA WITH VARB(2)RESID=0
                STATISTICS      ALL

     VARIABLE           MEAN      STANDARD DEV      CASES

     VARA             0.0449            0.2466         41
     VARB             1.4002            0.4899         41

                  VARA       VARB

     VARA         1.00000    0.45990
     VARB         0.45990    1.00000

      * * * * * * * * * * * * * M U L T I P L E   R E G R E S S I O N * * * * * * * * * * * * *

     DEPENDENT VARIABLE..    VARA
     VARIABLE(S) ENTERED ON STEP NUMBER  1..    VARB

     MULTIPLE R           0.45990                ANALYSIS OF VARIANCE      DF
     R SQUARE             0.21151                REGRESSION                 1.
ADJUSTED R SQUARE         0.19129                RESIDUAL                  39.
STANDARD ERROR            0.22173

     ----------------- VARIABLES IN THE EQUATION -----------------

VARIABLE           B          BETA      STD ERROR B         F

VARB            0.31260      0.45990      0.07460       10.461

MAXIMUM STEP REACHED

      * * * * * * * * * * * * * M U L T I P L E   R E G R E S S I O N * * * * * * * * * * * * *

     DEPENDENT VARIABLE..    VARA

                                                    SUMMARY TABLE

     VARIABLE                                MULTIPLE R   R SQUARE   RSQ CHANGE   SIMPLE R

     VARB                                      0.45990    0.21151     0.21151     0.45990
```

SEQNUM	OBSERVED VARA	PREDICTED VARA	RESIDUAL
1	-0.27988236	-0.12084480	-0.1590355
2	-0.15639C0	-0.12[illegible]480	-0.[illegible]1191E-01
3	-0.66[illegible]54E-01	-0.12[illegible]480	0.5395751E-01
4	0.2[illegible]02[illegible]E-01	-0.12[illegible]4[illegible]C	0.1[illegible]89C83
5	0.13[illegible]94	-0.12[illegible]4[illegible]C	0.2579174
6	0.76[illegible]0[illegible]E-01	-0.12[illegible]4[illegible]C	0.1973541
7	-0.5442733E-01	-0.12[illegible]4[illegible]C	0.6642067E-01
8	-0.28275[illegible]	-0.12[illegible]4[illegible]C	-0.1619059
9	-0.2737[illegible]	-0.12[illegible]4[illegible]C	-0.1529478
10	-0.2106348	-0.12[illegible]4[illegible]C	-0.[illegible]970671E-01
11	-0.1703447	0.[illegible]4119[illegible]E-02	-0.1727565
12	-0.1119[illegible]71F-01	0.[illegible]4119[illegible]E-02	-0.1360[illegible]52E-01
13	0.1012403	0.[illegible]4119[illegible]E-02	0.9[illegible]2[illegible]45E-01
14	0.1942739	0.[illegible]4119[illegible]E-02	0.1918[illegible]C
15	0.2393559	0.[illegible]4119[illegible]E-02	0.2369480
16	0.1[illegible]0172	0.[illegible]4119[illegible]E-02	0.1[illegible]36053
17	0.7246327F-01	0.[illegible]4119[illegible]E-02	0.7005143F-01
18	-0.2047521	0.[illegible]4119[illegible]E-02	-0.2072039
19	-0.3[illegible]1[illegible]	0.[illegible]4119[illegible]E-02	-0.3705184
20	-0.3[illegible]0381	0.[illegible]4119[illegible]E-02	-0.3584498
21	-0.1057432	0.1155[illegible]19	-0.[illegible]215[illegible]46
22	0.1[illegible]23[illegible]	0.1155[illegible]19	0.1741741E-01
23	0.2736449	0.1155[illegible]19	0.1578234
24	0.[illegible]63149	0.1155[illegible]19	0.2324935
25	0.3974611	0.1155[illegible]19	0.2[illegible]16396
26	0.3766370	0.1155[illegible]19	0.[illegible]28155
27	0.3110424	0.1155[illegible]19	0.1[illegible]52210
28	0.1910917	0.1155[illegible]19	0.75[illegible]702EE-01
29	-0.4[illegible]3[illegible]E-01	0.1155[illegible]19	-0.1[illegible]66545
30	-0.2213[illegible]99	0.1155[illegible]19	-0.3372113
31	-0.2707951	0.1[illegible]9[illegible]49	-0.44[illegible]4600
32	0.3559197E-01	0.1[illegible]96[illegible]49	-0.1340729
33	0.2305334	0.1[illegible]96[illegible]49	0.[illegible]6[illegible]53E-01
34	0.3359264	0.1[illegible]96[illegible]49	0.1702615
35	0.4252694	0.1[illegible]96[illegible]49	0.2556045
36	0.4537[illegible]6	0.1[illegible]96[illegible]49	0.2840[illegible]6
37	0.4032727	0.1[illegible]96[illegible]49	0.2335578
38	0.3077655	0.1[illegible]96[illegible]49	0.1[illegible]10[illegible]6
39	0.5756100E-01	0.1[illegible]96[illegible]49	-0.1121039
40	-0.1567796	0.1[illegible]96[illegible]49	-0.3763944
41	-0.2117417	0.1[illegible]96[illegible]49	-0.3814065

PLOT OF STANDARDIZED RESIDUAL

-2.0 -1.0 0.0 1.0 2.0

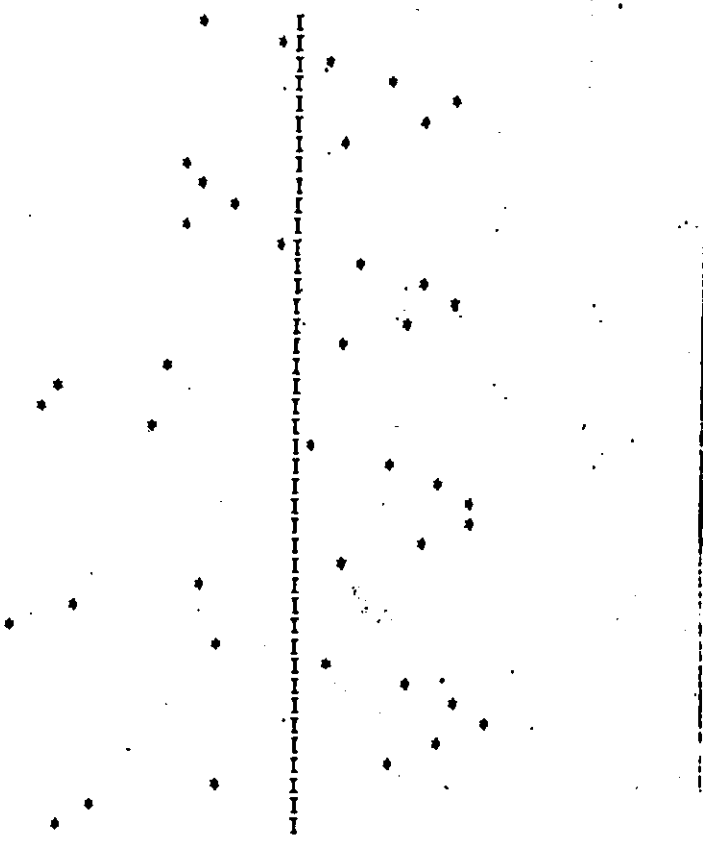

THIS SPSS JOB HAS TERMINATED NORMALLY.
THE JOB PROCESSED 27 CONTROL CARDS.
DURING THE JOB 0 ERRORS WERE DETECTED.